Cellular Operator Data Driven Solutions for Public Unlicensed Networks

Submitted to
Graduate School of Information Science and Technology,
Osaka University

January 2023

Srikant Manas KALA

List of Publications

Related Publications

The following articles and conference papers contributed directly to work presented in this thesis.

Journal Articles

(1) Srikant Manas Kala, Vanlin Sathya, Kunal Dahiya, Teruo Higashino, Hirozumi Yamaguchi, "Mitigating Trade-off in Unlicensed Network Optimization through Machine Learning and Context Awareness", *IEEE Access*, doi: 10.1109/ACCESS.2023.3235882, 2023.

(2) Srikant Manas Kala, Vanlin Sathya, Kunal Dahiya, Teruo Higashino, Hirozumi Yamaguchi, "Identification and Analysis of a Unique Cell Selection Phenomenon in Public Unlicensed Cellular Networks Through Machine Learning", *IEEE Access*, volume 10, 87282-87301, 2022.

(3) Srikant Manas Kala, Kunal Dahiya, Vanlin Sathya, Teruo Higashino, Hirozumi Yamaguchi, "LTE-LAA Cell Selection through Operator Data Learning and Numerosity Reduction", *Pervasive and Mobile Computing*, volume 83, 101586, 2022.

Conference Papers

(1) Srikant Manas Kala, Vanlin Sathya, Kunal Dahiya, Teruo Higashino, Hirozumi Yamaguchi, "Optimizing Unlicensed Coexistence Network Performance Through Data Learning", in *Proceedings of the Mobile and Ubiquitous Systems: Computing, Networking and Services (MobiQuitous 2021)*, vol. 419, pp. 128–149, January 2022.

(2) Srikant Manas Kala, Vanlin Sathya, Eitaro Yamatsuta, Hirozumi Yamaguchi, Teruo Higashino, "Operator Data Driven Cell-Selection in LTE-LAA Coexistence Networks", in *Proceedings of the International Conference on Distributed Computing and Networking (ICDCN 2021)*, pp. 206–214, June 2021.

(3) Srikant Manas Kala, Vanlin Sathya, Winston KG Seah, Hirozumi Yamaguchi, Teruo Higashino, "Evaluation of Theoretical Interference Estimation Metrics for Dense Wi-Fi Networks", in *Pro-*

ceedings of International Conference on COMmunication Systems & NETworkS (COMSNETS 2021), pp.351–359, June 2021.

(4) Srikant Manas Kala, Vanlin Sathya, Seah Winston KG, Bheemarjuna Reddy Tamma, "CIRNO: Leveraging capacity interference relationship for dense networks optimization", in *Proceedings of the 2020 IEEE Wireless Communications and Networking Conference (WCNC 2020)*, pp. 1-6, June 2020.

Miscellaneous Publications

Journal Articles

(1) Vanlin Sathya, Srikant Manas Kala, Kalpana Naidu, "Heterogenous Networks: From small cells to 5G NR-U" *Wireless Personal Communications*, 1-32, November 2022.

(2) Vanlin Sathya, Srikant Manas Kala, S Bhupeshraj, Bheemarjuna Reddy Tamma, "RAPTAP: a socio-inspired approach to resource allocation and interference management in dense small cells" *Wireless Networks*, volume 27, 441-464, 2021.

(3) Vanlin Sathya, Srikant Manas Kala, Muhammad Iqbal Rochman, Monisha Ghosh, Sumit Roy, "Standardization advances for cellular and Wi-Fi coexistence in the unlicensed 5 and 6 GHz bands" *GetMobile: Mobile Computing and Communications*, volume 24, 1, 5-15, 2020.

List of Abbreviations

AR Augmented Reality

BBU Baseband Unit

CAPEX Capital Expenditure

ED Energy Detection

eLAA Enhanced Licensed Assisted Access

ETACS Extended Total Access Communication System

FCC Federal Communications Commission

FeLAA Further Enhanced Licensed Assisted Access

IoT Internet of Things

LBT Listen Before Talk

MIMO Multiple Input Multiple Output

NPRM Notice of Proposed Rule Making

NR New Radio

NR-U New Radio in Unlicensed

OFDM Orthogonal Frequency Division Multiplexing

OPEX Operational Expenditure

OPEX Operational Expenditure

QoE Quality of Experience

QoS Quality of Service

RB Resource Block

RRH Remote Radio Head

RRM Radio Resources Management

RSD Residual Standard Deviation

SON Self Organizing Network

AR Augmented Reality

VR Virtual Reality

4G Fourth generation of mobile networks

5G Fifth generation of mobile networks

LAA Licence Assisted Access

LTE-A Long Term Evolution Advanced

RMV Regression Model Validity

SINR Signal to Interference & Noise Ratio

LTE Long Term Evolution

LTE-U Long Term Evolution Unlicensed

Abstract

Unlicensed coexistence networks and spectrum-sharing standards help cellular operators meet the ever-increasing demand for mobile data through the efficient utilization of unlicensed bands. However, several incumbents are already operational in these frequencies rendering the wireless environment extremely dynamic and unpredictable. Consequently, increased transmission conflicts and differing quality of service (QoS) requirements present new challenges in harmonious coexistence and spectrum sharing. Cellular networks are also undergoing consistent densification, increasing the overhead and complexity of network optimization. Despite their versatility, the classical network optimization models seem ill-equipped to offer solutions in real-time to facilitate harmonious coexistence and spectrum sharing. Recent studies show that classical optimization techniques are not sufficient to offer latency-critical applications and services in the unlicensed bands. As a result, challenges in unlicensed cellular networks are best solved through a data-driven approach, leveraging machine learning for network analysis, performance prediction, anomaly detection, and performance optimization.

The first challenge to this empirical approach is the collection and extraction of unlicensed network data. After all, a machine learning model is only as reliable as the data it is fed. Thus, data-driven solutions for successful unlicensed operation of Licensed Assisted Access (LAA) in 5 GHz and New Radio in Unlicensed (NR-U) in 6 GHz require operator data from current cellular deployments. Unfortunately, given the high cost of network monitoring applications and the limited geographical presence of these new networks, access to cellular network data is limited.

Next, methodologies and frameworks must be devised to leverage the gathered data. These frameworks will help solve problems ranging from network performance analysis to network optimization and also in investigating new phenomena unique to unlicensed bands. For example, comparative analysis of unlicensed network standards proposed by standardization bodies is usually measurement-based. A data-driven performance analysis is lacking. Likewise, performance analysis of unlicensed network mechanisms, such as the cell selection process, requires a methodology based on machine learning.

In addition, a hybrid data-driven optimization approach is necessary for optimal network performance with low convergence times. A largely unexplored problem in machine learning-based dense unlicensed network optimization is the accuracy-speed trade-off, i.e., achieving high accuracy in optimization objectives with minimal time costs. More importantly, the proposed hybrid optimization techniques should be validated on real-world network data. Only then can novel solutions be tailored

for the new cellular standards for the unlicensed spectrum.

Finally, a new phenomenon in unlicensed cellular deployments and their impact on network performance should be investigated through data analysis and machine learning. New findings will make way for new high-performance solutions, such as cell selection initiated by the user device in future unlicensed bands.

This thesis seeks to address these challenges in a comprehensive end-to-end fashion. The first problem entails identifying data-driven methodologies for the analysis and optimization of unlicensed network standards. This work investigates network feature relationships (NFRs) in unlicensed LTE-WiFi (LTE-U and LTE-LAA) networks through supervised learning of network data collected from an unlicensed experimental testbed. The experiments were carried out on a coexistence testbed consisting of both the unlicensed LTE standards (LTE-U & LTE-LAA) and two Wi-Fi standards (802.11n/ac) on multiple channel bandwidths.

A data-driven comparative analysis of different LTE-U and LAA network configurations is performed through learning model parameters such as R-sq, residual error, outliers, choice of predictor, *etc.* In addition, LTE-U & LTE-LAA are contrasted on signaling and user data traffic and resource block allocation. Thereafter, a hybrid optimization approach that combines machine learning and network optimization called Network Feature Relationship-based Optimization (NeFRO) framework is proposed. NeFRO improves upon the conventional optimization formulations by utilizing the feature-relationship equations learned from network data. It is demonstrated to be highly suitable for time-critical dense unlicensed networks through two optimization objectives, *viz.,* network capacity and signal strength. NeFRO is validated against four recent works on network optimization. NeFRO is successfully able to reduce optimization convergence time by as much as 24% while maintaining accuracy as high as 97.16%, on average. Further, the work investigates the use of more precise higher-order NFRs in optimization formulations and the consequent trade-off that arises between the increase in convergence time (Speed) and the nearness to optimal results (Accuracy). It demonstrates the relevance of context awareness of the network conditions and the traffic environment in mitigating the trade-off. To that end, the context-aware network feature relationship-based optimization (CANEFRO) approach is proposed and validated through decision matrix analysis. CANEFRO demonstrates the impact of network context on the degree of feature relationship (2^{nd} & 3^{rd} degree polynomials), the objective of optimization (SINR and Capacity), and the network use-case (Accuracy vs. Speed). CANEFRO is also used to contrast LTE-U & LTE-LAA optimization performance. In particular, decision matrix analysis demonstrates a higher decision score for LAA by as much as 42% as compared to LTE-U.

Next, this work focuses on data gathering from real-world LAA deployments. A dataset is created from LAA networks of three major cellular operators in Chicago, *viz.,* AT&T, T-Mobile, and Verizon. The data was extracted through a computer-vision-based system developed for a reliable network monitoring application. The engineered system enables data extraction at scale, low cost, high accuracy

and for multiple cellular technologies.

The gathered operator data is analyzed through several supervised machine learning algorithms. The effect of cell selection on LAA network capacity and network feature relationships is studied. Insightful inferences are drawn on the contrasting characteristics of the Licensed and Unlicensed components of an LTE-LAA system. Further, a cell-quality metric is derived from operator data and is shown to have a strong correlation with unlicensed coexistence system performance. To validate the ideas, two state-of-the-art cell association and resource allocation solutions are implemented through the NeFRO framework. Validation results show that data-driven cell selection can reduce Unlicensed association time by as much as 34.89%, and enhance Licensed network capacity by up to 90.41%. Further, with the vision to reduce the computational overhead of data-driven cell selection in LAA and 5G New Radio Unlicensed networks, the performance of two popular numerosity reduction techniques is evaluated.

Finally, this work highlights a unique phenomenon related to Physical Cell Id (PCI) observed in public LAA deployments. Notably, the licensed and unlicensed carriers of a device may have the same PCI or different PCIs. The phenomenon is triggered by the combined effect of unlicensed deployment architectures and cell selection mechanisms. Consequently, the phenomenon will intensify in the 5G NR-U, whose public deployment will soon begin. It is also desirable to accurately identify the PCI scenarios at the device for improved cell selection and network performance. The impact of the phenomenon on the LTE, LAA, and Wi-Fi components is demonstrated in three steps: First, the variation in network performance prediction accuracy in PCI scenarios is examined. Second, the efficacy of numerosity reduction techniques used in data-driven cell selection is evaluated in both PCI scenarios. The third step entails comparing operator data analysis with network measurements. On-site experiments are conducted at the same PCI and different PCI sites to study differences in real-time network performance. A controlled LTE-WiFi coexistence environment is created and multiple traffic categories are considered. Finally, a class-weight-based solution is proposed for PCI scenario identification. Despite the high data imbalance, an f-score of 0.75 and an AUC-ROC of 0.84 are achieved for LAA, with a minimalist feature set consisting of SINR and Throughput.

Thus, this thesis seeks to improve unlicensed network performance through a wholesome data-driven approach. It includes experiments on unlicensed network testbeds, new methodologies for comparative performance analysis, network data collection from real-world deployments, data analysis, and predictive modeling, and new solutions for network optimization and mechanisms. One of the significant achievements of this work is the release of an LAA network dataset for easy access to the broader research community. Together, these contributions can help operators tap into the unharnessed potential of the current and future unlicensed bands.

Contents

List of Figures

List of Tables

Chapter 1

Introduction

The first generation (1G) cellular networks were commercially released in the late 1970s. The primary goal of these analog communication systems, such as the Extended Total Access Communication Systems (ETACS), was to deliver voice services to consumers. With the foray of digital communication in the second generation (2G) networks launched in the 1990s, there was a transcendental shift in cellular communication technology and services. Since then, there has been constant innovation in cellular technology. Mobile networks have been frequently upgraded through periodic releases incorporating new standards and paradigms such as spectrum sharing. Consequently, network capacity, quality of voice and data services, privacy and security, and energy efficiency of cellular devices have improved significantly. The commercially available 5G networks deliver average data rates of about 200 Mbps, and can potentially offer up to 20 Gbps downstream rate [1]. The datarate of 51.2 Kbps, available to the Apollo 11 spacecraft that landed on the moon, pales in comparison to what an average smartphone user enjoys today [2]. Cellular data consumption has also consistently surged. The global monthly average data consumption was pegged at 12GB/smartphone for the year 2021 [3]. Mass adoption of data-intensive mobile services, such as live streaming, high-definition video, and Augmented/Mixed Reality, is expected to drive the global monthly data demand by three-fold to 40 GB/smartphone by the year 2027 [3].

To support this data demand, greater spectrum allocation, and efficient spectrum utilization go hand in hand. Available spectrum is typically utilized in three ways, through licensed operation (e.g., 4G LTE and 5G NR), unlicensed operation (e.g., LTE-WiFi coexistence on 5 GHz, Wi-Fi 2.4 GHz), and spectrum sharing (e.g., CBRS, Wi-Fi 5 GHz in UNII-2, Wi-Fi 6E and 7 in 6GHz). Given that the licensed spectrum is a scarce resource, unlicensed coexistence and spectrum sharing offer opportunities for maximal spectral utilization. To that end, cellular operators have deployed Licensed Assisted Access (LAA) services – the first public unlicensed cellular deployments in the 5GHz band.

However, to be able to share spectrum or facilitate the coexistence of multiple radio technologies in a band, a deeper understanding of the existing spectrum utilization is crucial. For example, federal operations are the main incumbent in the Wi-Fi 5 GHz UNII-2 band. Soon, Wi-Fi 6E will expand

Wi-Fi 6 or NR in unlicensed (NR-U) capabilities in the 6GHz unlicensed band, and Wi-Fi 7 will enhance these capabilities by a factor of 40x with multi-link aggregation. Thus, it is imperative that coexistence efficiency of cellular, Wi-Fi, and other incumbents in the shared spectrum be closely studied with respect to parameters such as bandwidth, usage frequency, density, resource allocation, etc.

This can only be achieved through the analysis of existing data from network deployments. Without access to this data, it is difficult to investigate how efficiently the spectrum is being used and to identify the practical challenges to fair coexistence. Thus, access to cellular network data is vital for the research community.

1.1 Unlicensed Coexistence and Spectrum Sharing

Licensed spectrum is a limited and expensive resource. Thus, there has been a consistent push from industry and standardization bodies such as 3GPP, and ETSI for a greater utilization of the unlicensed spectrum by Long-Term Evolution (LTE) cellular networks. The two paradigms that can help operators tap into the unharnessed potential of the unlicensed bands are unlicensed coexistence and spectrum sharing.

1.1.1 Unlicensed Coexistence Networks

To ensure fair coexistence of existing incumbents with unlicensed cellular operation, two LTE-WiFi coexistence standards were prescribed and adopted, which are: *LTE license assisted access* (LTE-LAA) proposed by 3GPP and *LTE in unlicensed spectrum* (LTE-U) proposed by industry forum. The Federal Communications Commission of the United States of America (FCC) deregulated 500 MHz spectrum in the 5GHz band for unlicensed cellular operation in coexistence with Wi-Fi. After a prolonged LTE-U vs. LAA debate, cellular operators globally backed LAA. By 2020, 38 operators in 21 countries were deploying LAA networks in the 5GHz band, as compared to only 3 countries where LTE-U deployments were commercially operational [4]. LTE-LAA was hailed as a 3GPP benchmark for fair coexistence of LTE with existing incumbents such as Wi-Fi networks in the unlicensed bands. It also served as a successful technological precursor to the 5G New Radio-Unlicensed (5G NR-U) [5]. Encouraged by these outcomes, toward the end of 2018, FCC issued a Notice of Proposed Rulemaking for unlicensed operation in the 6 GHz band. It prescribed guidelines for unlicensed coexistence of cellular services with existing incumbents such as Wi-Fi access points (APs) in the 6 GHz band (5925-7125 MHz). These prescriptions were adopted in April 2020. Likewise, the European Commission decided to allocate 480 MHz (5925- 6725 MHz) of spectrum in the 6 GHz band to harmonize unlicensed coexistence of cellular and Wi-Fi systems.

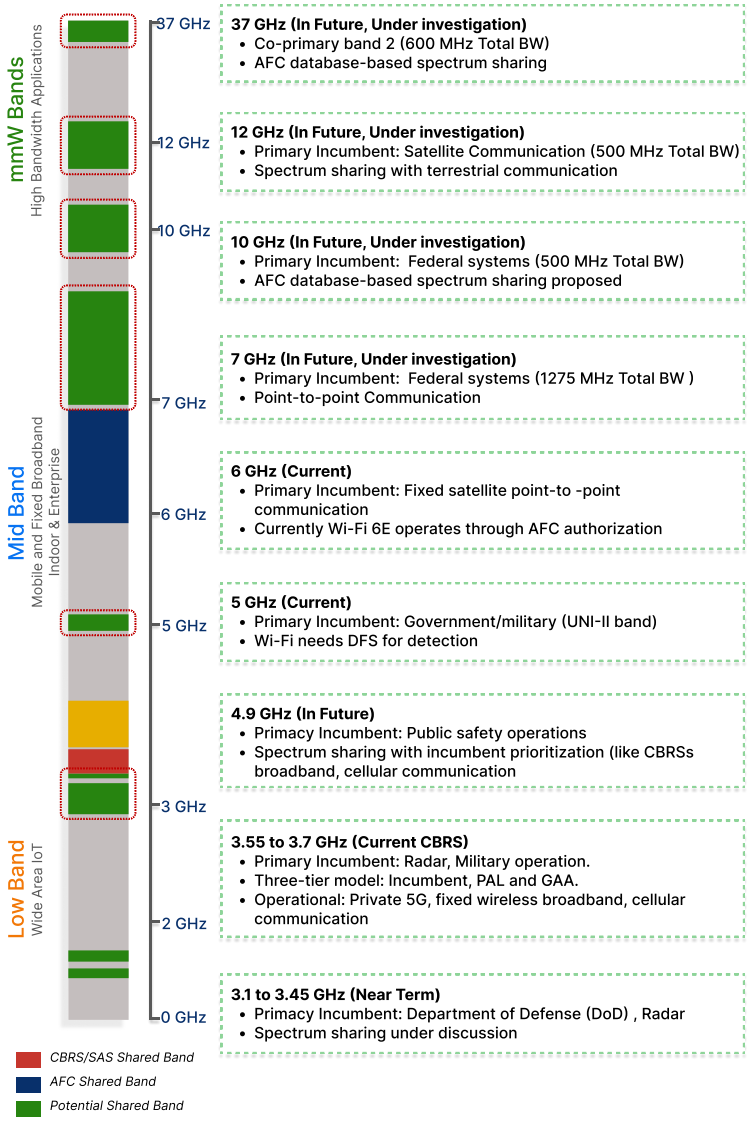

Figure 1.1: Opportunities in the Unlicensed Spectrum

1.1.2 Spectrum Sharing

Traditionally, regulators have allocated spectrum to mobile operators only after clearing out the incumbent users. However, in addition to coexistence, the unlicensed bands can also be utilized through spectrum sharing where the primary incumbent(s) or primary user(s) can be military communications, radar or satellite transmissions, and Broadcast Auxiliary Services (BAS). During times or in areas where the primary incumbent is inactive, secondary incumbents/users can operate in the medium. Examples of secondary incumbents include Wi-Fi in 5 GHz UNII-2 or Citizens Broadband Radio

Service in 3.5GHz (3550 MHz to 3700).

Three spectrum sharing mechanisms are operational or under consideration [6]. The most prominent is the Citizens Broadband Radio Service (CBRS) approach, currently operational in the 3.5 GHz Band in the US. The other two are Licensed Shared Access and Concurrent Shared Access such as *club licensing* [6].

CBRS uses dynamic sharing to support three tiers of prioritized or controlled access to the spectrum. The highest priority tier with the most protection comprises incumbents, such as radars and satellite services. Prioritized Access License (PAL) holders form the secondary tier. PALs purchase the rights to use the available spectrum (up to a maximum of 40 MHz) when the top-tier incumbent is not using it. The lowest tier offers a General Authorized Access (GAA) to any service willing to use the spectrum when available with the least protections. In areas where the top-tier incumbent is not utilizing the spectrum, the PAL and GAA tiers get access to reserved portions of the spectrum. Additionally, FCC has mandated all tiers to look up the Spectrum Access System (SAS) database, which facilitates the spectrum sharing model by regulating and managing access. In case a band is not registered as being used in the SAS database, PAL and GAA tiers can access each other's reserved portions in the band.

Second, is Licensed Shared Access [6]. It has a two-tiered structure where primary incumbent(s) are license holders who can sub-license the spectrum to secondary service providers such as mobile operators. The secondary tier can use the shared spectrum when not in use by the incumbent. The first such spectrum-sharing model was operational in Europe in the 2.3 GHz band, and more sophisticated models are under development.

The third mechanism for sharing spectrum is the concurrent shared access such as *club licensing* [6]. Unlike the first two mechanisms, this approach considers a single tier of users and allows them to coordinate and share spectrum with each other. Thus, mobile operators can share spectrum to enhance the quality of services (QoS) and the overall efficiency of spectrum usage.

1.1.3 Opportunities in the Unlicensed Band

The successful initial implementations of the above two paradigms have encouraged regulators, standardization bodies, and industry organizations to initiate discussions on opening other underutilized frequencies for coexistence and sharing. A detailed overview of ongoing discussions with band-specific highlights is presented in Figure 1.1.

Although high-band terahertz range frequencies, such as mmWave, have fewer incumbents and offer high bandwidths, the mid-band frequencies offer a more balanced combination of transmission range and bandwidth. Consequently, most potential bands under consideration are in the 1 GHz — 12 GHz range, essentially making the mid-band the primary driver of coexistence and spectrum sharing systems. However, it will also make it the most crowded, exacerbating the challenges and bottlenecks observed in the 5GHz unlicensed operation. The Federal Communications Commission (FCC) in the U.S. recently created rules for the 6 GHz band that would allow unlicensed services to coexist with

existing incumbents in the band, mainly high-power fixed microwave links and lower-power broadcast auxiliary services. It is expected that in addition to WiFi, this band will also be used by cellular systems deploying 5G NR-U, similar to the use of the 5 GHz band by LAA.

Let us consider the recently deregulated 1200 MHz spectrum (5925 MHz–7125 MHz) in the UNII bands 5, 6, 7, and 8 in the US. In the 6 GHz band, apart from Wi-Fi 6E, unlicensed cellular services will coexist with other existing incumbents, primarily the high-power fixed point-to-point microwave services and lower-power BAS. Despite these additional constraints, reliable and improved QoS is expected from unlicensed services. To that end, IEEE and 3GPP organized a workshop on coexistence networks in 2019 to discuss existing challenges and propose feasible solutions for the next generation of standards covering WI-Fi 6E and 5G NRU operation in the 6 GHz band.

Correspondingly, the current deployments in the 5 GHz band also serve as the best training ground for improved 6 GHz unlicensed and spectrum-sharing operation. The challenges faced in LTE-WiFi coexistence will resurface in 6 GHz band as well. However, lessons from the 5 GHz band deployments can be learned only through collaborative research and analysis for which access to network data is of utmost importance. Without LAA network data analysis, empirical ground truth regarding efficiency of various network mechanisms will be difficult to determine. Findings such as the type of services coexisting in the unlicensed band or the impact of cell selection on LAA performance [7,8] would not have been possible. Likewise, lessons learned from LAA deployments will also pave the way for robust and low-friction spectrum sharing systems enabling NR-U operation in 6GHz and beyond.

1.1.4 Utility of Data-driven Solutions

Machine Learning algorithms make it possible to formulate the problem of estimating network performance as a prediction problem. In the recent past, several state-of-the-art studies have used the family of regression algorithms, decision trees, support vector machines, neural networks, and other AI/ML techniques for feature relationship analysis and network performance prediction [9–13]. AI/ML algorithms can help analyze several aspects of network feature relationships such as strength, independence, and causality [10,11]. Invariably, the goal of applying AI/ML algorithms is to improve network performance. For example, learning 802.11n feature relationships can facilitate improved configuration selection and enhanced rate adaptation [9]. Similarly, they can be used to design link adaptation algorithms and improve network throughput [10,12].

In the 6 GHz band, the spectrum will not only be shared between cellular (5G) and Wi-Fi (802.11ax) but also other incumbents, viz., broadcast auxiliary services, military/ship radars, fixed microwave transmissions, and weather or terrestrial satellite systems. Thus, data-driven evaluation of current unlicensed LAA networks will help the primary incumbent(s) understand (a) How efficiently the spectrum is being utilized and (b) How fairly are other radio technologies (e.g., LAA, Wi-Fi) coexisting/sharing the spectrum. Apart from operators, analysis of LAA network data will also help government bodies draft better coexistence/spectrum-sharing policies and make expeditious decisions.

Further, network bottlenecks can be easily identified. For instance, it was learned that it is difficult to predict network throughput by looking at SINR or RB allocation alone. Further, for different locations, cells, or operators, the importance of SINR or RB in determining network capacity differs (sometimes operators aggregate with more than one channel with different bandwidths). This problem becomes more challenging with a larger feature set with tens or hundreds of network features. AI/ML techniques such as Permutation Feature Importance, Principal Component Analysis, and t-distributed stochastic neighbor embedding can help determine the network parameters most relevant to overall network performance in a given context.

Another problem of interest could be to predict the probable range of Throughput or SINR with high confidence for a given set of network features. This can be modeled as a regression problem. Likewise, classification models based on AI/ML algorithms can be used to solve a variety of important problems, including the PCI confusion/collision, choice of primary channel for operation, choice of LTE/5G vs. LAA/NR, identifying when career aggregation is enabled, understanding which bandwidth (5, 10, 15 or 20 MHz), Rank (1 or 2), MIMO (2x2 or 4x4) is selected in a given context, etc. Even when there is insufficient network data for specific scenarios leading to (extreme) class imbalance, low-cost AI/ML algorithms are efficient at learning the network context.

Current and future unlicensed specifications will include millimeter wave (mmWave) bands. These bands offer ultra-high capacity with channel bandwidths in hundreds of MHz. However, propagation loss and atmospheric attenuation of the signal limit their coverage. From a network optimization perspective, this is particularly important as optimization formulations ensuring fair coexistence must be hyper-localized and should converge quickly. This makes a strong case for machine learning-driven optimization. For example, the current solutions for the initial access optimization problem in the mmWave bands are either based on conventional beam sweeping or formulated as a combinatorial optimization formulation [14]. Both may lead to high convergence times in dense mmWave coexistence networks with multiple incumbents, especially when the optimization model has to be hyper-local. Other typical problems that can be addressed through data-driven analysis and optimization in the mmWave bands include coverage optimization and traffic-steering for mmWave hetnets [15, 16].

Thus, the data-driven ideas and methodologies proposed in this thesis hold relevance for unlicensed cellular networks, including the mmWave bands.

1.2 Overview of the Research Problems Addressed

1.2.1 Gathering and Extraction of Cellular Operator Data

It is relevant to study the characteristics of current LAA cell selection mechanisms and their influence on network performance by analyzing operator data collected from LAA deployments. Most studies on unlicensed cell selection so far have been conducted on experimental LAA testbeds or through simulations [17–21] and not on real-world LTE-LAA networks. Data-driven solutions to optimize the

unlicensed LAA operation in 5 GHz and NR-U in 6 GHz will be effective only if the underlying machine learning models are trained on operator data from current cellular deployments. Unfortunately, due to expensive network monitoring applications and the limited geographical presence of new unlicensed networks, there is limited access to cellular network data.

Thus, the first problem addressed in this thesis is the gathering and extraction of unlicensed network data from public LAA deployments. A dataset from LAA networks of three major cellular operators in Chicago, viz. AT&T, Verizon, and T-Mobile is created. A computer-vision-based system is designed which can extract data for multiple cellular technologies at scale and with high accuracy.

1.2.2 New Data-driven Techniques and Frameworks

Another major challenge is that new techniques and frameworks are needed to utilize the gathered network data. This is particularly true for network performance optimization, as conventional optimization techniques are insufficient for highly dynamic unlicensed bands. Unlicensed band optimization requires harmonious coexistence and frictionless spectrum sharing. More importantly, solutions are needed in real-time and must support latency-critical services. New data-driven solutions are needed to meet these requirements.

New methodologies for network performance analysis using machine learning are also of great interest. Currently, network performance analysis is primarily measurement-based, i.e., the focus is on the values of important network parameters. For example, the comparative analysis of the unlicensed network standards, viz., LTE-LAA and LTE-U, presented in several prominent works, is usually measurement-based. The LAA vs. LTE-U debate has raged since the two standards were proposed. However, measurement-based comparative studies have been unable to definitively conclude why LAA eventually emerged as the preference of cellular operators globally. Thus, a new data-driven performance evaluation is needed, which calls for a deeper analysis of network data using machine learning. It can be used to focus on relationships between network variables to better understand the ambient network environment. In unlicensed networks, data-driven performance analysis can help analyze the efficiency of mechanisms such as the cell selection process.

This thesis proposes (a) a machine learning-based methodology for network performance analysis and (b) a hybrid data-driven optimization framework for unlicensed networks. It performs a comparative analysis of LTE-U and LTE-LAA using network feature relationships (NFRs) through supervised learning algorithms. Network data was collected from experiments on an unlicensed experimental testbed comprising both the unlicensed LTE standards (LTE-U & LTE-LAA) and two Wi-Fi standards (802.11n/ac) on multiple channel bandwidths. The data-driven analysis compares the performance of LTE-U and LAA network configurations by analyzing model parameters such as R-sq, residual error, and outliers. Further, the relevance of network context is shown by contrasting LTE-U & LTE-LAA on signaling and user data traffic patterns such as SINR, Throughput, and resource block allocation. The findings of the data-driven comparative analysis of LAA and LTE-U indicate why LAA has emerged

as the global standard for unlicensed cellular networks.

The second data-driven solution proposed in this thesis combines machine learning and conventional network optimization. The hybrid approach is called the Network Feature Relationship-based Optimization (NeFRO) framework. NeFRO utilizes the feature-relationship equations learned from the network data by considering them as constraints in conventional optimization formulations. By doing so, NeFRO reduces the convergence time (Speed) while maintaining high closeness to optimal results (Accuracy). NeFRO is shown to be suitable for time-critical services and applications in dense unlicensed networks. To validate NeFRO, two optimization goals,*viz.,* network capacity and signal strength, and four recent solutions on network optimization were considered. NeFRO demonstrates a reduction in optimization convergence time or "Speed" of as much as 24% while maintaining nearness to baseline optimal values or "Accuracy" as high as 97.16%, on average.

The thesis also evaluates two more aspects of machine learning-based network optimization. First is the use of more precise higher-order NFRs in optimization formulations and the consequent trade-off that arises between the increase in convergence time (Loss in Speed) and near-optimality of results (Gain in Accuracy). Second, it demonstrates the relevance of context awareness of the ambient network conditions and traffic environment in the performance of the optimization model. It also explores the possibility of utilizing context awareness in mitigating the trade-off. To that end, this thesis proposes a context-aware network feature relationship-based optimization (CANEFRO) approach. CANEFRO is validated through decision matrix analysis. It highlights the relevance of network context in (a) the selection of feature relationship equations for NeFRO (between 2^{nd} & 3^{rd} degree polynomials), (b) the optimization objective (SINR and capacity), and (c) the requirement of the service or application (Accuracy vs. Speed). CANEFRO also enriches the comparative evaluation of LTE-U & LTE-LAA in terms of context-aware optimization. Through a decision matrix analysis, it reveals a higher decision score for LAA by as much as 42% when compared to LTE-U.

1.2.3 Performance Enhancement of LAA Networks and New Findings

New methodologies for data-driven analysis and optimization should be functional in real-world deployments. The objectives are threefold: (a) data-driven performance analysis of current unlicensed deployments, (b) demonstrate possibilities for improvement in network processes through data-driven optimization (NeFRO), and (c) identify new phenomena that are unique to unlicensed networks. Thus, the solutions proposed in this thesis are applied to the extracted LAA network data.

Through operator data analysis, this thesis identifies opportunities to improve network performance and efficiency. In particular, it focuses on the impact of cell selection decisions in small cells of an LTE-LAA system. The cell selection mechanisms employed by cellular operators in LTE HetNets based on signal-to-interference plus noise Ratio (SINR) and transmission power are unsuitable for LTE-LAA deployments. Further, the impact of cell association on the performance of an LAA network and its components has not been studied comprehensively. Cellular operators already employ AI/ML to

enhance network operations [22]. Thus, cell selection mechanisms for LTE-LAA based on real-time cell quality metrics will add significant value to the operators and end-users.

This thesis analyzes the impact of cell selection on a combined LTE-LAA system and its licensed and unlicensed components by considering PCI as a categorical parameter [8]. Supervised AI/ML algorithms are also used to learn the SINR-Capacity relationship in the licensed (LTE) and unlicensed (LAA) components and insightful inferences drawn on their contrasting characteristics. In addition, the analysis shows a correlation between a cell quality metric derived from operator data and coexistence network performance. The NeFRO approach is applied to operator data for two state-of-the-art cell association and resource allocation optimization solutions. Operator data-driven cell selection leads to a reduction in association time (by up to 34.89%) and enhanced network capacity (by up to 90.41%). Finally, two existing solutions to operator data numerosity reduction are discussed with the goal of accelerating cell selection in dense unlicensed networks. Data analysis reveals a clear distinction in the performance of LTE and LAA components when their respective data is subjected to numerosity reduction.

It was learned that this relationship varies significantly in licensed and unlicensed components. LAA typically shows a stronger relationship (higher R-sq) for various AI / ML techniques, including decision trees and neural networks [7,8]. Further, the feature importance of SINR in predicting network capacity is much higher for unlicensed networks than for licensed networks [7, 8]. The reason is that LAA networks were characterized by high resource block allocation and lower user density, making device throughput more dependent on signal quality received.

Furthermore, From a cellular operator perspective, in coexistence networks, challenges of synchronization are also exacerbated by densification and can only be addressed through a distributed approach to large-scale network optimization [23]. Network performance optimization can also benefit from data-driven inputs. A hybrid approach that combines AI/ML with a theoretical constraint-based optimization formulation can greatly enhance network performance. For example, feature relationship equations learned from network data for a response variable such as SINR or Throughput can serve as a constraint in an optimization model [10, 13]. Doing so enriches the optimization model with context from the ambient network environment, making it more empirical and data-driven. There is sufficient evidence to indicate that network operators already employ AI/ML to further optimize their processes, such as cell selection [22]. Thus, a publicly available LAA dataset will pave the way for new research on data-driven network optimization.

Finally, the data analysis in this thesis reveals a unique Physical Cell Id (PCI) related phenomenon in the unlicensed cellular deployments. Notably, the licensed and unlicensed carriers of a device may have the same PCI or different PCIs, thereby spawning two PCI scenarios in which all unlicensed network sites can be categorized. However, due to the nascent stage of unlicensed deployments, the impact of this phenomenon on coexistence network performance is unexplored. It appears desirable to accurately identify the two PCI scenarios for improved network performance through use-cases such

as device initiated cell-selection. But the inherent data imbalance makes the classification problem challenging. This thesis addresses these problems through the following approach. Operator data from three LAA cellular providers is gathered and the dataset is analyzed using machine learning (ML) algorithms. The impact of the two PCI scenarios on the LTE and LAA components is demonstrated in three steps: (a) The variation in network performance prediction accuracy in the two scenarios is examined. (b) The suitability of numerosity reduction techniques in both PCI scenarios is evaluated through their impact on performance prediction models. (c) A comparison of the operator data analysis with the network measurements is performed. On-site experiments are conducted at the same PCI and different PCI sites to study the difference in real-time network performance. For a comprehensive evaluation, a controlled LTE-WiFi coexistence environment is created and multiple traffic categories are considered. Finally, the major challenge of the prediction of PCI scenarios is formulated as an imbalanced classification problem. The proposed class-weight-based solution uses a minimalist feature set of only two features, viz. SINR and Throughput. The weighted classifier identifies the PCI scenarios of a mobile device with an AUC of 0.71 and 0.84 in the ROC curve, for LTE and LAA components, respectively.

To summarize, this thesis aims to enhance the performance of unlicensed network performance through a data-driven approach. Although the experiments, data collection, data analysis, and ML-based solutions are for LAA networks, they will add great value to 5G-NRU networks as well. The work in this thesis involves experiments on unlicensed network testbeds (LAA and LTE-U), new data-driven frameworks for network analysis, data collection and extraction from public LAA networks, operator data analysis, feature relationship analysis and predictive modeling, and data-driven solutions for network optimization. This thesis also makes a large LAA dataset publicly available for the benefit of the wireless/cellular networks community. Combined, the dataset, analysis, and solutions presented in this thesis will aid cellular operators in maximizing the spectral utilization of current (5GHz) and future (6GHZ and beyond) unlicensed bands.

The thesis is organized as follows. A review of existing research studies relevant to unlicensed cellular networks is presented in Chapter 2. Therafter, Chapter 3 presents methodologies for data-driven analysis and optimization of unlicensed networks. The ideas presented in this chapter are validated on data from an experimental testbed. To apply them to data from real-world deployments, a detailed description of operator data collection and extraction is presented in Chapter 4. Next, this chapter presents an analysis of the performance of LAA networks with respect to cell selection and Physical Cell Id. Chapter 5, discusses a new phenomenon related to cell selection choices unique to unlicensed cellular operation and its implications on LAA network performance. Finally, the conclusions are presented in Chapter 6.

Chapter 2

Literature Review

This chapter presents a brief overview of the state-of-the-art and recent developments in the unlicensed band cellular operation. It also highlights the new challenges and complexities that LAA and future unlicensed cellular networks will face.

2.1 Literature Review on Unlicensed Network Optimization

In the unlicensed bands, the spectrum is shared by cellular (4G/5G), Wi-Fi (802.11ac/ax), and several incumbents such as broadcast auxiliary services, military and ship radars, fixed microwave transmissions, and weather or terrestrial satellite systems. In licensed frequencies, cellular operators only have to contend with intra-cell and inter-cell interference. However, in the unlicensed band, cellular operation suffers conflicting transmissions from other coexisting radio transmissions. Apart from interference mitigation, it is also necessary to ensure fair and harmonious coexistence with other incumbents. This adds additional constraints on network mechanisms such as resource allocation and scheduling. Finally, the constant ongoing densification of coexistence systems due to a variety of small cells and access points makes unlicensed network optimization extremely challenging. The following sections review these dimensions in great detail.

2.1.1 Unlicensed Networks: Interference and Densification

Interference is a serious bottleneck to the routine network performance management tasks such as efficient resource allocation, optimal transmission scheduling, guaranteeing and maintaining QoS standards *etc.* Unfortunately, estimating the intensity of interference and its impact on a wireless network is an NP-Hard problem [24].

2.1.2 Densification in Unlicensed Networks

Several interference characterization studies show that while densification may lead to an initial gain in LTE-WiFi coexistence system capacity, network performance eventually deteriorates with the rise

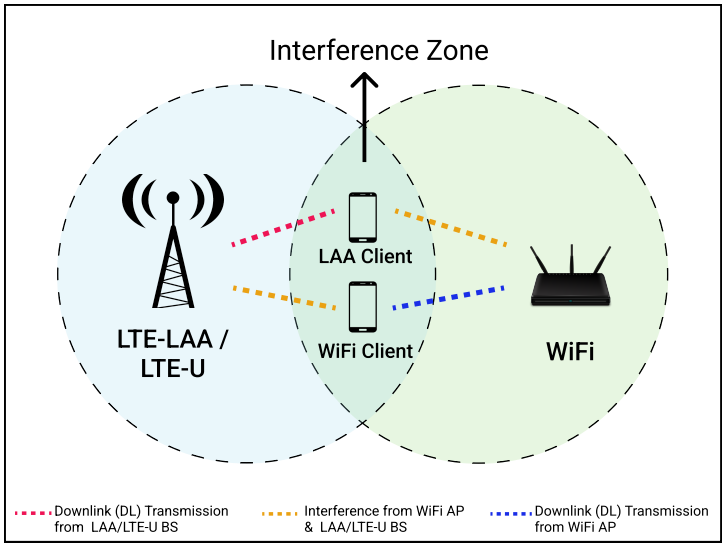

Figure 2.1: Interference in the Unlicensed Band

in density [25, 26]. The decrease in inter-AP/inter-SC distance does not necessarily lead to gains in network capacity due to the increased interference in DNs/UDNs [27].

Coexistence networks in the unlicensed band will experience new interference-related challenges. As shown in Figure 2.1, the densification of LTE-WiFi coexistence systems will exacerbate the adverse impact of interference. Densification in unlicensed coexistence will also worsen the asymmetric adverse impact on WiFi due to the overlapping LTE system and vice versa. To address these problems, several solutions are being proposed. For example, optimal interference control and offloading strategy for LTE-WiFi coexistence networks is presented in [28]. Another recent study has suggested a new cooperative Listen Before Talk (LBT) mechanism using zero forcing (ZF) precoding to overcome co-channel interference in dense coexistence networks [29]. New network architectures aimed at maximizing dense coexistence network capacity through the use of well-known techniques such as the almost blank subframe (ABS) scheme have also been proposed [30].

However, most studies on interference characterization of coexistence networks are primarily simulation-based and limited to highlighting the challenges posed by interference [27, 31]. Greater insight into the relationship between network variables in a dense unlicensed network, such as capacity and interference, is required. However, such data-driven studies on network feature relationships in the unlicensed band are lacking. For example, the analysis presented in [13] is limited to demonstrating the distinction in the characteristics of the SINR-Capacity relationship between experimental networks in normal-density and dense/ultra-dense unlicensed networks. The impact of factors *e.g.,* unlicensed LTE variant, Wi-Fi standard, the bandwidth allocated, and signaling data, *etc.,* on the feature relationships in the network also remains unexplored [27, 31, 32].

2.1.3 Analyzing Network Performance through Feature Relationships

Network performance is known to have an inverse relationship with interference [24]. Network capacity is usually the primary indicator of the QoS of a network, while secondary metrics include transmission loss and end-to-end latency. Therefore, capacity interference relationship (CIR) analysis and modeling have been the focus of numerous works [24, 33–35].

Due to the spatially and temporally dynamic nature of interference endemic in a wireless network, an exact quantification of CIR is a highly challenging task [24, 34–36]. A precise mathematical representation is not often achievable. This is even more true for the unlicensed band, where the probability of potential transmission conflicts from incumbents and coexisting technologies is extremely high.

At the same time, for high efficiency in unlicensed spectral utilization and fair coexistence, understanding the impact of interference is vital in unlicensed and spectrum-sharing systems. The conventional approach to analyze CIR was through theoretical models such as proposing the upper bound on maximal achievable throughput [35]. Such theoretical solutions usually require additional network-related information beforehand, such as the network layout and location of the nodes and often make assumptions about wireless network parameters such as the expected traffic load, *etc.* [34–36]. Given the complexity of unlicensed systems, i.e., a large number of coexisting technologies with varied architectures, it is infeasible to have prior knowledge of respective network parameters.

Thus, instead of theoretical models, an empirical or data-driven approach seems more suited for the unlicensed band. In the recent past, several state-of-the-art studies have used machine learning algorithms to better understand relationships between network variables. These studies have applied regression algorithms, neural networks, and other machine learning techniques to network data for a data-driven analysis [9–13]. This approach is useful because AI/ML algorithms can help analyze several aspects of network feature relationships (NFR), including the strength of the relationship between variables, feature importance, the interdependence of variables, and causality [10, 11]. The learned feature relationships can be used to predict and improve network performance. For example, NFRs in an 802.11n network were used to improve network configuration selection and rate adaption [9]. They can also lead to better link adaption algorithms and, most importantly, offer enhanced network capacity [10, 12].

However, the current literature on unlicensed networks lacks a data-driven feature relationship analysis of network performance. For example, most comparative studies on unlicensed cellular standards viz., LAA and LTE-U are *measurement based*, *i.e.,* the performance analysis is done by comparing several network performance evaluation metrics such as throughput, latency, packet loss ratio, channel occupancy times, number of re-transmissions, *etc.* In contrast, a *feature relationship analysis* looks for patterns in network data that can reveal relationships such as dependence, correlation, causation, *etc.,* between network variables. Thus, a more comprehensive experimental evaluation and data-driven analysis of unlicensed coexistence systems is required.

2.1.4 Optimization Challenges in Dense Networks

Several challenges in network management are resolved by modeling them as optimization formulations with varying contexts and diverse end goals. The popular ones are convex optimization, binary linear formulations, and mixed non-linear formulations [37, 38]. Solutions to several problems *viz.,* cost-efficient network deployment/operation [39], dynamic allocation of resources, energy efficiency [40], backhaul network design [41, 42], interference management [43], efficient spectrum sharing [44], and licensed/unlicensed band selection for transmission [42], are sought through a variety of optimization techniques.

While many of these problems are well-known in wireless networks, they assume new dimensions in unlicensed networks. Multiple incumbents, the requirement of fair coexistence, and increased network density make unlicensed network optimization extremely complex. For example, extra network information may be required, which includes network connectivity data, cache placement information, and timely sharing of locally determined metrics in a distributed architecture [45]. Optimization models must also account for temporal and spatial variation in network data which requires composite design parameters consisting of both discrete (e.g., remote radio unit selection) and continuous (e.g., beam-forming design) variables. The added requirement for network information in dense network optimization results in NP-hard mixed integer non-linear formulations [37], which in turn lead to higher computational overheads and increased convergence times. Further, scalability is a crucial aspect not just to find optimal solutions for complex problems in coexistence deployments but to also determine if such solutions are infeasible [37]. From a cellular-operator perspective, in coexistence networks, challenges of synchronization are also exacerbated and can only be addressed through a distributed approach to large-scale network optimization [23].

2.1.4.1 Need for Time-critical Optimization

A major motivation behind unlicensed coexistence deployments is to offer high QoS and low end-to-end delays to latency-critical services such as mobile AR applications and autonomous vehicles where the maximal tolerable delay might typically be $\leq$ 10ms [46]. Thus, the need for low association times and fast handovers in a dense unlicensed environment makes network optimization **time-critical**. However, consistent densification significantly increases network scale and complexity, which leads to high convergence times and computational overhead to arrive at optimal solutions [31]. Further, the cumulative effect of the new optimization challenges in unlicensed networks highlighted earlier has a far greater consequence in the form of increased latency.

This is a major potential challenge for ultra-low-latency AR applications, as already the current LTE/LTE-A deployments account for almost 30% of the end-to-end AR latency [47]. With densification, the latency problem will exacerbate and diminish the gains in throughput. Thus an important expectation from optimization techniques is low convergence time so that unlicensed networks can seamlessly facilitate latency-critical services to end-users seamlessly [31, 37].

2.1.4.2 Challenges to Time-critical Optimization

Some factors that contribute to high convergence times in unlicensed network optimization are highlighted below.

- Complex theoretical constraints: While using complex theoretical constraints may have worked in conventional/sparse network optimization, they are unsuitable for latency-critical applications. The complex network topology and the requirement of detailed network information in a DN/UDN cause substantial computational overheads in optimization formulations with complex constraints [48, 49].
- Simplistic constraint relaxation: Several network optimization solutions begin with complex theoretical feature relationships and, given their high resource demands, relax these constraints to arrive at simpler, easily solvable constraints [50]. Commonly employed simplification techniques include *constraint relaxation*, *i.e.,* linearizing the resource-intensive theoretical constraint by making context-specific assumptions or considering particular scenarios [50]. For example, simple *interference distribution functions* are assumed to derive computationally less intensive heuristics [51]. However, constraint-linearizations aimed only at *solving* the optimization faster overlook the practical viability of the model.
- Lack of ground-truth input: Usually, the theoretical constraints or constraint relaxation techniques are not motivated by real-world network data. Since unlicensed networks are characteristically different, new data-driven optimization solutions appear to be more suitable.

2.2 Unlicensed Operation: Relevant Aspects

This section discusses the aspects of coexistence in the unlicensed band that are relevant to the experiments and analysis presented in this work. These include the bands and channels on which LAA/NR-U and Wi-Fi operate, the feasibility of bandwidth combinations, channel access mechanisms, and Channel Access Priority Class (CAPC).

2.2.1 The 5 GHz Unlicensed Band

The 5 GHz Unlicensed National Information Infrastructure bands (U-NII bands) range from 5.15 to 5.85 GHz. Recently, a U-NII-4 band with four channels spanning 5.85 GHz–5.925 GHz, has been notified by the Federal Communications Commission through a Notice of Proposed Rulemaking [52]. Thus, a total of eight U-NII ranges have been prescribed by FCC, of which 1 to 4 lie in the 5 GHz range and 5 to 8 are for 6 GHz. LAA coexists with IEEE 802.11a and higher Wi-Fi standards in the 5 GHz spectrum. Each U-NII band is governed by certain guidelines and restrictions with respect to usage and operation. For example, U-NII 1 (5.150–5.250 GHz) is a low-power band that has no restrictions apart from being limited to indoor use with 50 mW of maximum transmission power. U-NII-2 is

assigned mainly to radar systems. Therefore, unlicensed devices communicating in the band have to necessarily implement Dynamic Frequency Selection (DFS), giving priority to the radar signals. As a result, this band is seldom utilized by LAA and Wi-Fi. Therefore, although a substantial block of 560 MHz of the spectrum seems available, a much smaller fraction of about 160 MHz belonging to U-NII-1 and U-NII-3 bands is fully harnessed. It is noteworthy that Wi-Fi channels are 20/40/80 MHz wide, while 3GPP has specified 20 Mhz channels for LAA, with the possibility of aggregating up to 3 LAA channels.

Table 2.1: Channel Access Priority Class in LAA Downlink

DL CAPC	**Initial CCA**	**CWmin**	**CWmax**	**TXOP**	**QCI**
1 (Voice)	25 μs	30 μs	70 μs	2 ms	1, 3, 5, 65, 66, 69, 70
2 (Video)	25 μs	70 μs	150 μs	3 ms	2, 7
3 (Best Effort)	43 μs	150 μs	630 μs	8 ms, 10 ms	4, 6, 8, 9
4 (Background)	79 μs	150 μs	10.23 ms	8 ms, 10 ms	–

2.2.2 Channel Access Priority Classes

An operator uses Channel Access Priority Classes (CAPCs) for specific types of traffic when UEs transmit data on the uplink (UL) and downlink (DL) over an LAA carrier. Four CAPCs are specified for LAA in 3GPP Release 15 [53]. Table 2.1 presents the details of the LAA DL CAPC classes along with specific values for each class for parameters *viz.,* QoS Class Identifier (QCI), Clear Channel Assessment (CCA) duration, maximum and minimum contention windows (CW_{Max}, CW_{Min}), and Transmission Opportunity (TXOP) duration. A data traffic category is assigned a specific TXOP duration based on its CAPC. For example, video and voice data have TXOPs of 3 ms and 2 ms, respectively, to meet end-user QoS guarantees. Given the low latency requirements of these data flows, small data packets are used. In contrast, for traffic categories such as data download in the background and best effort, LAA employs large packets to optimize network throughput with a maximum TXOP of 8 ms. To meet QoS guarantees, 3GPP prescribes that operators use CAPCs according to the standardized QCI to which the data traffic belongs. However, operators are free to employ non-standardized QCIs so long as a suitable CAPC is used for data traffic. In uplink transmission, LAA eNB determines the CAPC of the traffic by considering the QCI with the least priority in a Logical Channel Group.

Similarly to LAA, Wi-Fi classifies traffic into Access Categories (ACs) depending on the type of traffic and priority. Wi-Fi (802.11ac) ACs for various types of traffic *viz.,* video, voice, background data, and best-effort data, with the corresponding values for parameters *viz.,* Arbitration Inter-frame Spacing (AIFS), CW_{Max}, CW_{Min}, and TXOP are presented in Table 2.2.

Table 2.2: Access Categories in 802.11ac

Access Category	**AIFS**	**CWmin**	**CWmax**	**TXOP**
Voice (AC_VO)	18 μs	27 μs	63 μs	2.08 ms
Video (AC_VI)	18 μs	62 μs	135 μs	4.096 ms
Best Effort (AC_BE)	27 μs	135 μs	9.207 ms	2.528 ms
Background (AC_BK)	63 μs	135 μs	9.207 ms	2.528 ms

2.2.3 Channel Access Mechanisms

LTE-LAA employs a Listen-Before-Talk (LBT) mechanism to access the unlicensed channel. The mechanism resembles the Carrier-sense Multiple Access with Collision Avoidance (CSMA/CD) MAC protocol of Wi-Fi. LBT facilitates a better coexistence of LAA with Wi-Fi than LTE-Unlicensed (LTE-U), which has a duty-cycle mechanism [54]. LAA eNB and UEs sense the channel prior to transmitting on the LAA SCell. The LAA eNB/UE LAA will defer for an initial CCA duration, depending on the CAPC of the traffic. Subsequently, LBT triggers a random back-off period in the range of (0, CW_{size}), where CW_{size} is assigned a value between CW_{Min} and CW_{Max} according to channel conditions. If the back-off is successful, the LAA eNB/UE starts transmitting.

Wi-Fi makes use of the CSMA/CD mechanism, which ensures that an AP/device transmits only when the channel is idle, and the station has not finished a successful transmission immediately prior to sensing the channel. The device waits for an initial sensing period of Distributed Coordination Function Inter-frame Space (DIFS) for IEEE 802.11n and below or AIFS for amendment 11ac and above. If the Wi-Fi node is contending for access immediately after successful transmission, it continues to sense the channel for an initial length of DIFS/AIFS, until the channel is idle again. If the channel is detected to be busy, a random back-off period in the range of (0, CW_{size}) is selected.

LAA's LBT is compatible with CSMA/CD of Wi-Fi, which reduces collisions during transmissions and leads to fair coexistence and enhanced network performance [55]. Furthermore, Wi-Fi has an energy threshold of -62 dBm and a preamble detection threshold of -82 dBm. Since the LAA LBT has an energy threshold of -72 dBm, its vulnerability to interference from Wi-Fi APs is reduced, which also facilitates fewer fluctuations in signal strength at the LAA UE. Finally, upon getting access to the channel, an LAA eNB/UE can transmit data for a TXOP length of up to 10 ms if it has prior information that a Wi-Fi device does not coexist in the unlicensed band. However, onsite measurements reveal that for most types of traffic (e.g., data, data plus video/streaming, etc.) LAA LBT generally allows for a maximum TXOP of 8 ms to the UE for transmission.

2.3 Cell Selection: Mechanisms and Challenges

2.3.1 Cell Selection Procedure in LTE

The high-level cell search, camping, and selection mechanisms are well laid out in the LTE specifications, leaving the finer details of intelligent implementation to the cellular service providers. The cell selection mechanisms may vary across operators and across different LTE flavors, especially LTE-LAA coexistence deployments, owing to the paradigm-specific considerations. This section presents an overview of the cell selection mechanism prescribed in LTE.

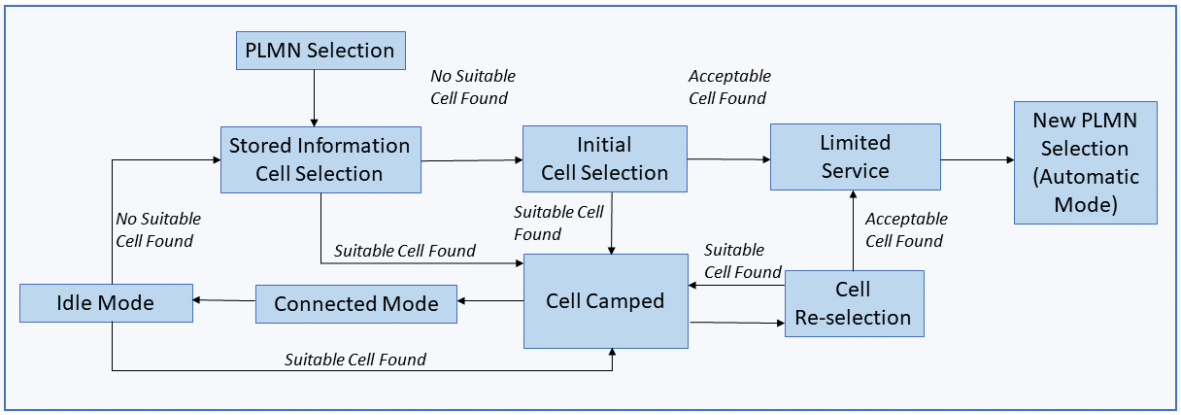

Figure 2.2: High-level Cell Selection Procedure in LTE

A high-level LTE cell selection mechanism is illustrated in Figure 2.2, and it involves the following main steps.

2.3.1.1 Cell Search

A UE needs to learn the PCI of a cell, the information pertaining to the signal quality, and establish timing and frequency synchronization with a small cell. This requires scanning available frequencies for signals from one or more cells in proximity. The LTE synchronization process is two-fold, involving a primary slot synchronization (PSS) (5ms periodicity) and a secondary synchronization signal (SSS) which helps achieve the frame synchronization. Together, PSS and SSS pass on the PCI information to the UE, which then gathers the cell's signal quality and associated details by monitoring the reference signals and the broadcast channel, respectively.

2.3.1.2 Cell Selection

There are two primary cell selection mechanisms. First is the *initial cell selection*, where the UE does not need to be aware of the active E-UTRA RF channels and may scan the supported E-UTRAN bands for available carrier frequencies. A UE will select the *suitable Cell i.e.,* the cell with the strongest signal/carrier to camp on. If no suitable cell is available, the UE will pick an *acceptable Cell* to camp

on. The second is the *stored information cell selection*, where the cell selection decision of the UE is guided by cell quality and carrier channel information stored from earlier cell measurements. In case a Suitable Cell is not available for camping, the UE initiates the first procedure. This is a fast and efficient procedure, and vendors (*e.g.,* Ericcson) seem to employ this mechanism in combination with learning and prediction systems for optimal cell selection [22].

2.3.1.3 Cell Re-selection

UE continues to monitor the network information and signal-quality parameters of the cell it is latched on to and also of the neighboring cells. Based on certain measurable criteria and the priority of carrier frequencies, it may choose to perform cell re-selection and camp on the most suitable cell available.

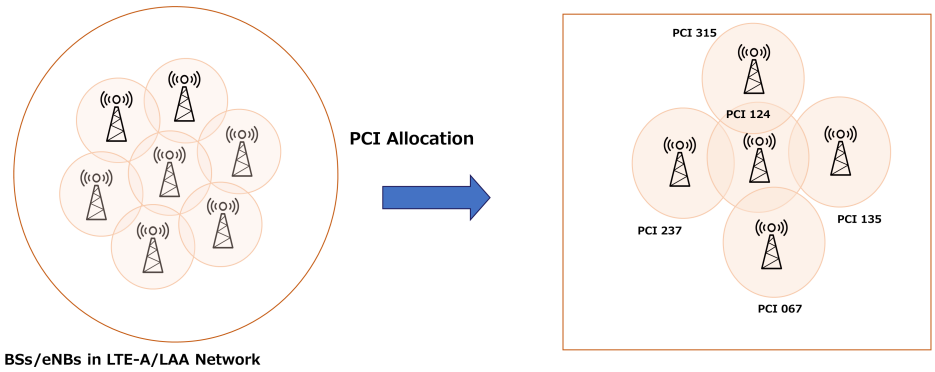

Figure 2.3: Role of PCI in Cell Selection

2.3.2 Role of PCI in Cell Selection

With the adoption and proliferation of new cellular standards, a wide variety of base stations, from Macro cells to low-power Femtocells, are being deployed. The consequent increase in network complexity presents new challenges in the planning, management, and maintenance of cellular networks. The efficient operation of cellular networks, especially LAA/5G-NRU deployments, requires reliable mechanisms for network configuration and reconfiguration with minimal human intervention. This served as motivation for the paradigm of Self-Organizing Networks (SON), where seamless and uninterrupted service is provided to the end-user through small cells capable of self-configuration [18].

The first and most important step in a cellular SON is *cell identification*, without which optimal cell selection and handover to user equipment (UE) are not possible. At the physical layer, the identification of a cell/eNB is done with the help of Physical Cell Id (PCI) in LTE-A/LTE-LAA and 5G NR-U. PCI allocated to a cell/eNB (Figure 2.3) is used to discover and identify the cell/eNB when a cellular device initiates the association process or during a handover, [56]. The high-level cell selection process in LTE, LTE-A, and LTE-LAA is presented in Figure 2.2. In these cellular standards, the PCI of a cell

is generated using the Primary Synchronization Signal (PSS) and the Secondary Synchronization Signal (SSS), using the expression ($PCI = 3 \times SSS + PSS$), where $PSS \in \{0, 1, 2\}$, and $SSS \in \{0, \ldots, 167\}$. Therefore, a typical PCI in LTE-LAA is always in the range of [0,503]. While PCIs in 5G NR/NR-U are generated in a similar fashion, 1008 unique PCIs are available, as $SSS \in \{0, \ldots, 335\}$.

2.3.3 Challenges to Cell Selection in LTE HetNets

The popular approaches to cell search, selection, and camping are Reference Signal Received Power (RSRP) based cell selection, Cell Range Extension (CRE) using SINR, and adaptive cell selection employing techniques such as Q Learning [17, 56]. Nevertheless, several challenges arise during cell association in LTE HetNets [18, 22].

First, the transmission power, signal quality, and SINR-based solutions are simple to implement but inefficient in LTE-A HetNets and LAA coexistence networks. While some dense small cell configurations may ensure that devices receive equal or comparable power levels from all cells, there is an inherent transmit power asymmetry in HetNet deployments. This problem is likely to get worse in LAA deployments. Second, interference experienced by mobile UEs on the periphery of small cells from macro base stations also degrades network performance [56]. Further, the ambient channel conditions and resource allocation asymmetry during handovers pose additional challenges to cell selection for optimal network performance [22]. Adaptive cell selection algorithms such as Q-Learning-based CRE offer a more informed cell selection process but tend to be computationally expensive [17].

More practical solutions to cell selection and handover in LTE HetNets have been implemented by major industry players such as Ericcson [22, 57]. Cellular operators and third-party vendors have greater infrastructural resources to propose proprietary and patented solutions from a radio resource management standpoint. At a high level, these solutions rely on evaluating each cell on specific attributes and assigning it a *cell-quality metric* generated after a phase of real-time network-data learning. The metric helps make temporal predictions about the small cell's ability to meet QoS guarantees and is shared with the mobile UE to make an informed decision during cell selection [22,57].

This section briefly discusses the PCI allocation process and the challenges in unlicensed cell selection, followed by the unique PCI scenarios observed in LAA deployments.

2.4 New Cell Selection Challenges in the Unlicensed Bands

The traditional LTE/LTE-A cell selection process is generally dependent on parameters such as RSRP, RSRQ, SINR, and transmission power received at the UE. Although there is ample research to suggest that parameters associated with traffic QoS (e.g., Guaranteed Bit Rate), traffic load, and power/energy consumption at the UE ought to be considered, operators prefer practical cell selection and handover mechanisms that are SINR driven [58]. The simple approach works for cellular operators *viz.,* AT&T, T-Mobile, and Sprint as LTE/LTE-A HetNets do not suffer the adverse impact of interference from

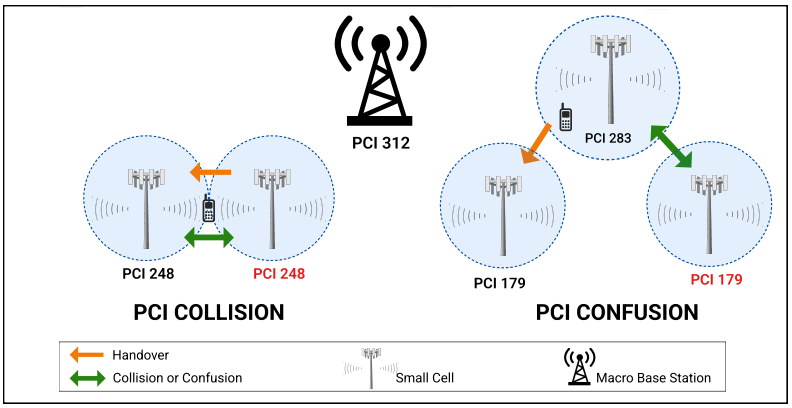

(a) Challenges in PCI allocation

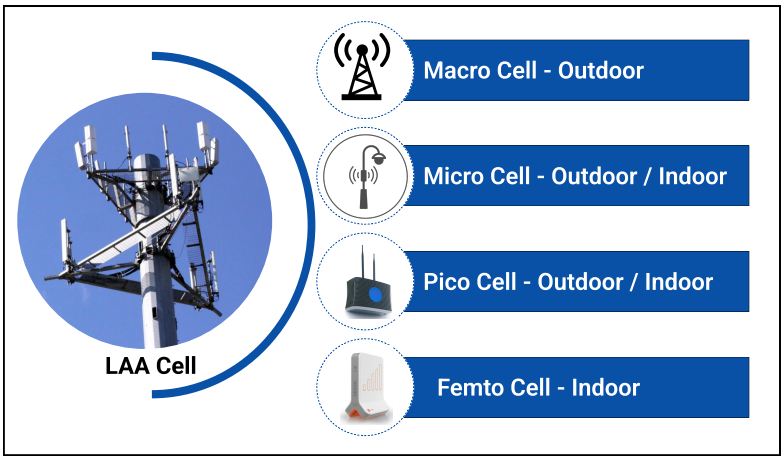

(b) Greater Competition for Limited PCIs

Figure 2.4: PCI Allocation and Challenges

external sources [59]. LTE/LTE-A networks operate in dedicated bands of the Licensed spectrum that are exclusive to specific cellular operators. Further, the co-tier and cross-tier interference experienced within the network is usually mitigated and managed through centralized and distributed resource allocation solutions [60].

In sharp contrast, unlicensed cellular networks have to contend with transmission conflicts from coexisting Wi-Fi APs on the same channel, which can drastically degrade the SINR. Furthermore, interference from rogue mobile hotspots and other sources, hidden node problems, and dense Wi-Fi (802.11n/ac/ax) network deployments adversely affect SINR in an unlicensed coexistence system such as LAA. This is particularly true in dense scenarios, where radio resources may not always be allocated to LAA. SINR-based cell selection is also less suitable in LAA due to interference from external Wi-Fi

transmissions, which typically causes fluctuation in SINR received at the LAA UE. As a result, cell selection and handover decisions made at the UE trigger frequent disconnections and re-attachments, degrading LAA performance. Thus, for efficient cell selection and radio resource allocation in LAA, additional information about the small cell is necessary to determine cell quality [8, 22].

Case in point, when LTE and LAA share a PCI, it implies that they share the same LTE backhaul, i.e., LTE Evolved Packet Core (EPC) with MME, P-GW, S-GW, HLR, etc., which ensures efficient splitting of resources. Additional signaling is required at the LAA secondary cell (Scell) for the UE to recognize that the component carrier belongs to the same LAA provider as the primary cell (Pcell), which in turn provides the Licensed carrier to the UE. In the Licensed band, PCI is sufficient for cell identification since multiple operators share a carrier only if the operators: (a) provide coverage to spatially/geographically separated areas, or, (b) share the network. Despite these provisions, two major PCI-related problems are encountered, which are illustrated in Figure 2.4(a) and briefly described below:

(1) PCI collision: Neighboring cells are assigned identical PCI, which poses a challenge during UE attachment and handovers.

(2) PCI confusion: Two different small cells within the same macro Base Station (BS) are assigned identical PCI, which poses a challenge, especially during handovers.

Since LTE-A/LAA has only 504 unique PCI values, strategic reuse and network planning provide reliable identification of cells/eNBs. However, with increasing network density and low-power cell deployment, as shown in Figure 2.4(b), an LAA cell has to compete with other small cells and macro cells for a limited number of PCIs, leading to a higher frequency of PCI collisions and PCI confusions [18]. An important reason is that cells/eNBs of different operators belonging to different Public Land Mobile Networks (PLMNN) may assign the same PCI to their respective eNBs [53, 61]. These challenges were adequately addressed in LTE/LTE-A networks through smart PCI allocation using mechanisms such as graph coloring, clustering, and network-initiated SI reading since operators controlled the Licensed bands allocated to them [18, 62]. However, the solutions prescribed for the unlicensed band, *viz.,* increasing the range of PCIs, broadcasting partly unique cell identities, and inter-operator coordination are difficult to implement in a shared spectrum [61]. Furthermore, the complexity of these challenges will increase as cellular operators and enterprise network providers deploy more Citizens Broadband Radio Service (CBRS) small cells operating on the LTE protocol stack [63]. The upcoming small cell deployments in the C-band spectrum are also likely to intensify the contention in PCI ID allocation.

Finally, 3GPP release 15 may also prescribe additional specifications for LAA processes [53]. For example, an LAA handover process entails the following specific steps. First, the eNB/small cell configures the UE with one Discovery Signal Measurement Timing Configuration window on one frequency for the serving cell and for each available neighboring cell. Second, the UE utilizes the allocated window to identify and measure Discovery Reference Signals from the neighboring cells.

Further, to overcome the challenges of hidden nodes (unlike LTE/LTE-A), the UE may measure the Received Signal Strength Indicator (RSSI) during an RSSI measurement timing configuration window and share the average RSSI and channel occupancy with the serving cell in the next reporting interval [53].

Solutions to the problems anticipated in LAA networks have been prescribed in 3GPP release 15, in 3GPP minutes of meetings, and in recent research work [53, 61, 64]. Prior to the proliferation of public LAA deployments, the analysis and solutions for LAA were validated primarily through theoretical modeling, simulations, and experimental testbeds [65–68]. After several cellular operators began offering LAA services globally, some studies have sought to conduct performance analysis of these networks through on-site measurements [8, 64, 69].

However, the new phenomenon observed in unlicensed deployments, which is presented in Chapter 5, is not yet identified, nor has its impact been analyzed using ML modeling and operator data analysis.

Chapter 3

Data-driven Analysis and Optimization of Unlicensed Networks

3.1 Introduction

There has been a consistent increase in latency-critical data traffic from services such as augmented reality (AR) and on-the-go video streaming [70]. The inability of existing LTE/LTE-A (Long Term Evolution/Long Term Evolution-Advanced) networks to meet the Quality of Service (QoS) requirements for uplink-heavy and bursty flows of AR applications deny the end-user a seamless experience [47].

To address these challenges cellular operators have taken recourse to harness the potential of the unlicensed spectrum through the operation of LTE in the 5GHz band in coexistence with Wi-Fi. Two unlicensed cellular standards were put forward, *viz., LTE in unlicensed spectrum* (LTE-U) and *LTE license assisted access* (LTE-LAA). The adoption of these standards has led to rapid deployment of LAA/LTE-U small cells in the 5GHz band where 500 MHz has been allocated for unlicensed LTE operation in coexistence with Wi-Fi access points (APs) [8, 26, 71]. Buoyed by this development, Federal Communications Commission (FCC) of the USA has decided to deregulate 1200 MHz for 5G NR-U (New Radio-Unlicensed) and Wi-Fi coexistence in the 6 GHz band as well [52].

However, in the unlicensed band, cellular operators have to coexist with existing incumbents such as Wi-Fi, radar operation, fixed satellite transmission links, and Broadcast Auxiliary Services (BAS) [71]. This increases the probability of transmission conflicts making the environment highly dynamic. Thus, new techniques and frameworks are needed to analyze unlicensed network performance.

3.1.1 Need for New Data-driven Solutions

The current approach to network performance analysis is measurement-based, i.e., it is dependent on the values of significant network variables observed in simulations and experiments. Let us consider

the prolonged LTE-U vs LAA debate [68, 72], which has essentially relied on the measurement-based analysis. Despite a significant body of work dedicated to the comparative analysis of the two standards, no definitive conclusion can be drawn. However, by 2021 38 operators in 21 countries were investing in LAA, while LTE-U deployments were commercially available in only 3 countries [4]. This definitely indicated an industry preference for LAA over LTE-U. Thus, new data-driven methodologies are needed, that can analyze network data through machine learning and offer deeper insights into network performance. As discussed in Chapter 2, feature relationships between network variables can provide a better understanding of the ambient network environment.

Secondly, the dense deployment of LTE/LTE-A, LAA, and 5G small cells magnify the scale and complexity of cellular networks. This leads to increased computational costs and longer convergence times to arrive at optimal solutions [31]. From the perspective of ultra-low-latency augmented reality (AR) applications and high-speed vehicular networks, this is extremely undesirable. A typical LTE/LTE-A network already contributes about 30% to the end-to-end latency in mobile AR [47]. Network densification will exacerbate the latency problem and undo the enhancement in network throughput achieved through the utilization of unlicensed spectrum. Thus, an important expectation from optimization techniques is low convergence times so that dense unlicensed networks can facilitate latency-critical services to end-users seamlessly [37].

Conventional optimization techniques have been at the core of cellular network operations. However, a data-driven optimization approach is more suitable for unlicensed band optimization [65]. This is due to the extremely dynamic network environment and additional requirements of harmonious coexistence and fair spectrum sharing in the unlicensed spectrum. More importantly, the solutions are needed in real-time and must support latency-critical services. Thus, new data-driven solutions are needed to meet these requirements. Data-driven optimization is a hybrid approach that combines the power of machine learning and traditional optimization to better support applications such as mobile AR and autonomous vehicles that need low end-to-end delays (typically $\leq$ 10ms).

Despite its suitability for unlicensed bands, machine-learning-based optimization is context-specific and application dependent. Applications such as mobile AR and autonomous vehicles need low association times and fast handovers. These constraints make optimizing performance and resource-allocation **time-critical** for these applications. This chapter refers to it as the "Speed" of the network optimization model. On the other hand, some applications and services such as VR-enabled telesurgery are resource intensive and require the highest-priority QoS Class Identifier for satisfactory end-user QoS [73]. To ensure maximal resource allocation, data-driven time-critical optimization solutions must be close to the theoretically optimal solutions. This nearness to optimal solutions is referred to as the "Accuracy" of the model.

Thus, apart from reducing convergence times for time-critical services new data-driven optimization solutions must address the challenge of Accuracy-Speed trade-off. Doing so requires intelligent selection of network feature relationships (NFR) learned from the network data to be used as constraints in the

optimization model. Typically, multiple feature relationships with varying polynomial degrees can be learned using machine learning algorithms. Thus, selecting a suitable NFR is a non-trivial problem.

Finally, network context must also be considered in the data-driven optimization solution. Context typically comprises the network configuration, ambient network environment, application's priority for Accuracy or Speed, the goal of optimization, the degree of learned feature relationships, etc [7, 74, 75]. For example, only signaling data and user-plus-signaling data would create two different network contexts. Moreover, since network context is extremely dynamic, the context-aware solution should be validated through an appropriate methodology.

To that end, this chapter explores a context-aware data-driven approach to unlicensed network analysis and optimization. Network performance analysis is performed through supervised machine learning algorithms to compare LTE-U and LTE-LAA networks. Further, learned Network Feature Relationships (NFRs) are used to accelerate network optimization while ensuring high accuracy vis-a-vis baseline optimization models. NFRs are also a suitable indicator of network context. Hence a context-aware approach is proposed that examines the performance of higher-order feature relationship models. It analyzes the trade-off involved in using higher-order NFRs with high R-sq in data-driven optimization.

3.1.2 Contributions

The specific contributions of this chapter are listed below.

- Experiments were conducted for multiple dense LTE-WiFi coexistence combinations and bandwidth variations on an experimental testbed.
- Comparative analysis of LTE-U and LAA networks was performed through feature relationship analysis (e.g., SINR-Capacity relationship) using machine learning (ML) algorithms.
- Demonstrated the importance of network context through differences in ML model parameters such as R-sq, residual error (RSD), outliers, etc.
- Utilized network feature relationships (NFR) to optimize performance through four state-of-the-art network capacity and signal strength optimization formulations.
- Analyzed Accuracy-Speed trade-off in using higher-order NFRs in optimization models for different coexistence configurations.
- Validated context-aware data-driven optimization through decision matrix analysis.

3.2 A Review of Related Works

A brief overview of research literature relevant to the analysis and solutions proposed in this chapter is presented below.

For wireless network performance analysis and modeling, understanding the interplay between various network parameters is crucial. The network context is also governed by network metrics such as throughput, signal plus interference, and noise ratio (SINR), resource block allocation, modulation coding scheme, etc. [74, 75]. Conventionally, the relationships between network parameters were determined through abstract theoretical models. For example, capacity interference relationship (CIR) analysis and modeling have been the focus of numerous works [24, 33–35]. Theoretical solutions invariably require additional prior network-related information e.g., the network layout, location of the nodes, etc. Further, due to the complexity of the problem (e.g., determining CIR is NP-hard), often assumptions are made about wireless network parameters such as the expected traffic load or expected mobility patterns of nodes in dynamic scenarios [24, 35]. However, network context is highly spatio-temporal and can be adequately represented only through machine learning models trained on network data.

Thus, a better approach to learning network context is by learning relationships between network variables through data analysis. Machine learning techniques such as regression algorithms, decision trees, and random forests can be used to learn Network Feature Relationships (NFRs) [8–13, 76]. NFR analysis unlocks deeper insights into various dimensions of network context such as the strength of the relationship between network variables (R-sq, accuracy, etc.), precision in the predictions of the response variable (residual error), presence of significant fluctuation in parameter values (Outliers), etc. In addition, NFR analysis can also reveal associations between network parameters such as dependence, correlation, causation, *etc.*. This approach is empirical and data-driven, as compared to the abstract theoretical solutions discussed in Chapter 2. Training models on network data also does away with the need for assumptions, approximations, and prior network information typically required in theoretical models [34, 36]. Further, the algorithms used in learning NFRs are not only reliable but also computationally less expensive, compared to both conventional solutions and more advanced machine learning techniques such as deep learning. This has encouraged the application of NFR analysis to analyze performance and learn context even in large-scale networks [11, 12].

The utility of feature relationship analysis in the unlicensed spectrum can be demonstrated through a data-driven evaluation of the unlicensed LTE standards, viz., LAA & LTE-U. The existing research literature on the comparative performance of the two standards is characterized by three features. First, the experiments are primarily conducted through simulations and often make assumptions or relaxations [67,68]. Second, the comparative analysis and the conclusions drawn rely on *measurements*, *i.e.,* through the comparison of important network parameters such as network capacity, signal plus interference, and noise ratio (SINR), resource block (RB) allocation, modulation coding scheme (MCS), latency, number of re-transmissions, *etc.* [68,72] Third, there is a limited focus on learning the network context. For example, the variation in performance of the LTE unlicensed standard with the variation in coexisting Wi-Fi standards is rarely studied. Likewise, network context is influenced by factors such as bandwidth allocation and signaling data. While measurement-based studies are a great first step

in network performance evaluation, learning and utilizing network context is highly desirable for the optimal performance of dense unlicensed networks [74,75]. Thus *feature relationship analysis* facilitates a deeper understanding of network performance and network context through machine learning models trained on network data.

Another major challenge is unlicensed network optimization. Due to the dense deployment of small cells and APs, and the presence of multiple coexisting incumbents, the unlicensed band is extremely complex and dynamic. For example, although densification may lead to an initial gain in system capacity, it has been shown that unlicensed network performance eventually deteriorates with an increase in density [25].

Typically, problems pertaining to network management *viz.,* dynamic allocation of resources, energy efficiency, interference management, efficient spectrum sharing *etc.*, are solved through optimization [23, 37, 38]. Although efficient solutions to many of these problems are available for licensed networks, they assume new dimensions in dense unlicensed networks. With increased spatial co-location of small cells and APs in coexistence deployments, the complexity of formulations, and consequently, the convergence time of optimal solutions increases significantly [48]. Due to the complex network topology, detailed network information is required for dense network optimization [31, 45]. The cumulative impact of these factors results in NP-hard mixed integer non-linear formulations [37], which lead to higher computational overheads and increased convergence times.

To overcome these challenges and reduce convergence times in dense network optimization, some measures can be taken. First, instead of complex theoretical constraints, constraints rooted in ground truth that are learned from network data should be considered. Second, simplistic constraint relaxation techniques should be avoided. For example, *i.e.,* linearizing the complex theoretical constraints by making context-specific assumptions or by considering specific scenarios [50].

Several recent studies have used machine learning to optimize vital network metrics, e.g., rate adaptation [9], link adaptation [12], and network throughput [10]. In particular, the learned feature relationships can be utilized to improve network performance. For example, learning 802.11n feature relationships can facilitate improved configuration selection and enhanced rate adaptation [9]. Likewise, they can be used to design link adaptation algorithms and improve network throughput [10, 12]. Thus data-driven optimization seems to be a better solution for unlicensed networks.

Utilizing network feature relationships as in optimization However, the impact of the degree of feature relationship equations on the optimization goals and performance is not studied. In [65], we show that strong NFRs are characterized by high R-sq, low fluctuations in R-sq, and low mean squared error. These NFRs lead to high Accuracy, i.e., nearness to baseline optimal formulations. But the solution is restricted to only second-order polynomial NFRs and the Accuracy-Speed trade-off involved in higher-order NFRs is not investigated. Further, a methodology for mitigating this trade-off based on the network context and the use case (application/service) is not explored either.

This chapter addresses these challenges. It focuses on the relationship between interference and net-

work throughput or the Capacity-Interference relationship (CIR), as interference is a serious bottleneck to network performance management.

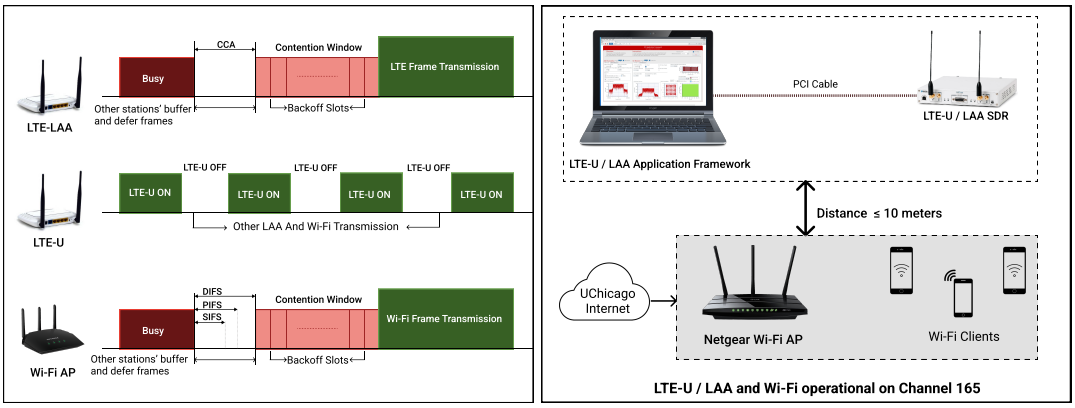

(a) Channel Access Mechanisms

(b) Representative Testbed

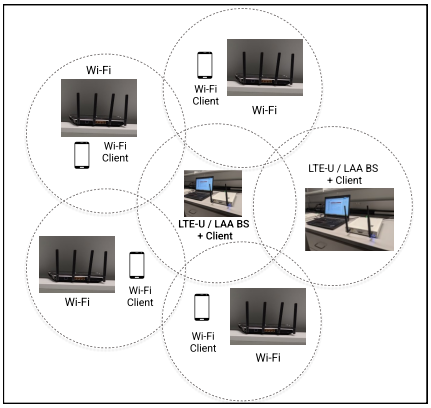

(c) Representative Topology

Figure 3.1: Testbed Design

3.3 Feature Relationship Analysis Methodology

This chapter seeks to leverage network feature relationships to analyze network context and optimize network performance. To that end, this section contains a discussion on LTE-WiFi experimental textbeds (LTE-U and LTE-LAA), the ML algorithms considered for feature relationship analysis, and the test scenarios considered in the comparative context analysis of LTE-U and LAA.

3.3.1 Network Design Considerations

For efficient utilization of the unlicensed band, LTE and Wi-Fi coexistence must be fair and cooperative. To achieve fair coexistence between the two radio access technologies, two standards for unlicensed LTE

were released, viz., LTE-U and LTE-LAA. However, the two standards employ different mechanisms for medium sensing and access, illustrated in Figure 3.1(a). While LTE-U has a load-dependent duty-cycle mechanism, LTE-LAA relies on a Listen-Before-Talk (LBT) mechanism. LAA's LBT is compatible with the CSMA/CD MAC protocol of Wi-Fi, ensuring a more fair coexistence with 802.11 WLANs compared to LTE-U.

Testbed Design LAA/LTE-U testbed are created using the National Instruments *NI RIO* platform, shown in Figure 3.1(b). The NI Labview system provides 3GPP prescribed PHY implementation and supports flexible configuration of system parameters such as transmission power, LAA transmission opportunity (TXOP), LTE-U duty cycle ON & OFF, etc. The Wi-Fi platform comprises of Netgear wireless routers which support both 802.11n and 802.11ac in the 5 GHz band. The Wi-Fi testbed allows easy configuration of MAC and PHY layers parameters such as channel bandwidth, transmission power, CW_{min}, CW_{max}, etc. Relevant technical specifications related to the testbed are presented in Table 3.1.

The experiments were performed in an indoor setting at the University of Chicago. Multiple coexistence configurations were implemented through combinations of LAA-LTE/LTE-U, 802.11n/802.11ac, and varying bandwidths (5, 10, 15, & 20MHz) to account for cross-talk interference. The interference from LAA was kept below Wi-Fi's clear channel assessment (CCA) threshold by regulating LAA's power spectral density (PSD). Further, as shown in Figure 3.1(c), random dense coexistence networks were created by maintaining an internodal distance $\leq 10m$ between nodes in the testbed. SINR and Capacity data was gathered through the experiments. It is noteworthy that apart from the dense scenario, multipath fading due to obstacles such as walls and furniture, makes this experimental setup suitable for studying CIR in coexistence networks.

Table 3.1: Experiment Parameters.

Parameter	**Value**
Number of nodes	6
Transmission Power	23 dBm
Operating Frequency	5 GHz
LTE-U/LAA RF Transmission	Loopback
LTE Transmission Channel	PDSCH, PDCCH
Data Traffic	Full buffer
WiFi Channel Access Protocol	CSMA
LAA Channel Access Protocol	LBT

*PDSCH - Physical Downlink Shared Channel

3.3.2 Machine Learning Algorithms for Relationship Analysis

Next, the feature relationships in the LTE-WiFi coexistence data gathered from the experimental testbed are modeled as a regression problem.

Let N represent the number of training points and let dimensionality of the feature vector be denoted by D. Then, the unlicensed network data can be represented as $\{\mathbf{x}_i, y_i\}_{i=1}^{N}$, where $\mathbf{x}_i \in \mathbb{R}^D$ is the feature vector and $y_i \in \mathbb{R}$ is the ground truth value for i^{th} training point. The goal is to learn a mapping $f : \mathbf{x}_i \rightarrow y_i$ where x_i is the predictor (SINR or Capacity) and y_i is the response (Capacity or SINR).

3.3.2.1 Machine Learning Algorithms

This chapter considers the following basket of learning algorithms for the regression analysis:

Linear Regression: This group of algorithms learns a linear relationship by solving $\arg\min_{\mathbf{w},b} \sum_{i=1}^{N} ||(\mathbf{w}^\top \mathbf{x}_i + b) - y_i||_2^2 + \alpha \mathbf{w}^\top \mathbf{w}$ [77]. Here, the weight vector is denoted by $\mathbf{w} \in \mathbb{R}^D$ and the bias term is $b \in \mathbb{R}$. Further, the weightage (importance) of the l_2-regularization term is controlled by the hyperparameter denoted by α, which is set to zero for Ordinary Least Squares Linear Regression (OLS). However, for Ridge Regression (RR), α is set through k-fold cross validation (kCV).

Kernel Ridge Regression: A non-linear mapping is expected to be more suitable for the SINR-Capacity relationship, especially with respect to optimization [36]. Therefore, we use Kernel Ridge Regression [77] that employs non-linear transformations such as polynomial and radial basis function (RBF). Its goal is to solve $\arg\min_{\mathbf{w},b} \sum_{i=1}^{N} ||K(\mathbf{w}, \mathbf{x}_i) + b - y_i||_2^2 + \alpha \mathbf{w}^\top \mathbf{w}$. Here, $\mathbf{w} \in \mathbb{R}^D$ is the weight vector, $b \in \mathbb{R}$ is the bias term, and α is a hyperparameter defined above. It should be reiterated that α is the weightage of the regularization term that can help us avoid overfitting and lead to better performance on test data, especially in case of non-linear kernels. The experiments are performed for both radial basis function (RBF) and polynomial kernel (MPR).

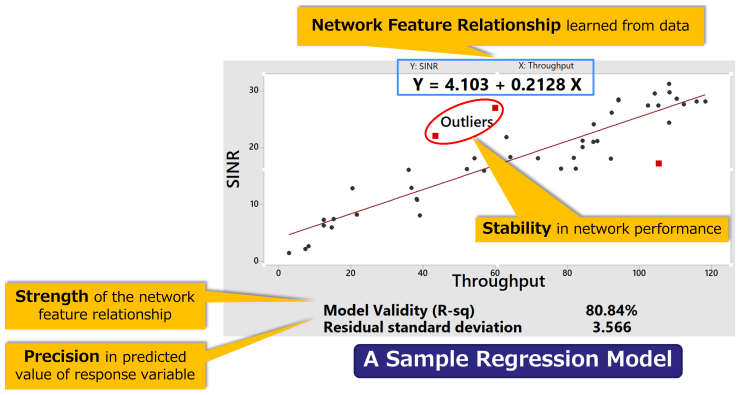

Figure 3.2: Analysis through Network Feature Relationships

3.3.2.2 Illustration of Network Feature Relationship Analysis

Figure 3.2 demonstrates how feature relationship analysis can be used to analyze network performance. A regression model learned on network data has certain important metrics such as R-sq, outliers, residual standard deviation or root mean error and a feature relationship equation. Each of these metrics offers an insight into the relationship between the network features considered in the model. R-sq conveys the strength of the relationship, i.e., with how much confidence can the variation in response variable be explained by the set of predictor features? Higher the R-sq, the stronger the network model, and the better the network performance. Likewise, % of outliers demonstrates the stability of the network in terms of fluctuation in the response variable (e.g., Throughput). More importantly, the feature relationship equation learned from network data is a reflection of the ambient network environment and can be utilized in network optimization. Thus, a strong, stable, and precise network model will imply better network performance.

3.3.3 Test Scenarios and Model Selection

Experiments were performed and data was recorded for CIR analysis for 40 Test Scenarios, represented as TS_i, where $i \in \{1 \dots 40\}$. A TS_i denotes a unique unlicensed coexistence configuration which is a combination of the unlicensed LTE standard (LTE-U/LTE-LAA), the Wi-Fi variant (802.11n/ac), bandwidth allocation (5, 10, 15, &20 MHz), and the response variable (SINR/Capacity). Eight new test scenarios (TS_i where $i \in \{33 \dots 40\}$) are considered, which involve experiments only for control and signaling data transmission in LTE-U and LAA, 802.11n/ac, for the 20 MHz band. These scenarios are compared with the respective control-plus-data transmission test scenarios. Further, the CIR selection for each TS_i is carried out through the following ML model selection scheme. Feature relationships that are 1–3 degree polynomials are learned and validated through k-fold cross validation (kCV). Further, higher-order terms are ensured to be statistically significant to avoid overfitting. To remove outliers, the local outlier factor (LOF) algorithm is used, which is an unsupervised technique that determines the deviation in the density of a sample with respect to its k neighbors.

Using this methodology, the context and performance of LAA & LTE-U networks is studied and a comparative analysis is presented in the next section.

3.4 Relevance of Context in Unlicensed Coexistence Networks

To delineate the network context, the parameters of the CIR model are observed and a comparative analysis of LTE-U & LAA is performed. The results are presented for scenario-specific comparisons in Figure 3.3, and configuration-level trends in Figure 3.4. Please note that only for Figure 3.4(b), a logarithmic scale is used to show "% Difference" due to a high variation in values. Relevant aspects that shape unlicensed coexistence network context, such as outliers, are also discussed.

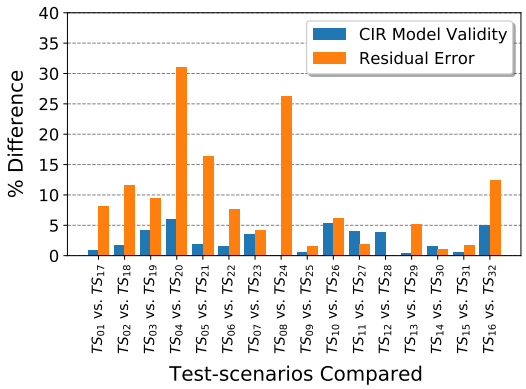

(a) LTE-LAA vs. LTE-U

Figure 3.3: Test Scenario Specific Comparative Analysis

3.4.1 Unlicensed Coexistence: LTE-U vs LAA

We begin with measurement-based observations on average network capacity, as most comparative studies focus primarily on this metric [68]. In 75% of the test scenarios, LTE-LAA outperforms LTE-U in coexistence with the corresponding Wi-Fi variant (n/ac). Likewise, in 87.5% scenarios, 802.11ac outperforms 802.11n in coexistence with the corresponding LTE variant (LTE-U/LAA). Further, LTE-LAA in coexistence with 802.11n/ac offers a higher SINR on average than LTE-U in all scenarios save one.

The LBT mechanism of LAA is quite similar to the CSMA channel access protocol of Wi-Fi and leads to a higher network capacity on average in LTE-LAA. LAA nodes sense the energy level on the medium (-72 dBm) prior to transmission, which mitigates co-channel interference from Wi-Fi and other LAA APs, ensuring higher SINR on average than LTE-U. On the contrary, LTE-U has a duty-cycle-based channel access mechanism which leads to inefficient transmissions and packet collisions in both the LTE-U and Wi-Fi components of the coexistence system.

3.4.1.1 R-sq or Regression Model Validity (RMV)

LAA and LTE-U models perform equally well, in a scenario-specific comparison with $\leq$5% difference in RMVs in 13/16 comparisons (26/32 scenarios). CIR in LAA seems to be only slightly better, as it outperforms LTE-U in the remaining 3 scenarios. In terms of average RMVs across all 32 scenarios, LAA and LTE-U are comparable, although LAA has a slight edge (<1%). Likewise, in LAA-WiFi-Predictor configuration combinations, LAA has a slight edge (0–2%). Prima facie, based solely on RMV, CIR does not appear to be impacted by the unlicensed LTE variant. However, RMV cannot be considered to be the only goodness-of-fit measure for feature relationships. A higher RMV is an indicator of the variation in the dependent variable explained by the model, but it does not indicate

how far the data points lie from the regression line. Moreover, the standard deviation of the RMV with kCV for a specific scenario must also be low. The analysis ahead explores these dimensions.

3.4.1.2 Residual Standard Deviation (RSD)

The ability of a feature relationship model to make accurate predictions is highly desirable for the model to be deployed in real-world network performance management. Thus, residual error, or RSD, is a measure of precision of the model's predictions and should ideally be low for a robust CIR.

A higher residual error is observed in twice as many LTE-U scenarios compared to LAA scenarios (5% margin of error). On average, LTE-U scenarios have a 6% higher RSD than LAA. Further, average residual error in all LTE-WiFi-Predictor network configurations is lower for LAA when compared to LTE-U. Thus, LAA models seem to be more precise in their ability to predict coexistence network performance, regardless of the response variable (Capacity or SINR).

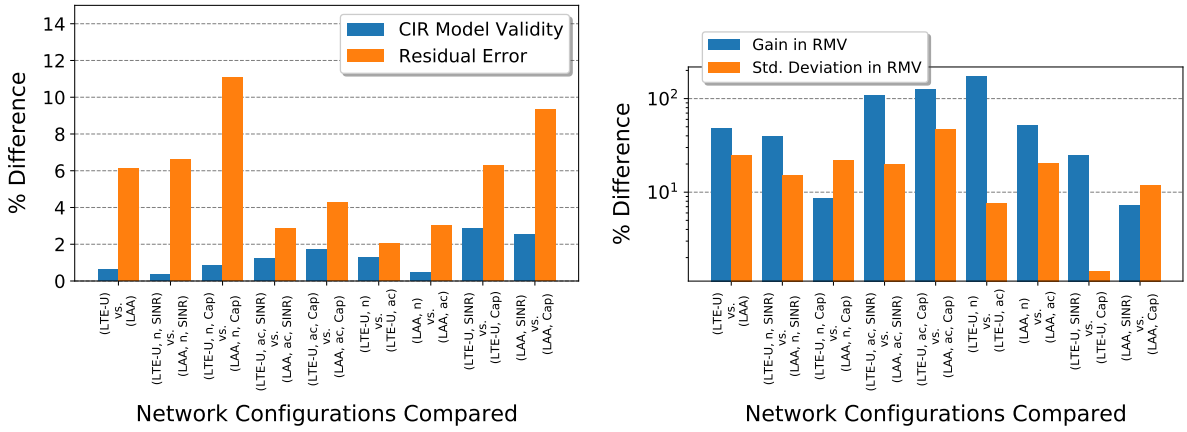

(a) Avg. RMV and Residual Error

(b) Avg. % Gain & Std. Deviation in RMV

Figure 3.4: Configuration-level Comparative Analysis

3.4.1.3 Gain and Standard Deviation in RMV

It is important to note the standard deviation (SD) in the validity of the CIR model when subjected to kCV, especially after LOF outlier removal. While outlier reduction yields higher RMVs, the Gain in RMV should be accompanied with low SD in RMV, averaged across all kCV runs. Thus, we consider high Gain and low SD as characteristics for stable CIR models.

LTE-U fares much worse than LAA in terms of both Gain and SD. LAA outperforms LTE-U by 47.67% in Gain and registers a 24.5% lower SD, averaged across all scenarios. A similar trend can be observed in LTE-WiFi-Predictor combinations as well. Thus, LAA has a higher gain after outlier removal along with a lower SD, which demonstrates the robustness of the LAA CIR models.

3.4.1.4 Outliers

For a network system, the outlier % may be considered to be a good indicator of the degree of fluctuation in network performance, and consequently the ability of a network to deliver the promised Quality of Service (QoS). However, selecting the outlier detection algorithm is a subjective choice. Although this chapter steers clear of making inferences based on outliers, we compare the outliers in the LTE-U and LAA data detected by the LOF algorithm with the outliers detected by "Minitab," a standard tool for data analysis [78]. Minitab's outlier detection algorithm labels samples with extreme "leverage points" and "large residuals" as outliers. As expected, the percentage of data points labeled as outliers is different in LOF and Minitab. However, LTE-U has a higher fraction of outliers compared to LAA in both LOF (by 9.11%) and Minitab (by 5.14%).

The reason for the high fluctuation in LTE-U can be attributed to the greater susceptibility of an LTE-U node to the unpredictable interference from Wi-Fi APs in its proximity. This primarily occurs during the LTE-U ON state, as there are no energy detection thresholds in LTE-U. Unlike LTE-U, Wi-Fi considers the energy threshold as -62 dBm and the preamble detection threshold as -82 dBm. Similarly to Wi-Fi, the LBT mechanism in LAA has an energy threshold of -72 dBm, making it less vulnerable to interference from Wi-Fi APs, and ensuring fewer extreme network performance fluctuations. Thus, LAA seems to offer more reliable performance from the perspective of end-user QoS experience.

3.4.1.5 Context in LTE-LAA vs LTE-U: A Feature Relationship Perspective

The analysis of various parameters of the data model underscores the relevance of the network context. The residual error, standard deviation in RMV, and % of outliers in LTE-U is higher than LAA, while the gain in RMV after outlier removal is lower. This is true for the majority of test scenarios regardless of the choice of Wi-Fi variant, predictor variable, and bandwidth allocated. Thus, CIR in LTE-LAA networks is qualitatively better in terms of the spread of data along the expected curve fit. This implies that LAA offers greater consistency in network performance and lower fluctuations in system variables, such as signal strength or throughput at the end-user device.

The impact of the network context has a strong correlation with macrolevel industry trends as well. The Global Mobile Suppliers Association (GMSA) report states that 38 operators in 21 countries have made investments in LAA compared to only 11 operators investing in LTE-U. In terms of global deployments, 30 operators are planning to deploy or are actively deploying LAA networks in 18 countries, in contrast to LTE-U, which is being deployed in only 3 countries. Furthermore, LTE-U deployments are designed with an upgrade path to LAA and eLAA [4]. Clearly, LAA is the preferred choice of industry for LTE unlicensed networks. From the perspective of network data analysis, this appears to be reasonable as LAA machine learning models indicate a more robust network performance and context than LTE-U.

A detailed data-driven network context analysis is presented in [65]. It includes a comparative

analysis of coexisting Wi-Fi standards and the impact of factors such as network bandwidth, the choice of predictor, and the optimization goal. The findings in [65] had hinted at three aspects that are relevant to the context and performance of unlicensed coexistence networks. These are resource block allocation, physical cell id (PCI), and control vs. user data. The impact of PCI on network performance and context has already been extensively demonstrated [7, 8, 76]. In the next section, we focus on the two remaining unexplored factors that influence the context and performance of an unlicensed network.

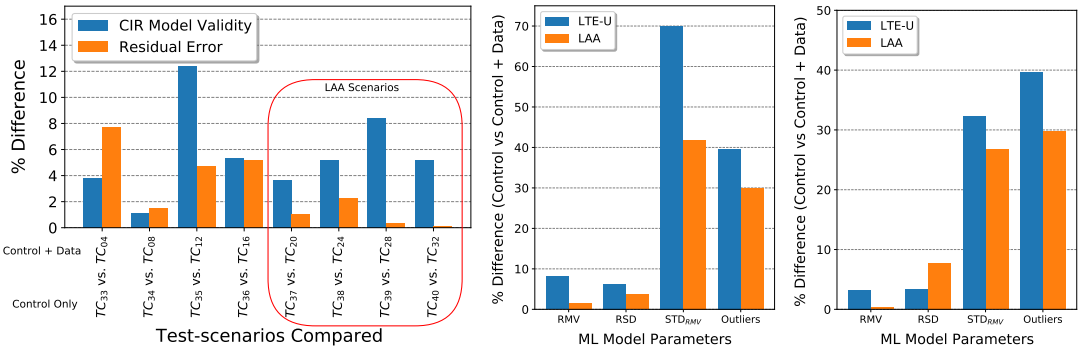

(a) Signaling vs User Data (b) Capacity as Response (c) SINR as Response

Figure 3.5: Impact of Signaling Data on Network Feature Relationships

3.5 Additional Factors that Impact Context

Feature relationships between networks variables are shaped by several other factors. In a public unlicensed cellular deployment, parameters such as Physical Cell ID, Resource Block (RB) allocation, Channel Quality Indicator, etc. often lead to more reliable data-driven network models. This is demonstrated in recent works on performance analysis and optimization of LAA operator deployments [7, 8]. However, these recent studies have not explored the impact of RB allocation. Additionally, while both [7, 8] present data-driven cell selection solutions, the impact of control signaling is not evaluated. Thus, this section expands on the comprehensive analysis of CIR presented in Section 3.4. It investigates two additional dimensions unique to this chapter, which are (a) variation of CIR in control signaling compared to control-plus-data transmission, and (b) impact of resource allocation on CIR. These aspects are explored ahead through data analysis and ML-based modeling of data gathered through 8 new test scenarios (TS_i, where $i \in \{33 \ldots 40\}$).

3.5.1 NFRs in Control vs Control+Data

In the recent data-driven cell selection solutions presented for LAA deployments [7, 8, 76] both control data and user data are considered, referred to as D_{C+U}. It remains to be seen whether the NFRs

differ in the scenario in which only control signaling data packets are transmitted (D_C). Furthermore, it is pertinent to study the variation of LAA and LTE-U NFRs in the two scenarios, namely, D_{C+U} and D_C. Because a significant variation in the parameters of the ML model can render the solutions derived from D_{C+U} less effective for cell attachment and handover.

3.5.1.1 Results and Analysis

To investigate these two challenges, additional experiments were conducted for both LTE-U and LAA. The experiments are run with coexisting Wi-Fi 802.11n/ac for the 20MHz band. The new eight control-only scenarios (TS_i, where $i \in \{33 \dots 40\}$) are compared with the respective D_{C+U} test scenarios.

The scenario-specific comparative analysis is presented in Figure 3.5(a), with LAA scenarios highlighted to contrast with LTE-U scenarios. It is evident that signaling-only and signaling-plus-user data models are qualitatively different, leading to feature relationships that differ significantly. This variation is quite prominent in terms of RMV, for both LTE-U and LAA. However, for LTE-U there is a greater fluctuation in the difference in RMV between the D_{C+U} and D_C models. In addition, the difference in residual error is also higher for most test scenarios compared to LAA.

Network configuration level analysis for ML models with Capacity and SINR as the response variable is presented in Figures 3.5(b) and 3.5(c), respectively. The comparative analysis of LAA and LTE-U further consolidates the findings presented in Section 3.4. The difference between ML model parameters such as RMV, standard deviation in RMV, residual error, and outliers, between the D_{C+U} and D_C models, is much more pronounced in LTE-U than in LAA. Further, for both SINR and Capacity models, LAA NFRs show lower variation between signaling-only and signaling-plus-user data.

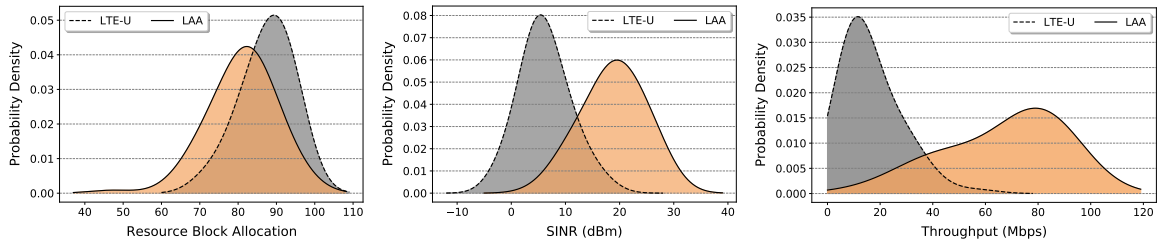

(a) Resource Blocks (b) SINR (c) Throughput

Figure 3.6: Probability Distribution of Network Variables

3.5.1.2 Explanation and Relevance

Both LTE-U and LAA transmit the control channel information over PUCCH, PDCCH, and PBCCH. Typically, LTE-U requires less control signaling than LAA. Due to its ON-and-OFF duty cycle mechanism, there is a lesser need for signaling information in PUCCH because there is no need to sense the

Table 3.2: Distribution Analysis of Network Variables

	Resource Blocks			SINR			Capacity		
Unlicensed Standard	Mean	Mode	Std Dev	Mean	Mode	Std Dev	Mean	Mode	Std Dev
LAA	81	84	8.3	18.9	18	5.4	66.9	89	20.5
LTE-U	87.5	93	6.5	6.2	5	4.3	16.4	10	10.6

medium for load, interference, etc. On the other hand, LAA needs to sense the medium for contention through CW_{min} and CW_{max} which vary, depending on the nature of the traffic.

Channel sensing in LAA ensures fair transmission and limited interference, enabling an operator to identify a better interface and select the ideal PCI for transmission. The fact that the signaling vs. signaling-plus-data feature relationships in LAA are comparable is desirable for data-driven cell selection. In sharp contrast, LTE-U experiences more interference with WiFi transmissions. The LTE-U ON message will interfere with nearby unlicensed band transmissions such as Wi-Fi or other LTE-U, leading to more retransmissions at the MAC layer (in terms of resource allocation) and RLC (in terms of queue and HARQ) by using additional radio resources. This explains a greater variation in network feature relationship parameters in signaling vs. signaling-plus-data compared to LAA transmission.

3.5.2 Resource Allocation in Unlicensed Coexistence

Resource Block (RB) allocation is an important network parameter that can influence network feature relationships such as CIR. In unlicensed LTE (LTE-U or LAA), the 20 MHz channel consists of 100 RBs, which are transmitted in the sub-frame within an interval of 1ms duration. Depending on the nature of traffic, the scheduler allocates the number of RBs necessary to satisfy the QoS/QoE. To investigate the distribution and impact of resource allocation two experiments were conducted for LTE-U and LAA, respectively. Thereafter, the probability density function (PDF) of the RB, SINR, and Throughput distributions in LTE-U and LAA is generated using kernel density estimation with a bandwidth estimator of 0.8. The results are presented in Figure 3.6.

We begin by exploring the characteristics of the distributions of the three network variables. It can be ascertained that except for SINR, the other two distributions for both unlicensed variants are skewed. For LTE-U, the RB distribution is left-skewed, while the Throughput distribution is right-skewed. In contrast, for LAA, both RB and Throughput distributions are left skewed. Thus, in LTE-U the SINR distribution seems to be influencing the Throughput distribution more than RB allocation.

Statistical analysis of the distribution is presented in Table 3.2. It is discernible from the statistics that the RB allocation is higher in LTE-U than in LAA. Taking into account the probability distribution, 87.53% samples in LTE-U have an RB allocation of 80 and higher, i.e., $P(RB \geq 80)$, compared to 54.70% in LAA. However, there is a drastic difference between the two standards and LAA performs

much better. For example, $P(SINR \geq 15dBm)$ or SINR equal to or greater than 15dBm is true for only 2% of the LTE-U samples compared to 67.3% samples in LAA. When combined, these results lead to an interesting Capacity distribution. Despite a higher allocation of RB, LTE-U offers much lower throughput values compared to LAA, with only 9.9% samples above 30Mbps compared to 96.4% samples in LAA.

A possible explanation is that, despite better RB allocation, high interference with coexisting Wi-Fi signals during the LTE-U On mode leads to increased packet retransmission. Corrupted symbols/bits over the air transmission render the RB utilization inefficient. Thus, poor SINR causes the LTE-U small cell to transmit a lower number of bits at a lower modulation coding scheme (MCS). Poor SINR combined with lower MCS results in a low overall system throughput or network capacity. Inefficient resource utilization may pose additional challenges in the fair sharing of the spectrum in the unlicensed band. On the other hand, LAA small cell are able to leverage the RB allocation more effectively to maximize network capacity.

Thus, features such as RB allocation and MCS have a clear impact on network feature relationships and, in turn, on the network context. Including these features in the data models is likely to offer improved feature relationships and greater gains in optimization accuracy [65]. However, application to network optimization must be done with caution, as constraints with additional features may lead to longer convergence times. Thus, accuracy-speed trade-off is a crucial aspect that must be considered in NFR-based optimization. This paper covers it at length in Section 3.7.

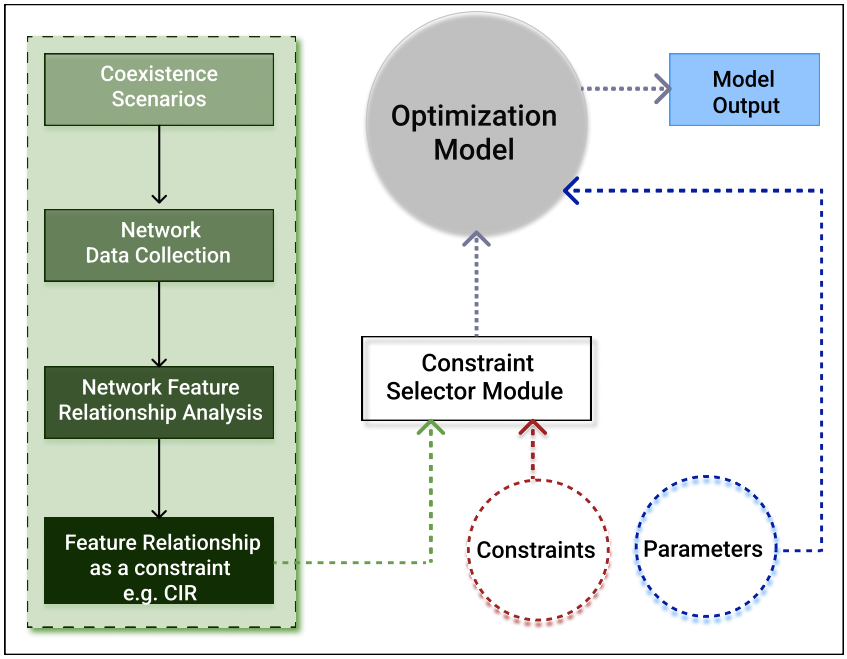

Figure 3.7: Network Feature Relationship-based Optimization

3.6 Utilizing Feature Relationships for Network Optimization

Optimal performance or resource allocation in a wireless network can be achieved through three broad frameworks, which are (a) optimization models, (b) machine learning techniques, and (c) a hybrid approach that combines the two called data-driven optimization [13, 79]. Although machine learning algorithms are commonly used for prediction and classification problems, feature relationships are particularly useful to reduce the computational overhead of unlicensed network optimization [45, 80].

3.6.1 Network Feature Relationship based Optimization

This chapter leverages the NFRs to enhance network performance, through the proposed ***Network Feature Relationship based Optimization*** (NeFRO) technique [65].

NeFRO is a data-driven approach which adopts the hybrid optimization methodology. As illustrated in Figure 3.7, NFRs learned from the network data serve as constraints in a model that aims to optimize dense unlicensed networks.The NeFRO framework overcomes the reliance on arbitrary assumptions and heuristics to relax complex theoretical constraints. NeFRO uses ML-based network feature relationship equations that reflect the ambient state of a wireless network.

The first step entails collecting data from network deployments at predetermined epochs. Next, low-cost machine learning algorithms are used to learn NFRs for each epoch. Robust NFRs from relationship models with high R-sq (RMV) are fed to *constraint selector module*, which chooses the constraints necessary for optimization formulation. Typically, the selector module is designed to compare the NFR learned for a feature vector $\{f_1, f_2, \ldots, f_n\}$ with the theoretical constraints associated with the feature vector. The rationale behind this step is that since the NFRs capture the ambient network environment, they can be used "as is" in the model, doing away with the need for arbitrary constraint relaxations. Despite its suitability, an NFR is tested for *convergence time viability*, by comparing its complexity and expected run-time vis-a-vis the theoretical constraint. Owing to its data-driven optimization approach, NeFRO is able to significantly reduce time costs of optimization while delivering results that are close to the values derived from theoretical constraints.

Although the illustration highlights the process-flow for a coexistence network, the NeFRO approach will apply similarly to network optimization in all wireless networks, with minor modifications, if required.

Benefits of the NeFRO Approach The proposed NeFRO framework offers several advantages over conventional network optimization. First, NFRs are learned from empirical data through ML algorithms for a given epoch. Thus, they reflect the ambient network environment better than theoretical constraints that involve similar network variables. Second, NFRs can be used "as is" in optimization without making any assumptions, unlike theoretical constraints, which often require context-specific relaxations and assumptions. Finally, if the data-driven NFRs are less complex than the corresponding theoretical constraints, the problem of arbitrary or forced relaxation of theoretical constraints is

automatically solved. Even when the learned NFRs result in computational overheads comparable to theoretical constraints, they ensure an informed network optimization process grounded in network data.

3.6.2 Implementation and Validation of NeFRO

Evaluation of NeFRO This chapter improves the metrics used for evaluation in [65]. Three simplified metrics are considered to evaluate NeFRO, viz., "Accuracy", "Speed", and "Optimization Gain". Accuracy of the NeFRO model demonstrates the closeness of the "NeFRO-optimal output" to the optimal value generated by the baseline optimization model. Thus, **Loss in Accuracy** can be defined as the *"(%) difference in the optimal value generated by the baseline model and the NeFRO-optimal value"*. The second parameter is the reduction in convergence time achieved by the NeFRO model to arrive at the NeFRO-optimal value. It is named **Speed**. Thus, **Gain in Speed** can be defined as the *"(%) reduction in convergence time achieved by NeFRO compared to the baseline model's convergence time"*. Together, the first two indicators are used to derive the "Accuracy Speed Trade-off" (Trade-off). In, this chapter *Trade-off* is defined in terms of *Optimization Gain*, where,

Optimization Gain (%) = Gain in Speed (%) - Loss in Accuracy (%)

For example, if the baseline model outputs an optimal solution of 100 and takes $10ms$ to converge, and the NeFRO generates 95 as the optimal solution and requires $9ms$ to arrive at the NeFRO-optimal value, then the Optimization Gain is 5%, and the Trade-off is acceptable.

A positive Optimization Gain justifies the Trade-off involved, especially when faster convergence time is highly desirable, such as an AR service communicating on an LAA or LTE-U channel. However, the lower the Loss in Accuracy, the lower the Trade-off, and more suitable is the optimization formulation. Thus, NeFRO uses data-driven NFRs to achieve the twin objectives of gain in Speed through *convergence time reduction* and high *Accuracy* with respect to the baseline optimization model. Please note that the Accuracy Speed Trade-off in dense network performance optimization is a major challenge in itself [48], and is addressed at length in Section 3.7. Next, the baseline optimization models and the validation methodology are discussed.

Baseline Unlicensed Network Optimization Models The proposed NeFRO framework is validated through four recent state-of-the-art studies that seek to optimize coexistence network performance. These include two studies that optimize end-user throughput or network capacity, and the remaining two works attempt to provide optimal signal strength to end-user equipment (UE). The LAA capacity optimization model presented in [81], is based on optimal resource allocation in an unlicensed coexistence network [81]. An LBT-compliant channel access solution is proposed in [82] for both LTE-U/LAA in the 5GHz band with the aim of maximizing network capacity through interference mitigation in the LTE-WiFi system. The two baseline capacity optimization models are denoted as COM_1 and COM_2, respectively in the discussion ahead. Regarding signal strength, the optimization

solution proposed in [83] improves network signal quality through strategic placement of nodes in the LTE-U and LAA networks. Next, the solution presented in [84], considers efficient spectrum usage of Wi-Fi APs along with optimal placement of nodes, for enhanced signal strength. The signal strength optimization models are henceforth denoted as SOM_1 and SOM_2, respectively.

Modeling of Unlicensed Network Optimization The General Algebraic Modeling Language (GAMS) [85], tool effectively models an unlicensed coexistence environment through the use of constraints. The SINR-related constraints account for the impact of LAA/LTE-U transmission on Wi-Fi APs and vice versa. Constraints concerning the number of active users connected to the LAA/LTE BS or Wi-Fi AP prevent the network from overloading. Similarly, constraints with respect to the user association threshold, such as an RSRP of -108 dBm, limit packet loss. Constraints concerning the placement of the BS or APs ensure that there are no blind spots or coverage holes in the network. Finally, resource allocation constraints are vital for modeling fairness in the coexistence system. For LAA and Wi-Fi, these include the sensing duration of LTE-LAA (LBT) and Wi-Fi (CSMA), ED thresholds (-62 dBm for Wi-Fi and -72 dBm for LAA) and the corresponding opportunities for data transmission. Similarly, for LTE-U, the duty cycle ON and OFF constraints are based on the number of contending nodes in the network.

Validation Methodology The methodology adopted to validate NeFRO entails the following steps. First, the four baseline unlicensed network optimization models are implemented in GAMS [85], for each of the test scenarios. That is, the implementations conform to the system configurations and network specifications considered. Second, *baseline optimal value* of the network parameter (SINR or Capacity) and the *convergence time* taken by the optimal baseline solution are recorded. The third step applies the NeFRO process to the baseline solutions. Thus, the complex theoretical constraints related to signal strength and/or network capacity in a baseline formulation are replaced with the data-driven CIR equations learned through ML algorithms. It is worth mentioning that baseline network capacity optimization formulations viz., COM_1 and COM_2, are considered for test scenarios where SINR is the predictor in the network ML model, and vice versa. Fourth, *NeFRO-optimal values* and *NeFRO convergence time* are recorded. In the fifth step, the NeFRO performance indicators are determined, viz., Gain in Speed, Loss in Accuracy, and Trade-off, from the observations made for baseline models (step two) and NeFRO models (step four),

Finally, NeFRO is assessed for its ability to reduce convergence time while ensuring a high Accuracy vis-a-vis the baseline optimization models. Therefore, *a high Gain in Speed, a low Loss in Accuracy, and a positive Trade-off will validate the NeFRO hypothesis.*

3.6.3 Optimization Results and NeFRO Evaluation

The NeFRO validation is performed through second-degree non-linear CIR models as the SINR-Capacity relationship in wireless networks is shown to be quadratic [36].

The results of the optimization simulations run in GAMS are presented in Figure 3.8 and Figure 3.9,

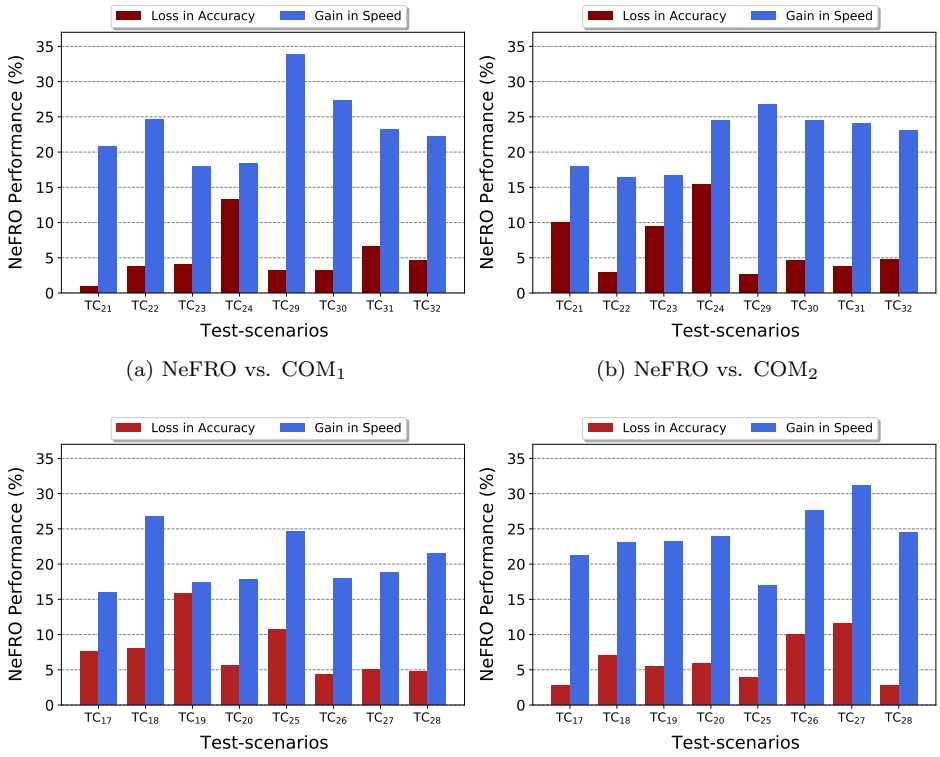

(a) NeFRO vs. COM_1

(b) NeFRO vs. COM_2

(c) NeFRO vs. SOM_1

(d) NeFRO vs. SOM_2

Figure 3.8: NeFRO Performance in LAA Capacity and SINR Optimization

Table 3.3: Performance Trends in Test-scenarios

NeFRO	**LTE-LAA Scenarios** (%)				**LTE-U Scenarios** (%)			
Parameter	COM_1	COM_2	SOM_1	SOM_2	COM_1	COM_2	SOM_1	SOM_2
Gain in Speed	23.54	21.75	20.11	23.98	9.9	10.95	5.83	6.4
Loss in Accuracy	4.96	6.69	7.72	6.18	5.03	3.88	3.62	2.84

for the LAA and LTE-U test scenarios, respectively. Further, Figures 3.8(a), 3.8(b), 3.9(a), and 3.9(b), present results for test scenarios where the objective is to optimize network capacity. The remaining figures show results for signal strength optimization test scenarios.

It can be discerned that NeFRO performs remarkably well by reducing the required convergence times while delivering NeFRO-optimal values very close to the optimal results of the respective baseline models. A scenario-specific evaluation of NeFRO can be performed by observing the difference in the length of bars of "Loss in Accuracy" and "Gain in Speed" for a particular test scenario. The greater the difference, the lower the Trade-off and the better the NeFRO performance. Two points are noteworthy. First, in LAA scenarios, NeFRO offers a significant reduction in convergence time, while in LTE-U

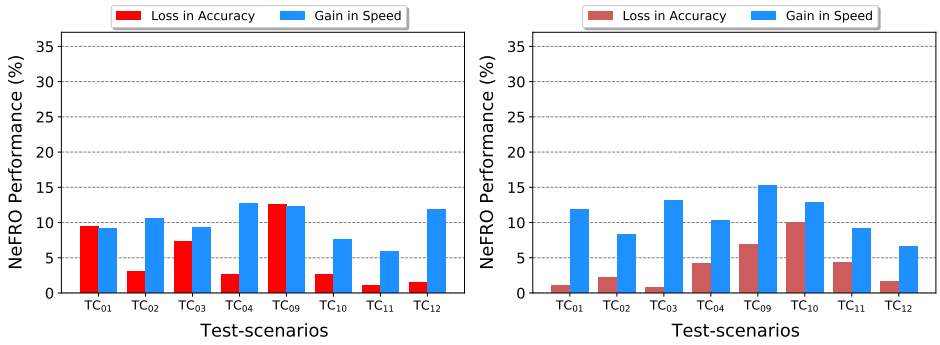

(a) NeFRO vs. COM_1

(b) NeFRO vs. COM_2

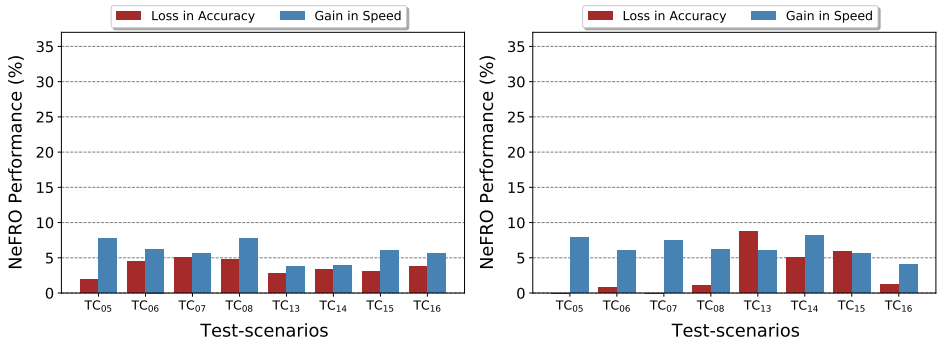

(c) NeFRO vs. SOM_1

(d) NeFRO vs. SOM_2

Figure 3.9: NeFRO Performance in LTE-U Capacity and SINR Optimization

scenarios, the Gain in Speed is somewhat subdued. Network optimization in LTE-U is inherently more challenging due to its channel access mechanism. Hence, it is more computationally intensive and requires a longer convergence time. Second, for LAA scenarios, the difference in NeFRO performance for capacity optimization and SINR optimization is negligible.

However, in LTE-U, there appears to be a noticeable difference in NeFRO performance for these two objectives. In particular, the Gain in Speed for SINR optimization in LTE-U is rather low, and for two specific SOM_2 test scenarios viz., TS_{13} and TS_{15}, it is lesser than the Loss in Accuracy, leading to a negative Trade-off. The average performance of NeFRO across all test scenarios for the four optimization models is presented in Table 3.3. Despite these specific instances, for both SOM_1 and SOM_2, the average Gain in Speed of NeFRO is higher than its average Loss in Accuracy, leading to an overall positive Trade-off.

In general, NeFRO outperforms the baseline model across all test scenarios and both unlicensed LTE variants by significantly reducing the convergence time (large Gain in Speed). The average Loss in Accuracy, as shown in Table 3.3, is also very low. Further, NeFRO seems to perform better in LTE-LAA scenarios compared to LTE-U, which can be expected based on the discussion and findings

presented in this chapter. Thus, the NeFRO framework stands validated.

Please note that these state-of-the-art optimization models are implemented for small-scale dense unlicensed coexistence scenarios on an experimental testbed. We expect that in a real-world network of much higher scale and density, the performance enhancement demonstrated by NeFRO will be far more pronounced.

3.7 Accuracy Speed Trade-off in Data-driven Optimization

The primary contribution of this chapter is context-aware data-driven optimization. Developing an understanding of the Accuracy-Speed Trade-off is the first step in that direction.

Within the hybrid optimization paradigm that leverages machine learning, *Accuracy-Speed Trade-off* implies that it is challenging to achieve high Accuracy while delivering results at high Speed. Although NeFRO is designed to deliver optimal results with high Accuracy and high Speed, essentially overcoming the Trade-off, its performance is invariably linked to the NFRs used as constraints. Multiple relationship models can be learned for a set of network features, depending upon objective criteria such as R-sq, outlier threshold, higher-order terms, *etc.* For example, a polynomial NFR of n^{th} degree with statistically significant higher-order terms (no overfitting) may represent the relationship more accurately through a higher R-sq. Strong NFRs lead to better results when used in tasks such as rate adaptation or throughput enhancement [9, 13]. Thus, the R-sq of an ML model trained on network data can be considered to be an indicator of its ability to optimize network performance. However, using a higher-order feature relationship in NeFRO may lead to a significantly longer convergence time. Hence, not all relationship models for a given feature set are suitable for dense unlicensed optimization through NeFRO.

These factors make the selection of an appropriate NFR for ML-based optimization a challenging problem. Thus, a prime objective of this chapter is to study *convergence time and accuracy trade-off* in using feature relationships of different degrees in data-driven optimization. In addition, it proposes a practical context-aware approach to selecting the appropriate NFR for the right use case.

3.7.1 Trade-off Evaluation in Methodology

The first step in this process is the evaluation of the Trade-off in data-driven optimization. To that end, the analysis in this section considers multiple network models for capacity-interference relationship (CIR) of different degrees (influences Speed) and R-sq (influences Accuracy).

Generating CIRs of Varying Degrees Kernel functions are varied in the ML algorithms discussed in Section 3.3.2, to generate feature relationship models of multiple degrees. A kernel function $K(\mathbf{x}, \mathbf{x}')$ allows us to compute the dot product in an arbitrary large space without the need to explicitly project features in high-dimensional space. In particular, $K(\mathbf{x}, \mathbf{x}')$ is defined as $exp(-\gamma||\mathbf{x} - \mathbf{x}'||^2)$ and $\gamma(\mathbf{x}^\top \mathbf{x}' + r)^d$ for radial basis function and the polynomial kernel, respectively. Here, γ, r, and

d are kernel-specific parameters. In particular, d controls the complexity of the decision function f, *i.e.,* setting $d = 1, 2, 3$ corresponds to learning a linear, quadratic, and cubic boundary in the case of the polynomial kernel. In practice, we prefer the polynomial kernel, as it can be easily plugged into the optimization routine, whereas the RBF kernel would require certain modifications. Nevertheless, the results are reported with both radial basis function (RBF) and polynomial kernel (MPR) for completeness.

SINR-Capacity relationship has been theoretically shown to be non-linear [33,36], hence the analysis presented considers CIR polynomials of degrees 2 and 3. Please note that data-driven CIRs can also be linear for specific network scenarios, e.g., when only a relatively linear section of the overall non-linear CIR curve is applicable to a system. In such scenarios, linear CIRs can have a high RMV or R-sq and may yield a better optimization performance, i.e., a lower Trade-off [13]. Since the experiments in this study were performed for the entire SINR range, linear models are not considered in the Trade-off analysis.

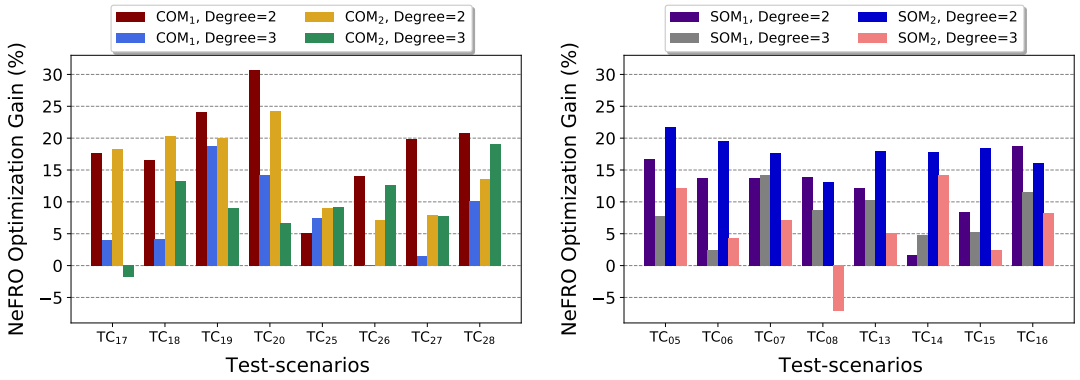

(a) NeFRO vs COM_1 & COM_2

(b) NeFRO vs SOM_1 & SOM_2

Figure 3.10: Impact of the Degree of NFR on LTE-U Capacity and SINR Optimization

Evaluation Methodology Comparative Trade-off analysis is performed for 2^{nd} and 3^{rd} degree polynomial CIRs through the baseline models that seek to maximize coexistence network performance through network capacity optimization (COM_1 and COM_2) and signal strength optimization at the UEs (SOM_1 and SOM_2). Next, as previously described (Figure 3.7), the theoretical constraints in the baseline models are replaced with the 2^{nd} and 3^{rd} NFRs learned from the feature relationship analysis. The NeFRO-optimal values and the convergence times are noted for the optimization objectives. Finally, the NeFRO-optimal and baseline-optimal values are compared to determine (a) Loss in Accuracy and (b) Gain in Speed.

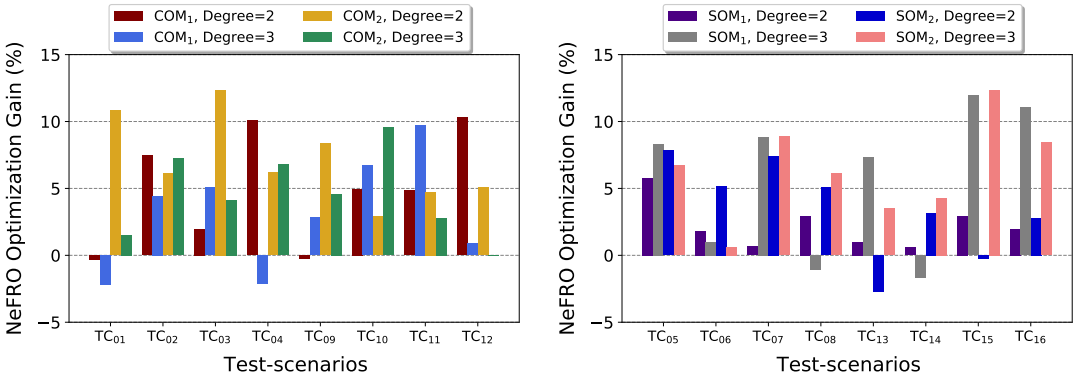

(a) NeFRO vs COM_1 & COM_2

(b) NeFRO vs SOM_1 & SOM_2

Figure 3.11: Impact of the Degree of NFR on LTE-U Capacity and SINR Optimization

3.7.2 Results and Analysis

The optimization simulation experiments are run in GAMS and the results are evaluated at the level of individual test scenarios and at the level of network configuration.

Scenario-specific Trade-off Evaluation The scenario-specific results are presented in Figure 3.10 and Figure 3.11, for LAA and LTE-U, respectively. For each test scenario, the "Degree" shows the order of the polynomial CIR used in NeFRO.

It is evident from the scenario-specific assessment that for NFRs of both polynomial degrees, NeFRO reduces run times while converging on NeFRO-optimal values that are extremely close to the baseline-optimal values. This is true for most test scenarios. Except in a few cases, even NFRs with "Degree=3" offer better overall performance than the baseline optimization models. In LAA scenarios, generally the magnitude of Optimization Gain decreases as the degree of the non-linear NFR increases from 2 to 3. Further, there is no unfavorable Trade-off in 2^{nd} degree polynomials and negative Optimization Gain in only two scenarios for 3^{rd} degree CIR.

Comparing 2^{nd} and 3^{rd} degree CIRs, the relative performance trends seem different for Capacity and SINR optimization models. In the former, as shown in Figure 3.10(a), 2^{nd} degree CIRs seem more suitable than 3^{rd} degree CIRs, except in one instance, TC_{25}. Since 3^{rd} degree CIRs perform slightly better for both optimization models in TC_{25}, the "context" of the scenario seems important. For signal strength optimization models (Figure 3.10(b)), the case is somewhat similar. In 6 of 8 test scenarios, 2^{nd} degree CIRs appear to be the better choice. However, for TC_{07} and TC_{14}, 3^{rd} degree CIR SOM_1 outperforms 2^{nd} degree. This, too hints at the fact that for a specific "context," network configuration, and the optimization objective, a higher degree CIR may offer a lower Trade-off.

In contrast to LAA, LTE-U optimization Trade-off trends are significantly different. Although NeFRO offers a positive Optimization Gain for both capacity and signal strength models for most

scenarios, the distinction between CIR of 2^{nd} and 3^{rd} degrees is not very pronounced. In capacity optimization (Figure 3.11(a)), 2^{nd} degree CIRs seem slightly more suitable and have a negative Optimization Gain for half the number of test scenarios. However, in LTE-U SINR optimization, the performance of CIRs of 2^{nd} and 3^{rd} degrees varies depending on the network configuration and optimization formulation. A possible reason for this could be that network optimization in LTE-U is often more complex owing to its duty-cycle-based channel access mechanism, leading to longer convergence times, regardless of the degree of NFR.

These findings highlight the importance of the network context and choosing the right NFR based on that context.

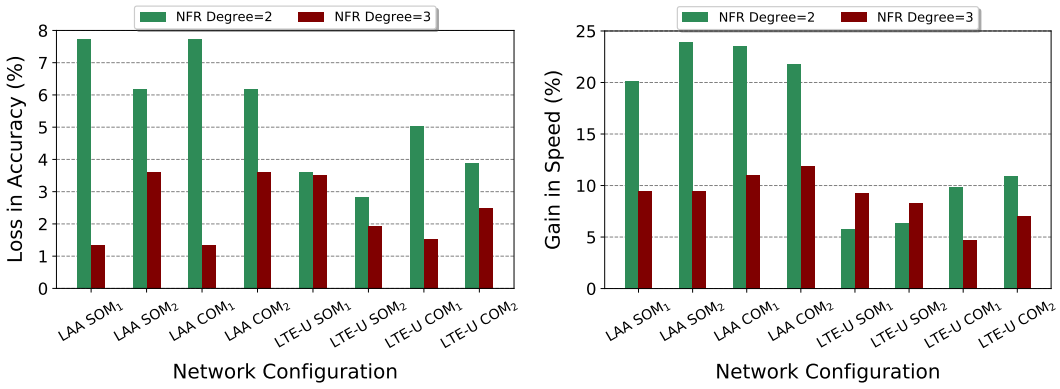

(a) Loss in Accuracy

(b) Gain in Speed

Figure 3.12: Trade-off Analysis at the Level of Network Configuration

Network Configuration Level Evaluation To investigate the relevance of context, it is important to see if the above Trade-off patterns are reflected at the macrolevel. Thus, the results of the network configurations are presented in Figure 3.12. It is evident that averaged across all test scenarios, NeFRO always ensures a positive Trade-off, for both LTE-U and LAA and all four baseline models, i.e., Gain in Speed is invariably higher than the Loss in Accuracy. On average, the Loss in Accuracy, is higher for LAA than it is for LTE-U, e.g., 2.98% and 4.7% for LTE-U and LAA SINR optimization, respectively. However, the average Gain in Speed, and as a result, the magnitude of average positive Trade-off, is higher for LAA than it is for LTE-U.

A comparison of 2^{nd} and 3^{rd} degree CIRs, offers great insight into the role of network context in NeFRO performance. The *network context*, as conceptually applied to this chapter, can be defined as "the sum total of the ambient network environment, network configuration, and the optimization objective." Looking at LAA optimization models in Figure 3.12, it is discernible that 2^{nd} degree CIRs offer a somewhat lower Accuracy but a much higher Speed, leading to a much higher overall Trade-off. Thus, at the configuration level, 2^{nd} CIRs lead to a higher Optimization Gain than 3^{rd} degree CIRs. However, considering Loss in Accuracy alone, the 3^{rd} degree CIRs perform much better, e.g., they

offer one fifth the loss for LAA SOM_1, compared to 2^{nd} degree CIRs. Thus, navigating the Trade-off becomes highly contextual. In scenarios where high Accuracy is important, despite the overall higher Optimization Gain, 2^{nd} degree CIRs may not be suitable.

The impact of context with respect to network configurations is more clearly brought out in LTE-U signal strength optimization. Here, for both LTE-U SOM_1 and LTE-U SOM_2, the 3^{rd} degree CIRs show better Accuracy and higher Speed. Therefore, it seems to make more sense to use 3^{rd} degree CIRs for this network configuration and 2^{nd} degree CIRs for other configurations.

In general, it can be inferred that the NeFRO approach improves the baseline models regardless of the type or degree of the NFR. Furthermore, it seems to benefit the LAA-WiFi coexistence optimization more than LTE-U. Most importantly, the NFR for data-driven optimization must be chosen based on the network context. This finding underscores the importance of the awareness of network context, which is a nontrivial problem, and a practical solution is presented in the next section.

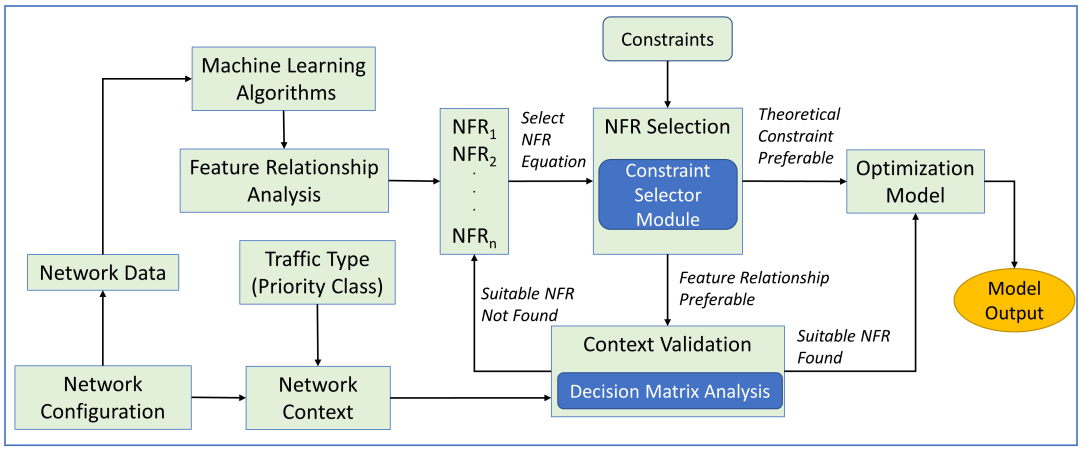

Figure 3.13: Context Aware Network Feature Relationship based Optimization

3.8 Context Aware Optimization

The findings of Trade-off analysis have highlighted that data-driven optimization of unlicensed coexistence network performance requires context awareness. The network context has several components. A major aspect of the network context is the nature of the traffic requested by the UE, such as voice, video, live streaming, file download, etc. Each traffic type has a different QCI index, EPS bearers, and channel access priority. Mobile network operators distinguish between different types of traffic to ensure high QoS at the UE and prioritize data traffic based on these parameters. Thus, voice traffic has high priority, and the packets need to be transmitted more frequently to avoid performance degradation, e.g., voice quality. Similarly, a file download service/application demands higher resource block allocation at the MAC layer to maintain an excellent data rate. Another aspect of context can be the

number of users connected to base station as that shapes the traffic load, congestion, and resource allocation.

The awareness of the context for network optimization is easily understood through cell selection mechanisms [76]. Data-driven cell selection is increasingly becoming the norm in industry [22, 57, 76] and solutions to improve the cell selection process have also been presented in recent academic studies [7, 8]. A context-aware optimization of signal strength would enhance the efficiency of the cell association process. For example, the context, i.e., ambient radio (LTE-U or LAA) condition and data demand, can guide the operator cell selection mechanisms in deciding which PCI needs to be enabled as an additional carrier for carrier aggregation or dual connectivity.

The discussion in this section proposes a context-aware NFR-based optimization framework (CANeFRO). The hypothesis is then validated through context-aware optimization choices made through *decision matrix analysis* [86].

3.8.1 Context Aware NeFRO

A high-level schema of the context-aware NFR-based optimization framework (CANeFRO) is presented in Figure 3.13. CANeFRO introduces an element of context awareness in the NeFRO approach discussed in detail earlier. It also provides for an improved selection of NFR through context validation. In this chapter, decision matrix analysis (DMA) or the Pugh method is used to calibrate the network context on a weighted scale [86]. The important aspects of CANeFRO illustrated in Figure 3.13 are discussed below.

A strong network feature relationship is reflected in the high R-sq of the ML model and is likely to improve the performance of the data-driven optimization model [9, 13, 76]. Since the CIR is non-linear, a higher-order CIR often offers a better regression fit, thereby ensuring a higher RMV or R-sq. Therefore, it seems desirable to utilize it in a NeFRO model for enhanced accuracy. However, a higher-order CIR will also increase the time cost of the optimization model that utilizes it. Thus, the choice of NFR should be motivated by the context. For example, a high-performance use case, such as remote surgery using a virtualized digital twin will prefer Accuracy over Speed [73], while high Speed will be preferred in on-the-go video streaming.

To reflect a varying context, a decision matrix is considered. On the X-axis, weights are assigned to Loss in Accuracy and Gain in Speed for each individual test scenario. Thus, context can be defined as $C \rightarrow (X, \Upsilon) \mid X \rightarrow Weight_{Acc}, \Upsilon \rightarrow Weight_{Spd}$, where C is the network context, X is the weight assigned to Loss in Accuracy, Υ is the weight assigned to Gain in Speed, $\text{Weight}_{Acc} \in [1, 0]$, $\text{Weight}_{Spd} \in [0, 1]$. Thus, the context changes from the use case (e.g., remote surgery) where Accuracy takes the highest priority and Speed takes the lowest priority, i.e., $C \rightarrow (1, 0)$ to the use case (e.g., live streaming) where Speed takes the highest priority and Accuracy takes the least priority, i.e., $C \rightarrow (0, 1)$. All other network contexts or use cases fall between these two extremes.

Subsequently, the decision score $S(C_k)$ for a given context is computed as follows.

$$\mathbf{S}(C_k) = \frac{\sum_{i=1}^{n} X_{TS_i}\Delta_{-}\ \text{Accuracy}_{TS_i} + \Upsilon_{TS_i}\Delta_{+}\ \text{Speed}_{TS_i}}{n}$$

where Δ_{-} refers to loss, Δ_{+} refers to gain, C_k is the k^{th} network context, X is the weight assigned to Loss in Accuracy, Υ is the weight assigned to Gain in Speed, TS_i is the i^{th} test scenario, n is the number of test scenarios in a network configuration, and k is the number of contexts.

Finally, the decision scores for each network context are computed for LAA and LTE-U, for both optimization objectives, for CIRs of 2^{nd} and 3^{rd} degrees, and all four baseline optimization models.

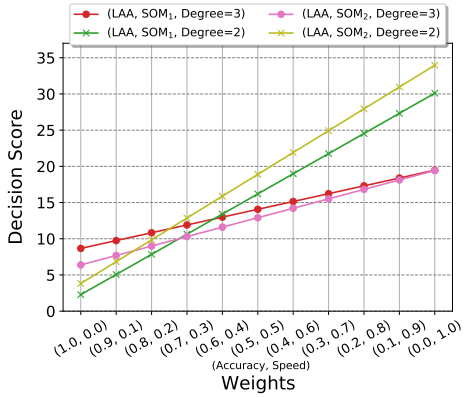

(a) LAA Signal Strength Optimization

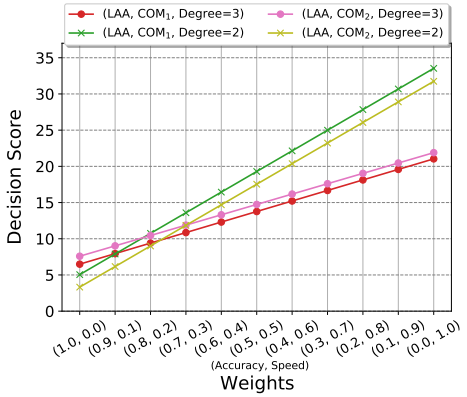

(b) LAA Network Capacity Optimization

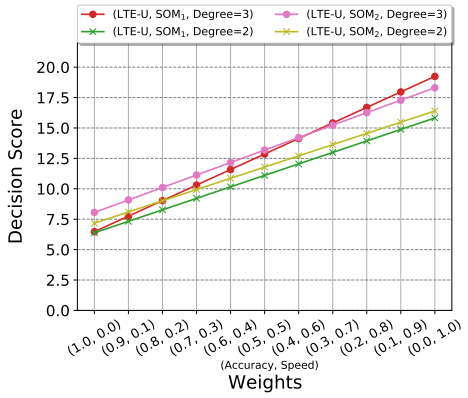

(c) LTE-U Signal Strength Optimization

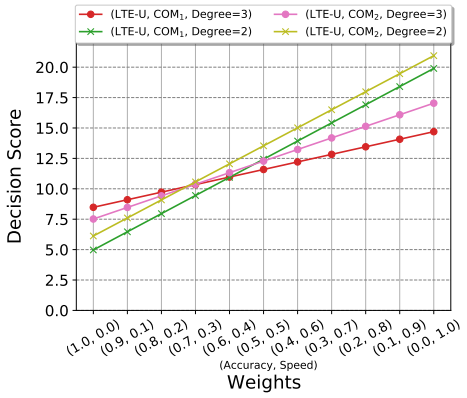

(d) LTE-U Network Capacity Optimization

Figure 3.14: Accuracy-Speed Trade-off Analysis in Data-driven optimization

3.8.2 Evaluation of Context-Aware NeFRO

The results of the decision matrix analysis for context-aware NeFRO are presented in Figure 3.14. It can be noticed that the context has an immense bearing on data-driven optimization and the choice

of NFR. Given the multitude of test scenarios considered in this chapter, for simplicity, the decision scores are averaged across individual test scenarios for a single unlicensed coexistence standard, viz., LTE-U and LAA.

For both standards, the optimization objective, i.e., providing maximum SINR and Capacity to the UE, and the optimization formulation, viz., SOM_1, SOM_2, COM_1, and COM_2, determine the best NFR for the context, shaping the overall decision score. For example, 2^{nd} degree LAA SOM_2 CIR outperforms 2^{nd} degree SOM_1. However, the reverse is true for 3^{rd} degree CIRs in LAA signal strength optimization (Figure 3.14(a)). Moreover, the performance difference stays more or less constant for 2^{nd} degree NFRs for all use cases, but for 3^{rd} degree the decision scores converge for high-Speed use cases, viz., (0.1, 0.9) and (0.0, 1.0). Similar contextual variability can be observed in other plots as well.

We now focus on the performance variation between LTE-U and LAA. For LAA, the performance of the signal strength and capacity optimization models follows a similar pattern (Figures 3.14(a) & 3.14(b)). 2^{nd} degree NFRs outperform 3^{rd} degree NFRs as for all use cases where the weight assigned to Speed (faster convergence times) is ≥ 0.3. Furthermore, 3^{rd} degree NFRs are the clear choice in use cases where no compromise in optimization accuracy is tolerable.

In sharp contrast, LTE-U demonstrates different trends for signal and capacity optimization goals, and there is a greater contextual variation in the choice of NFR. The first point of marked difference is that the decision score for LTE-U models is lower than LAA by up to 42%. This holds true for all four NeFRO optimization models. Second, for both SINR optimization models (Figure 3.14(c)), 3^{rd} degree NFRs are a better choice, for all use cases. Thus, regardless of the priority class of the traffic type and latency requirements of the use case, 3^{rd} degree NFRs outperform 2^{nd} degree NFRs. Further, the trends in the decision score presented in Figure 3.14(d) reveal that both types of CIR perform better in capacity optimization models for an almost equal number of use cases. Therefore, 3^{rd} degree NFRs are more suited in quadrant 3 use cases, where high accuracy is desirable and 2^{nd} degree NFRs are dominant in quadrant 2 use cases where high convergence speed is desirable.

From the above analysis, the impact of network context on data-driven optimization is evident. Thus, data-driven optimization solutions for real-world LAA deployments ought to consider the network context for a better end-user experience.

3.9 Conclusions and Way Forward

Unlicensed cellular networks and spectrum-sharing mechanisms face new challenges that require data-driven solutions for network optimization. An unexplored problem in the data-driven optimization of unlicensed networks is the Accuracy-Speed trade-off. This chapter took advantage of machine learning to improve the performance of classical network optimization techniques in dense unlicensed networks. It highlighted the relevance of network context in mitigating the trade-off by considering

multiple higher-order network feature relationships. A context-aware network feature relationship-based optimization framework (**CANEFRO**) was proposed and validated through decision matrix analysis. CANEFRO showed that the network context influences the choice of the feature relationship model and the optimization goal. It also demonstrated how network data and machine learning can be used to enhance the capabilities of classical network optimization.

Chapter 4

Data-driven Cell Selection in LAA Networks

4.1 Introduction

The exponential growth in data consumption has also pushed cellular operators to provide broad coverage and seamless connectivity through a dense deployment of Base Stations/eNodeBs (BS/eNB). They have rapidly standardized, adopted, and deployed new technological paradigms such as Long Term Evolution/Long Term Evolution-Advanced (LTE/LTE-A), heterogeneous networks (HetNets), and unlicensed coexistence networks. Spectral utilization has been maximized by opening up the 5 GHz and 6 GHz bands for unlicensed operation through LTE Licensed Assisted Access (LTE-LAA) and 5G New Radio (NR) in Unlicensed (NR-U) [87].

Cellular operators have begun rolling out LTE-LAA coexistence deployments globally, and their penetration is increasing at a phenomenal rate [88,89]. Since increasing the BS/eNB density to provide higher data rates is expensive and time-consuming [90], operators have chosen to deploy a large number of low-power small cells such as pico cells and femto cells. This trend is likely to continue in the next generation of unlicensed LTE-LAA and NR-U networks, giving rise to dense ($d \leq 10$m) and ultra-dense ($d \leq 5$m) network deployments (DNs/UDNs), where d is the inter-cell distance [91].

While LTE-LAA is capable of delivering high QoS by harnessing the unlicensed spectrum, the performance of dense LTE-LAA deployments will depend heavily upon efficient and fast cell association [92, 93]. Owing to the factors such as a new LTE-LAA coexistence deployment architecture, the type of backhaul connectivity available, and the vulnerability to interference from Wi-Fi transmissions, the solutions proposed for optimal cell association in LTE HetNets may not be suited for LAA deployments. The number of available Physical cell Ids is also limited to 504, so an additional challenge in LTE-LAA cell selection is that LAA has to compete with existing small cells and macro cells for PCI attachment. This can be observed in operator data, as sometimes the LTE and LAA components are camped on different PCIs.

Cell selection also influences packet-aggregation and routing of Licensed and Unlicensed coexistence data **[94,95]**, which in turn affect the network performance. Thus, it is of great interest to ascertain how cell selection affects LTE-LAA coexistence network parameters (e.g., Capacity) and network feature relationships (e.g., SINR-Capacity relationship). Further, the cell selection decision also determines the *association time* (AT) for a UE. In dense and ultra-dense deployments, AT becomes a critical parameter during the user association process.

The current studies available on PCI/cell selection in LAA have been conducted on experimental LAA testbeds or through simulations [17–21] and not on real-world LTE-LAA deployments. Thus a data-driven analysis of the current LTE-LAA cell selection mechanisms and their influence on network performance is needed.

It is noteworthy that the unlicensed networks coexist with other incumbents. Thus, it is necessary for the LAA/NR-U small cell to have real-time situational awareness of the wireless medium. Unlike LTE/LTE-A, LAA has to contend with interference from coexisting Wi-Fi APs and rogue transmissions in the shared Unlicensed spectrum. Thus, cell selection at the UE must be guided by network feature relationships (NFRs) learned from network parameters (features) such as signal-to-interference plus noise ratio (SINR), network capacity (Capacity), channel quality indicator (CQI), active user-density, channel usage, back-off indicator, *etc.* However, apart from the overhead of wireless sensing for situational awareness, storing large volumes of network data and learning feature relationships from them may impose excessive computational overhead. This is undesirable from the perspective of dense and ultra-dense LAA networks that are time-critical [13]. Thus, it is important to explore if instance-pruning can be successfully done on LTE-LAA operator data by studying the impact of numerosity reduction algorithms on network feature relationships.

The proposed work seeks to bridge this gap by analyzing operator data gathered from LAA deployments to investigate the impact of cell selection on the performance of its Licensed (LTE) and Unlicensed (LAA) components.[1].

4.1.1 Contributions

The primary contribution of this chapter is an operator data-driven approach to investigating challenges in cell selection in LTE-LAA deployments. The feature relationship analysis is conducted on a dataset of 7469 sample points collected from three cellular operators in the Chicago region. The idea is inspired by industry-proposed proprietary solutions that predict cell quality through network data analysis [22,57]. This thesis shows that transmission power or Reference Signal Received Power (RSRP) based cell selection may be simple and efficient but is less suited to LTE-LAA coexistence networks.

The specific contributions of this chapter are delineated below.

- Analysis of the effect of current LAA cell selection mechanisms on network capacity.

[1]The LTE and LAA components of the coexistence system are henceforth denoted as "Licensed" and "Unlicensed," respectively.

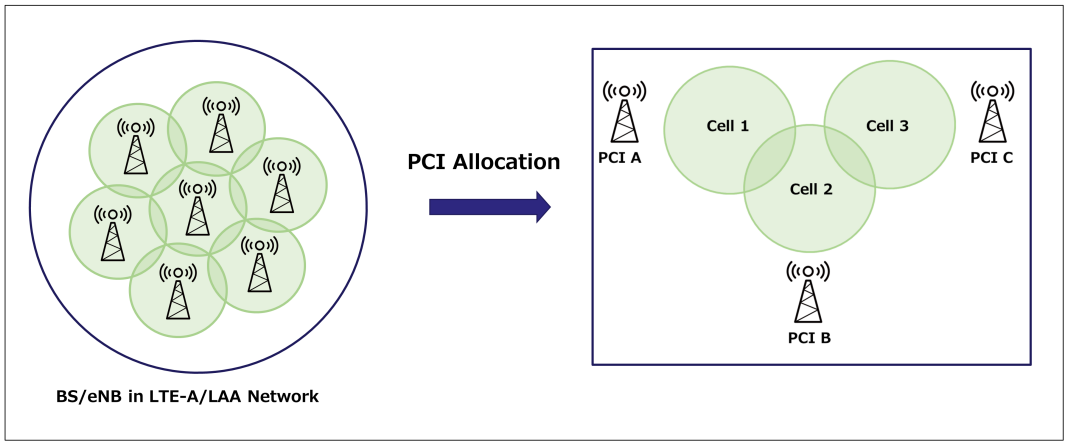

Figure 4.1: PCI Allocation in LTE-A/LAA

- LAA Feature Relationship Analysis: It ascertains if the relationship between network attributes such as SINR, Capacity, *etc.,* is independent of PCI as a categorical variable. LTE-LAA feature relationship is analyzed through several machine learning algorithms viz., Linear, Polynomial, Ridge, and Kernel RBF Regression, Decision Trees, Random forests, Gradient Boost, and Neural Networks.

- Data-driven cell-quality metric and network optimization: It demonstrates that the current cell selection algorithms employed by coexistence operators are not optimal. A cell-quality metric derived from network feature point relationships is used to improve the solutions of two state-of-the-art network optimization formulations.

- Data-reduction and feature relationships: Finally, it explores if the volume of operator data to be analyzed for cell selection can be reduced so as to accelerate cell selection while maintaining feature relationship validity. Two data numerosity reduction techniques, *viz.,* random sampling and k-medoids clustering are applied to both Licensed and Unlicensed components.

Concrete inferences are drawn on several new aspects of the LTE-LAA system, including differing characteristics of Licensed and Unlicensed components, the nature of feature relationships, and the choice of learning algorithms.

The next section presents the state-of-the-art in LTE-LAA cell selection and highlights the open challenges. For an overview of LTE cell-selection mechanisms, please refer to Chapter 2.

4.2 Related Research Work

This section presents the role of PCI, contrasts cell selection in LAA and LTE HetNets, and discusses the new challenges and open problems that need to be addressed in LTE-LAA cell selection.

4.2.1 Role of Physical Cell ID

Increasing network density and the rapid growth in small cell installation have presented new architectural and optimization challenges in LTE-LAA deployments. Further, as the number and density of small cells rise dramatically, it is necessary to devise a reliable and efficient means to identify these cells for self-configuration. The need for seamless network configuration/re-configuration and uninterrupted service to the user equipments (UEs) has spawned the idea of Self-Organizing Networks (SON) [18].

In a SON, the problem of physical layer identification of a cell in LTE-A/LTE-LAA/NR-U is solved through its physical cell ID (PCI). The PCI serves as the cell identity during cell selection when the UE is switched on, or during a handover, [56]. A PCI value is generated using two frequency synchronization signals *viz.,* the Primary Synchronization Signal (PSS) and the Secondary Synchronization Signal (SSS). A UE needs two signals to achieve time domain radio frame synchronization, subframe synchronization, slot synchronization, and symbol synchronization. They are also necessary for the determination of the center of the channel bandwidth in the frequency domain. PSS can take the values 0, 1, and 2, while SSS lies in the range of 0 to 167. Together, they generate a PCI value that lies between 0 and 503, through the expression [(3×SSS)+(PSS)]. For example, in Figure 4.1, Cells 1, 2, & 3 are allocated non-conflicting PCI values "A", "B", & "C," respectively, in the range of 0-503. However, given that there are only 504 unique values, PCIs are reused through strategic network planning to efficiently identify BSs and eNBs.

As a result, PCI search, selection, and attachment is a critical procedure in LTE-LAA/NR-U coexistence networks and is vital for delivering the guaranteed QoS to the end-user [18]. Improper or unplanned PCI allocation will lead to increased interruption of the Reference Signal (RS) which will in turn adversely impact signal coverage.

Solutions to cell selection problems in LTE/LTE-A networks have been proposed by both academia [18, 62] and industry [22, 57]. However, there are several open challenges to cell selection in LTE-LAA/NR-U coexistence which are discussed ahead. This chapter addresses some of these problems by analyzing LTE-LAA deployment data from three major cellular operators and demonstrates the impact that PCI has on LAA network capacity and feature relationships.

4.2.2 Cell selection: LAA Coexistence vs. LTE HetNets

Since the impact of cell association on LTE HetNet performance is well known, it ought to guide operator cell selection protocols [57]. However, traditional LTE HetNet cell association is generally SINR and transmission power based. Though several studies have suggested that metrics such as traffic load, QoS, and battery consumption should be considered during attachment and handover, due to practical reasons, the operator cell selection mechanism is primarily SINR driven [58]. A recent study also shows that handover and cell selection mechanisms in AT&T, T-Mobile, and Sprint HetNets are heavily dependent on SINR [59]. This simple approach works because LTE HetNets are not adversely affected by interference from external sources. Operators possess exclusively dedicated portions of the

Licensed spectrum and only have to address the challenges of internal co-tier and cross-tier interference through centralized or distributed solutions [60].

LTE-LAA networks are characteristically different as there is additional interference from external Wi-Fi sources, which can not be controlled and drastically impacts the SINR. Hidden node problems, mobile hot spots, and dense network scenarios also exacerbate the adverse impact of interference on SINR in an LAA system [87, 89]. Particularly in dense scenarios, radio resources are not always guaranteed to LAA. Further, interference from external Wi-Fi transmissions will cause the SINR at the LAA device to fluctuate continuously, and a cell selection decision based entirely on SINR will cause frequent disconnections and re-attachments [96]. Thus, a simple SINR-driven cell selection will lead to poor LAA network performance.

For efficient cell attachment and resource allocation in LTE-LAA, additional information associated with PCI is vital to ascertain cell quality. For example, when LTE and LAA share the same backhaul, *i.e.,* have a common PCI, resource splitting can be done more efficiently. It is also noteworthy that an LAA cell has to compete with other femto cells and macro cells for a limited number of PCIs, leading to a higher frequency of PCI collisions and PCI confusions [18].

The role of PCI in cell selection is also important from the point of view of deployment architecture. In the current coexistence deployments in the downtown Chicago region, it was observed that LTE and LAA components may have the same PCI or different PCIs. To minimize feedback delay from the UE and facilitate carrier aggregation in unlicensed coexistence, LTE and LAA cells are placed in close proximity and may share the same PCI. However, the Licensed and Unlicensed carriers may be camped on cells with different PCIs as well. In the same PCI architecture, the coexisting LTE and LAA components share a common backhaul, which is more suited for the splitting of LTE and LAA data and packet aggregation. However, the different PCI architectures may operate differently leading to a variation in network performance and end-user QoS. Therefore, the cell-selection decision may be influenced by the deployment architecture a UE is active in.

This chapter demonstrates that cell quality has a definitive impact on LTE-LAA coexistence network performance and that cell selection must be motivated by metrics based on real-time data and not SINR alone. The proposed network optimization solution takes PCI information into consideration, which when compared to the baseline models helps to improve the optimal results.

4.2.3 LAA Cell Selection: Open Challenges

Investigating cell selection and its impact on unlicensed coexistence networks is highly relevant as they differ characteristically from the existing LTE HetNets. While a significant research effort has been dedicated to optimal cell selection in LTE, LTE-A, and LTE HetNets, the impact of cell selection in LTE-LAA networks remains largely unexplored [21, 92, 93]. Moreover, the existing work on cell association in coexistence networks is validated on network prototypes or through simulation [17–20].

One reason is that LTE-LAA/NR-U deployments are still in their early stages and were not widely

available, although that situation is rapidly changing. Secondly, LAA cell selection mechanisms will evolve over time as the solutions based on SINR and signal strength gradually prove to be less suitable. Solutions similar to LTE HetNets are expected to be rolled out by industry players like Ericsson, whose micro Radio 2205 [97] is the radio primarily used in most 5GHz band coexistence LAA deployments.

Currently, a data-driven approach that may facilitate an informed cell selection by the UE in the unlicensed band is lacking in the research literature. This gap can be bridged by investigating the impact of PCI (cell selection) on the relationships between system variables in an unlicensed network. The relationships between network feature points such as Capacity, SINR, Bit Error Rate, *etc.,* are generally investigated through machine learning algorithms [9].

More importantly, cell selection based on some measure of recent cell quality or cell performance is likely to reduce cell association time and enhance network performance [22,57]. This chapter amply demonstrates this aspect by using a data-dependent cell-quality metric in network optimization. The next section discusses the data gathering and extraction exercise from public LAA deployments.

4.3 LAA Operator Data Gathering and Extraction

LAA deployments are the precursor to 5G-NRU systems that will soon be publicly available. Being the first commercially available unlicensed cellular standard, there are several challenges and problems that are unique to the LAA networks. Analysis of network data can reveal new insights that can help improve not just the performance of LAA networks but also of unlicensed cellular systems in the 6 GHz band.

Greater access to a real-world network dataset adds value to the research community and society at large in two ways. One, it makes it possible to leverage AI/ML to analyze the data and answer a variety of questions on network performance formulated as a classification or a regression problem. Researchers can utilize the LAA network dataset to predict network performance (e.g., network Throughput) with confidence through the recorded Phy layer parameters (features) such as EARFCN, RSRP(LTE), PCI, PLMN, Band, TAC, ECellID, SINR, BLER, Ant eNB T/Rx, Transmission Mode, Rank, RB, CQI, MCS, etc. Two, it often leads to new insightful findings about current deployments, which can help operators, researchers, end-users, and policymakers make informed decisions. Let's discuss each of these value propositions in some detail.

The democratization of data access is constrained by geographical proximity to state-of-the-art networks and the high cost of network monitoring tools and applications. Moreover, researchers have to contend with the usual challenges in data-sharing, which include, and are not limited to, data management, data security, and regulatory constraints. Further, even though cellular operators and industry professionals have access to their own network's data, it creates data silos, reducing the gains of collaborative research.

Overcoming these barriers to democratic and universal access to cellular network data requires low-

cost gathering, accurate extraction, and periodic release of data. This chapter makes a contribution towards these goals by sharing a dataset on public Licensed Assisted Access (LAA) networks [98].

Table 4.1: A list of cellular networking monitoring tools used by researchers

Monitoring App	Subscription Cost	Iperf Traffics	Root Access	QXDM Logs	4G and 5G	CSV Export	Spectrum
XCAL [99]	High	Yes	Yes	Yes	Yes	Yes	Licensed and Unlicensed
Qualipoc [100]	High	Yes	Yes	Yes	Yes	Yes	Licensed and Unlicensed
NSG [101]	High	Yes	Yes	Yes	Yes	Yes	Licensed and Unlicensed
SigCap [5]	Open-source	In Progress	No	No	Yes	Yes	Licensed and Unlicensed
CellInfo [102]	Open-source	No	No	No	Yes	Yes	Licensed and Unlicensed
FCC [103]	Open-source	Yes	No	No	Yes	Yes	Licensed and Unlicensed

4.3.1 LAA Dataset: Relevance and Challenges

It follows from the discussion thus far that a dataset from public LAA deployments comprising important network parameters is of great relevance. However, it is also a challenging task to create such a dataset.

4.3.1.1 Relevance and Value-add

The released LAA deployment data [98] will add a lot of value by helping the wider research community (a) Identify new challenges in unlicensed coexistence and spectrum sharing and (b) Propose data-driven solutions for existing and future unlicensed networks. Innovative AI/ML-based solutions may also be included in future specifications by standardization bodies. The LAA network dataset being released may potentially complement the primary incumbent network database. This seems necessary according to the report of the Global System for Mobile Communications Association, the international body that represents the interests of cellular operators. GSMA states, "(Spectrum) Sharing will only be useful for operators if the proposed band is harmonized for mobile use." [6]. It also calls upon the regulators for simple and investment-friendly coexistence and sharing frameworks that (a) Support reliable and high cellular QoS (b) Allow operators to voluntarily share their spectrum, and (c) Incentivize incumbents to share unused bands with high demand from other users [6]. To achieve these objectives, regulators and primary incumbents can use the released dataset. It will help develop a more comprehensive understanding of spectrum sharing, vis-a-vis other operational wireless technologies.

Further, the gathered data is from multiple operators, mitigating the problem of data silos. It may also encourage government entities to release their data in the unlicensed or shared spectrum, in the spirit of collaborative research.

Open-source applications like Sigcap, CellInfo, and FCC APP offer some Phy layer information such as RSRP, RSRQ, EARFCN, and PCI. However, for AI/ML-based network analysis, detailed and accurate network information (e.g., Resource Block (RB), SINR, Throughput, etc.) is required which is difficult to get at scale. Thus, creating such a dataset is a non-trivial exercise.

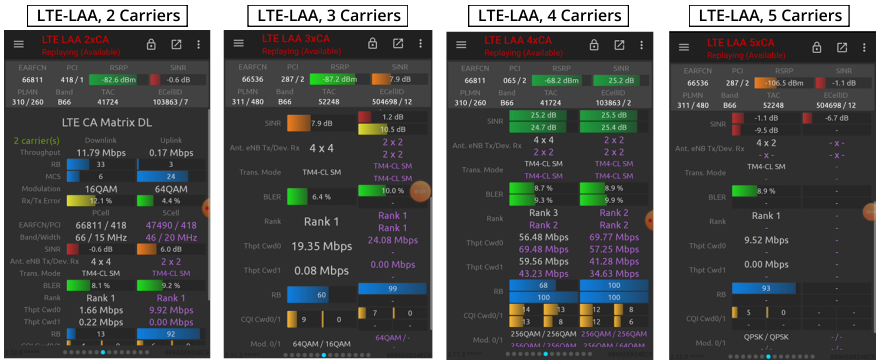

(a) LAA

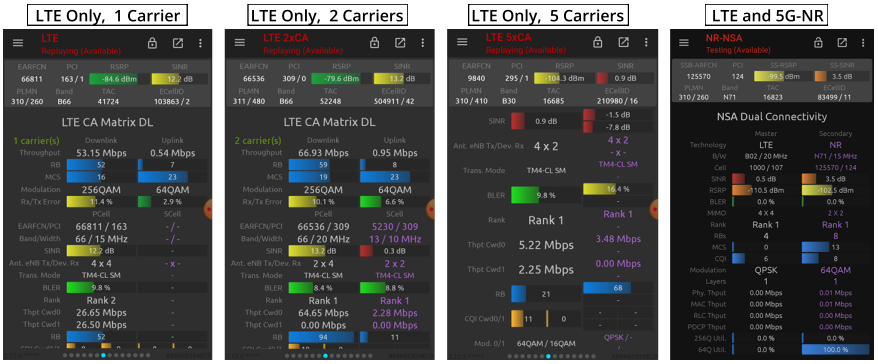

(b) LTE and 5G-NR

Figure 4.2: Relevant Data screen-types of NSG App

4.3.1.2 Challenge: Expensive Network Monitoring Applications

To determine the efficiency of spectrum usage by an operator through AI/ML models, values of important network parameters (features) are required, e.g., SINR, Throughput, RB, Channel Quality Indicator (CQI), Modulation Coding Scheme (MCS), etc. Only a handful of applications can extract these features on mobile devices with the latest chipsets that need to be rooted. A list of subscription-based and open-source tools along with their features is presented in Table 4.1. Paid applications generally offer tiered freemium subscriptions for monitoring and exporting network data. The free versions have limited utility, e.g, Network Signal Guru (NSG) does not currently allow 5G-NR monitoring in the free tier. The basic subscriptions come with monitoring capabilities and can range from tens to

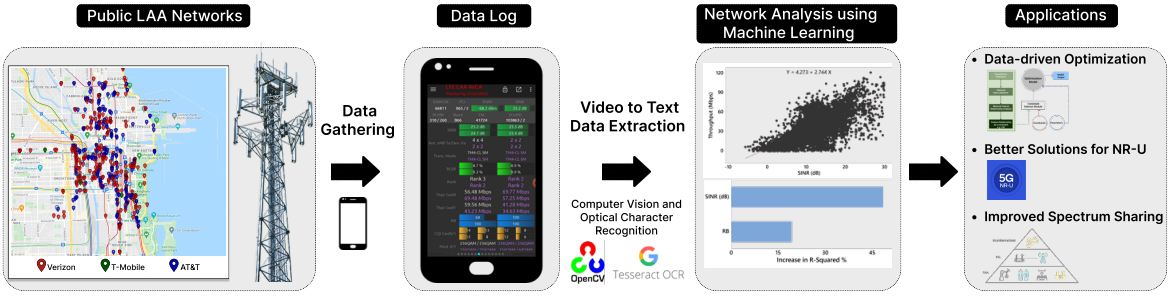

Figure 4.3: Data Gathering and Extraction for AI/ML Analysis

hundreds of dollars per month. However, for AI/ML analysis and modeling, network data is required at scale, typically in multiple thousands of samples. To be able to export the gathered data into a format suitable and sufficient for AI/ML analysis these applications charge up to tens of thousands of dollars every year. For example, Xcal, may cost up to $50 thousand for a year-long subscription. A plausible reason for the high cost is that cellular operators are secretive about their data as it could be leveraged to draw inferences on their proprietary technology and strategic processes [8].

However, most chipset vendors such as Qualcomm and cellular operators themselves are often equipped with state-of-the-art network monitoring tools such as QCAT, QXDM, and other applications. On the other hand, academic researchers, especially from the developing world, are denied access to data from the latest unlicensed deployments due to the exorbitant cost of the applications. It is noteworthy, that Mobile Insight [104] and SigCap [5] are very useful open-source applications. SigCap, in particular, is easy to install, displays real-time network information on the mobile device, and allows passive network monitoring [5]. However, NSG was chosen, as it delivers precise information on a larger set of PHY layer parameters and has an overall better interface. Thus, NSG offers a better user experience and functionality for LAA data collection at scale. It also allows for capturing mobility data within the background mode with high stability.

Nevertheless, expensive subscriptions of NSG and other applications, make it virtually impossible for the broader research community to have access to LAA deployment datasets. Our innovative computer-vision-based solution makes it possible to overcome this obstacle by extracting data from NSG screens shown in Figure 4.2 and releasing it to the community for AI/ML analysis.

4.3.2 Data Collection and Extraction

The data was collected in the period 2020–2021 in different areas of downtown Chicago. LAA deployments of three major cellular operators, viz., AT&T, T-Mobile, and Verizon, were considered. Data was collected with both stationary and mobile devices. The overview of the data gathering and extraction process is shown in Figure 4.3. The initial observations were made using multiple tools, some of which are presented in Table 4.1. Network Signal Guru (NSG) application developed by Qtrun Technologies

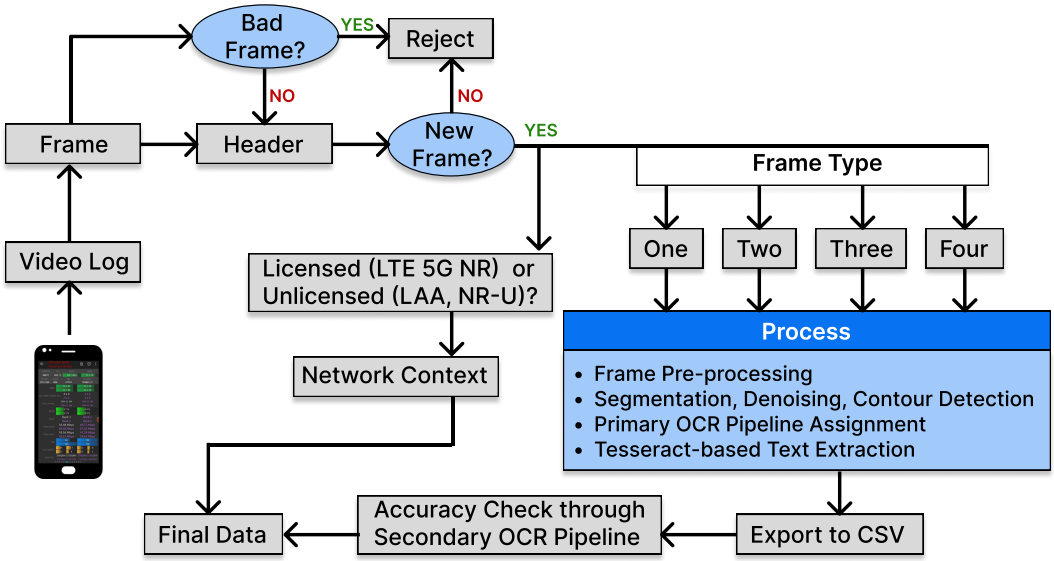

Figure 4.4: Schema of the Data Extraction Process

was selected as the primary data gathering tool for this dataset [101]. NSG supports multiple cellular standards such as LTE, LAA, and 5G-NR. Some of the relevant data screens for LTE-only, LTE-LAA, and 5G-NR are presented in Figure 4.2.

It's discernible that NSG provides more detailed information than open-source alternatives such as SigCap or FCC Speed Test. This includes information on bandwidth, signal strength, Physical Cell ID (PCI), resource blocks allocated (RB), throughput, Modulation Coding Scheme (MCS), Rank, etc. While it may suffice to make note of the observed data manually for network monitoring purposes, data-driven network solutions require thousands of samples for reliable modeling and prediction of network performance. Unfortunately, NSG doesn't permit extracting this data in the free tier of its freemium model. In the basic subscription tier, NSG allows capturing the monitoring session as an encrypted log in DLF format which can only be decoded by the NSG application on another device with a basic subscription. However, retrieving data in a file format desirable for data analysis such as ".CSV" or ".txt," is only possible with a more expensive subscription. This essentially prevents easy and affordable access to PHY layer data for AI/ML modeling and analysis.

To extract LAA data at scale for research and make it available to the wider research community, a solution based on computer vision and optical character recognition was engineered. The high-level schema of the data extraction system is shown in Figure 4.4. The rendering of the encrypted log was converted into a video and then into individual frames. Unique frames with the desirable frames were then identified and processed through our extractor built using the computer vision and deep-learning-based tesseract OCR engine.

Building the extraction system was a difficult task for several reasons. The constant change in net-

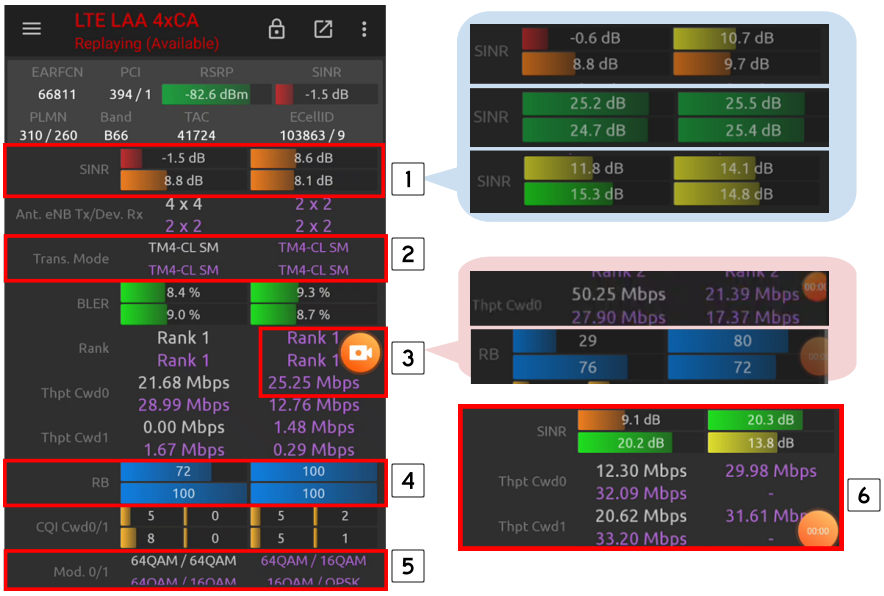

Figure 4.5: Challenges in Data Extraction

work parameters causes frequent toggling of the NSG screen. Likewise, the constant fluctuations in parameter values drastically alters the user interface making the frame too dynamic for a generic solution to process accurately. Our LTE-LAA monitoring logs consist of seven different frame screens/layouts with similar fields. Thus network context, i.e., LTE or LTE-LAA or 5G-NR, number of carriers, etc., needs to be learned on the fly and data must be extracted based on the context. Further, most parameter fields on the NSG frame are unique entities from the perspective of image processing and OCR pipelines, requiring specific techniques for near-perfect accuracy. A sample frame highlighting the major challenges to high extraction accuracy, numbered from one to six, is presented in Figure 4.5. The challenges include (1) Different background colors with varying levels of overlap for a single field requiring fine-tuned image processing and contour detection (2) Different text colors requiring different image-processing pipelines (3) Elements of UI overlapping parameter values requiring custom-tailored denoising (4) Identifying narrow strips of data fields in a toggling frame (5) Partial or cut-off fields (6) Multiple problems in the same field: missing data, different colors, varying background overlaps over values and noise.

The data extractor shown in Figure 4.4, was designed to overcome these constraints, ensure high accuracy, reduce data wastage, work across network types and frame types, and allow extraction at scale. Despite the multiple challenges, the extraction system works remarkably well with close to 100% accuracy. It also weeds out irrelevant frames and duplicate frames, speeding up the extraction process. Over 10000 samples are extracted with one or more of the following parameters EARFCN, PCI, RSRP, SINR, PLMN, Band, TAC, ECellId, SINR, Ant. eNB Tx, Trans. Mode, BLER, RANK, Throughput

Cwd0/Cwd1, RB, CQI Cwd0/Cwd1, and MCS [98].

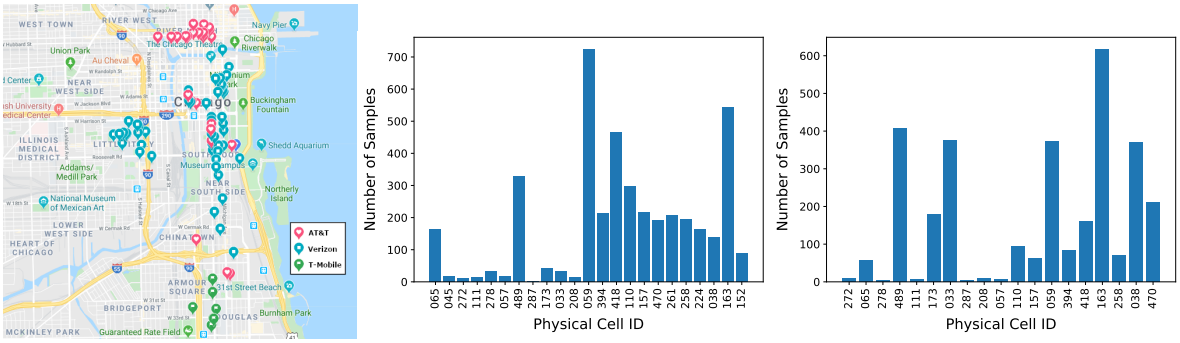

(a) LAA Deployments in Chicago (b) Unlicensed PCIs (c) Licensed PCIs

Figure 4.6: LAA Deployments and PCI Sample Sizes

4.4 Research Methodology and Metrics

This section discusses the research methodology and a detailed description of machine learning algorithms used to analyze the extracted network data.

4.4.1 Operator Data Description

The LAA operator data used in the analysis presented in this chapter is gathered from unlicensed deployments of AT&T, T-Mobile, and Verizon in the downtown Chicago region shown in Figure 4.6 (a). The LTE-LAA dataset has 7469 samples from the three operators and is large enough to make reliable inferences. In the extracted dataset, 59.94% samples are of Unlicensed PCIs and the remaining belong to Licensed PCIs. The sample sizes of significant Licensed and Unlicensed PCIs are shown in Figures 4.6 (b) and 4.6 (c), respectively.

4.4.2 Methodology and Metrics

The LTE-LAA cell selection analysis employs eight supervised machine learning techniques *viz.,* Linear regression, Ridge Regression, Kernel Ridge (RBF) Regression, Multivariate Polynomial Regression, Decision Tree, Random Forest, Gradient Boost, and Feed Forward Neural Network. This allows operator data to reflect the nature of the relationship between the network feature points, rather than fitting the real-world data onto an assumed theoretical function.

The feature relationship equations for network optimization are obtained from Multivariate Polynomial regression. Thereafter, the learning algorithms are subjected to *k-Fold Cross-validation (kCV)*, where $k = 5$. The training-testing approach to feature relationship analysis does not yield accurate

results [9]. kCV is a more rigorous approach to validating feature relationships through supervised learning.

For a more comprehensive and accurate analysis, three categories of the LTE-LAA operator data were considered, *viz.,* Combined (Unlicensed and Licensed coexistence data), Licensed coexistence, and Unlicensed coexistence. These data categories were analyzed through several machine learning algorithms to ascertain (a) the impact of PCI on network performance, and (b) how PCI-specific feature relationships can be leveraged to optimize it further. Feature relationships for models "With PCI" as a categorical parameter are compared to the models where PCI is not considered, denoted by "Without PCI." The objective is to understand how cell selection impacts the Licensed and Unlicensed components of an LTE-LAA coexistence system.

After studying the impact of cell selection at the LTE-LAA component level, a more granular analysis at the level of individual cells is carried out. The motivation is to ascertain if PCI-specific network feature combination analysis may yield a reliable quantitative measure of cell quality which can enhance cell selection mechanisms in coexistence networks. Finally, operator data is subjected to non-parametric *numerosity reduction* through sampling and clustering techniques while maintaining high relationship model validity.

In regression and classification, R-sq is a measure of the ability of the predictor (e.g., SINR) and categorical variables (e.g., PCI) to explain the response variable (e.g., Capacity). In this chapter, the magnitude of R-sq is considered to be the **Validity** of the feature relationship model, and the two terms are used interchangeably. Model **Validity** is used to explain the impact of PCI, and it also serves as a measure of cell quality for efficient cell association.

4.4.3 Machine Learning Algorithms for Relationship Analysis

The feature relationships within the gathered LAA operator data can be modeled as a regression problem to estimate network capacity using SINR and PCI feature points. Let N be the number of training points and D be the dimensionality of the feature vector. Then the network data can be represented as $\{\mathbf{x}_i, y_i\}_{i=1}^{N}$, where $\mathbf{x}_i \in \mathbb{R}^D$ is the feature vector and $y_i \in \mathbb{R}$ is the ground truth value for i^{th} training point. The objective is to learn a mapping $f : \mathbf{x}_i \rightarrow y_i$ where x_i denotes SINR and PCI (predictor) and y_i denotes network capacity (response). The following basket of algorithms is considered for the analysis:

- **Ordinary Least Squares Linear Regression**: This algorithm tries to learn a linear mapping by solving $\arg\min_{\mathbf{w},b} \sum_{i=1}^{N} ||(\mathbf{w}^\top \mathbf{x}_i + b) - y_i||_2^2$. Here, $\mathbf{w} \in \mathbb{R}^D$ is the weight vector and $b \in \mathbb{R}$ is the bias term.

- **Ridge Regression**: Ridge Regression improves over Ordinary Least Squares Linear Regression by introducing an $l2$-regularization term. The aim is to learn a linear mapping by solving $\arg\min_{\mathbf{w},b} \sum_{i=1}^{N} ||(\mathbf{w}^\top \mathbf{x}_i + b) - y_i||_2^2 + \alpha \mathbf{w}^\top \mathbf{w}$. Here, $\mathbf{w} \in \mathbb{R}^D$ is the weight vector, and $b \in \mathbb{R}$

is the bias term as defined earlier. Moreover, α is a hyper-parameter (set via validation) that controls the weightage of the regularization term.

- **Kernel Ridge (RBF) Regression**: SINR-Capacity relationship is expected to be non-linear [36], which indicates that a non-linear mapping might be more suitable. Kernel Ridge Regression [77] makes use of non-linear transformations such as polynomial and radial basis function (RBF). Its goal is to solve $\arg\min_{\mathbf{w},b} \sum_{i=1}^{N} ||K(\mathbf{w}, \mathbf{x}_i) + b - y_i||_2^2 + \alpha \mathbf{w}^\top \mathbf{w}$. Here, $\mathbf{w} \in \mathbb{R}^D$ is the weight vector, $b \in \mathbb{R}$ is the bias term, and α is a hyper-parameter as defined earlier. $K(a, b)$ is a kernel function that allows to compute dot product in an arbitrary large space without the need to explicitly project features in high dimensional space. In particular, $K(\mathbf{a}, \mathbf{b})$ is defined as $exp(\frac{-||a-b||^2}{2\sigma^2})$ for RBF kernel where σ is a free parameter.

- **Polynomial Regression**: Multi-variate Polynomial Regression (MPR) is a machine learning technique that is almost invariably used for ascertaining the relationship between feature points in the system being analyzed, such as a wireless network [9, 105, 106]. MPR is also considered to be a Kernel Ridge Regression with a polynomial kernel in literature. The only difference is that $K(\mathbf{a}, \mathbf{b})$ is defined as $(\mathbf{a}^\top \mathbf{b} + c)^d$ for polynomial kernel where c is a free parameter and d is the degree of the polynomial.

- **Neural Networks**: Neural Networks [107] learn the mapping as a sequence of feed-forward layers in contrast to hand-crafted kernel functions used by Kernel Ridge Regression. It aims to solve
  $\arg\min_{\mathbf{G}} \sum_{i=1}^{N} ||\mathbf{w}^\top g(\mathbf{x}_i) + b - y_i||_2^2 + \alpha \mathbf{G}^\top \mathbf{G}$. Here, $g := g_1(g_2(..))$ is a sequence of non-linear transformations, *i.e.,* g_1, g_2, *etc.*, $\mathbf{G}$ denotes the model parameters including parameters in function g, the weight is vector $\mathbf{w}$, and the bias term is b. Moreover, α is a hyper-parameter as defined earlier. For example, a neural network with 1-hidden layer can be seen as: $g(x) := \sigma(\mathbf{G}\mathbf{x})$, where σ is a non-linearity such as sigmoid or Rectified Linear Unit (ReLU), and $\mathbf{G}$ is a weight matrix. The number of layers, the number of neurons in each layer, non-linearity, and α are hyper-parameters for the network which are tuned using kCV.

- **Decision Tree**: Decision Trees [108] are another family of algorithms that recursively partition the data points in order to minimize the mean-squared error at each node. Decision trees are especially suitable for applications involving categorical features. The *depth* of the tree is a hyper-parameter determined via kCV. Moreover, Minimal Cost-Complexity Pruning [108] is used to avoid overfitting.

- **Random Forests**: Here, an ensemble of decision trees is used in order to reduce variance and improve performance on the test set. In particular, Random Forests [109] use the *bagging strategy* to sample the training set for each tree. Finally, the predictions of each tree are combined at test time. The number of learners, *i.e.,* trees, the number of samples in bootstrapping, *etc.,* are the

hyper-parameters for this algorithm in addition to hyper-parameters for a single decision tree regressor, which are tuned via kCV.

- **Gradient Boosting**: Another way to learn an ensemble of trees is to use the *boosting strategy* [110] instead of bagging. It learns multiple decision trees in succession, where more emphasis is given to the training points where the model is performing poorly. Similar to Random Forests, the number of trees, number of samples used to train each tree, *etc.*, are the hyper-parameters for this algorithm in addition to hyper-parameters for a single decision tree regressor, which are tuned through kCV.

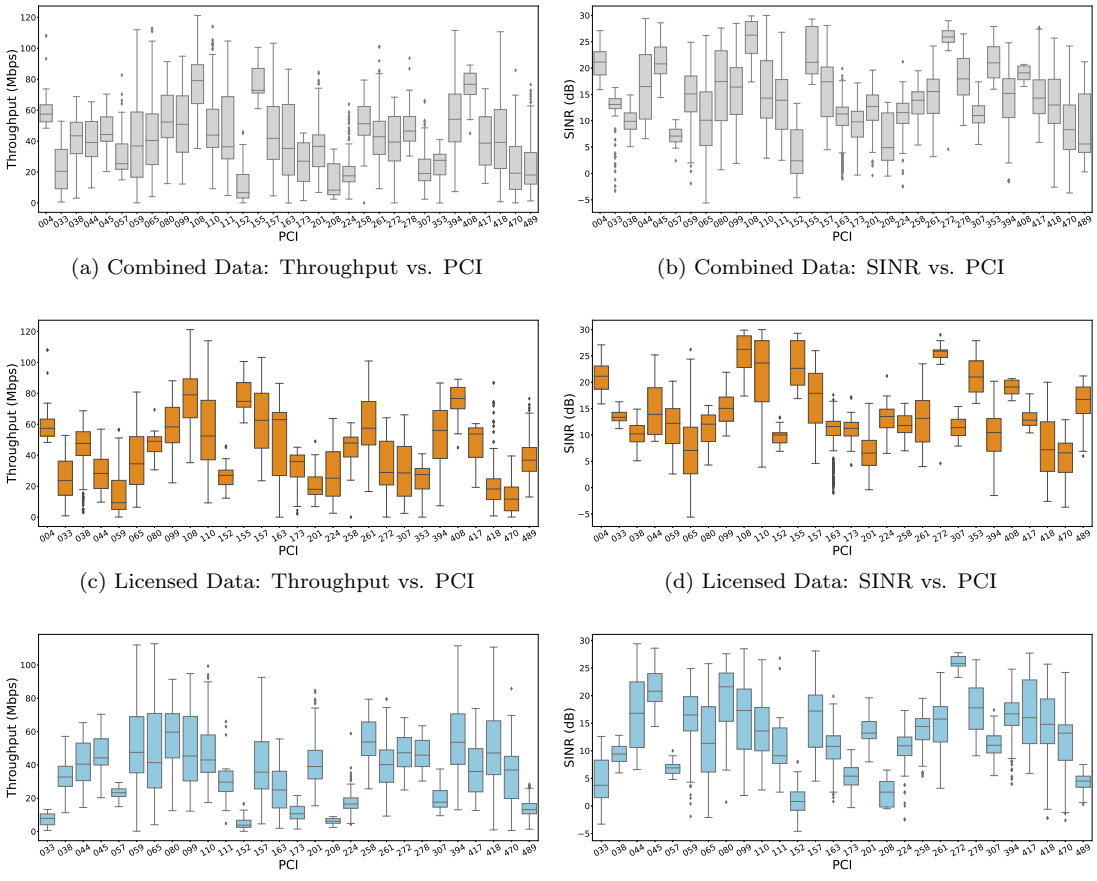

(a) Combined Data: Throughput vs. PCI

(b) Combined Data: SINR vs. PCI

(c) Licensed Data: Throughput vs. PCI

(d) Licensed Data: SINR vs. PCI

(e) Unlicensed Data: Throughput vs. PCI

(f) Unlicensed Data: SINR vs. PCI

Figure 4.7: PCI and Coexistence Network Feature Points

4.5 PCI & LAA Coexistence Capacity

A detailed description of cellular data analysis and the impact of PCI on coexistence network capacity is presented in the following subsections.

4.5.1 Capacity Variability with Cell Selection

Let's begin with the analysis of how the distribution of the total network capacity varies with PCI values. Instead of simplistic measures of central tendency such as mean, mode, or median, the boxplot is used to show the dispersion and variability of Throughput with PCI. A boxplot offers a more detailed visual representation of data through the interquartile range (25^{th} percentile to 75^{th} percentile), outliers, and median, among other relevant information.

The Throughput-PCI variability analysis for the combined coexistence data is presented in Figure 4.7 (a). The distribution of Throughput is not uniform across PCI, which is evident from the varying interquartile ranges and fluctuating median values. If the dispersion patterns of Throughput and SINR vis-à-vis PCI are similar, then an argument can be made that the fluctuation in network performance is dependent on the signal strength and quality, and the apparent impact of PCI is visible simply because a dependent variable (Throughput) was treated as an independent variable. No concrete conclusions can be made, and further variability analysis of SINR with PCI is required.

Hence, Figure 4.7 (b) presents an SINR-PCI variability analysis for the same list of PCIs. By comparing the two distribution chapters/chapter3/BoxPlots/, prima facie, it can be discerned that for some PCIs, a high median SINR does not correspond to a high median Throughput, and the reverse is equally true. This trend is more prominently visible in both Licensed and Unlicensed components of the operator data, shown in Figures 4.7 (c), 4.7 (d), 4.7 (e), and 4.7 (f). For example, for PCI 059, the Licensed median SINR is high ($\approx$ 13 dB), but the corresponding Licensed median Throughput is relatively quite low ($<$ 10 Mbps), while for PCI 470 a comparable Throughput median is observed at a much lower median SINR. In Figure 4.7, a greater impact of PCI is visible on the Licensed coexistence data. For PCIs 155, 353, 004, and 408, the standard deviation in network capacity is 23.90, while that in SINR is only 6.06. These four cells have comparable median Licensed SINR values, but their median Throughput values differ significantly.

A similar trend can be found through outlier analysis. While cell 418 shows outliers in Licensed network capacity above the 1^{st} quartile, no outliers are detected in the SINR data. Interestingly, cell 224 has outliers in the Unlicensed data for both Throughput and SINR, but they lie at opposite ends of the data range.

The data shows that cell selection has an immense bearing on network performance. A possibility of the inexplicable variation in feature points could be the dependence on variables that have not been accounted for, such as resource block (RB) allocation. For example, the observed RB allocation to a UE in the Unlicensed spectrum was very close to 100, on average. This can be attributed to low initial

adoption of LAA devices at the time of data gathering. This will certainly change with the increase in LAA network penetration and a decrease in LAA smartphone prices. While the scope of this chapter is limited to determining the impact of PCI selection on network capacity, it sufficiently demonstrates that this impact is real and can not be attributed to variables (such as RB) external to the feature combination considered.

4.5.2 Multivariate Regression with PCI as Categorical Variable

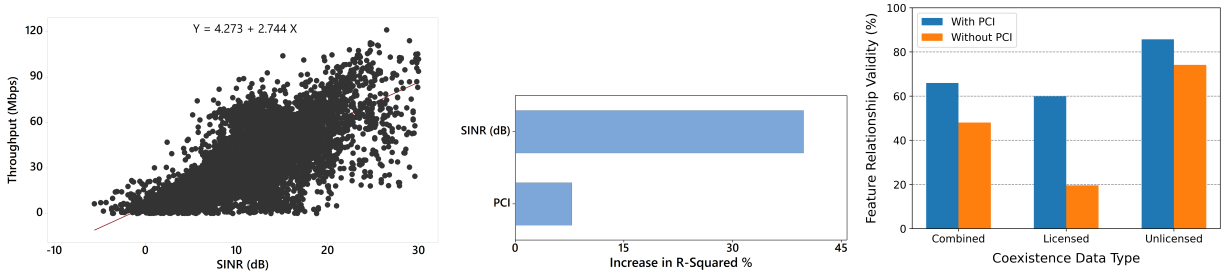

(a) Capacity-SINR Relationship (b) Impact of PCI on Validity (c) Relationship Validities

Figure 4.8: Combined Data Feature Relationship Analysis

If the SINR-Capacity relationship can be better explained with PCI as a categorical variable, this will offer definitive proof that the PCI selection process can be further improved. Figure 4.8 illustrates the SINR-Capacity relationship with and without PCI as a categorical variable and the impact of PCI on the Validity of the model. Two inferences can be made from the spread of the data in the scatter-plot of Figure 4.8 (a). First, the relationship of this feature combination may depend on other system variables. Second, analyzing the Licensed and Unlicensed components of the coexistence operator data *combined* may not be ideal. A low model validity of 48.06 gives strength to these suspicions, and both can be confirmed through further regression analysis. Multivariate polynomial regression with PCI as an additional predictor leads to a 36% increase in model Validity (65.32). Figure 4.8 (b) compares the impact of SINR and PCI on Validity, and it is discernible that the effect of PCI is significant.

To evaluate the inference on coexistence data segregation, this analysis is repeated for Unlicensed and Licensed data. The Validity of the baseline (without PCI) SINR-Capacity relationship for Combined, Licensed, and Unlicensed data is presented in Figure 4.8 (c). When PCI is not considered, the Validity of models is quite low. R-sq of the SINR-Capacity feature association varies considerably, being quite high for the Unlicensed data and low for Licensed data. The noteworthy point is that regardless of the Validity of the baseline model, upon using PCI as a categorical parameter, there is a significant increase in Validity. The R-sq doubles for Licensed data and shoots up by as much as 15.58% for Unlicensed data (Figure 4.8 (c)). This conspicuous improvement in model Validity is irrefutable evidence of the impact of PCI on coexistence network data. Next, these observations are validated through several machine learning algorithms.

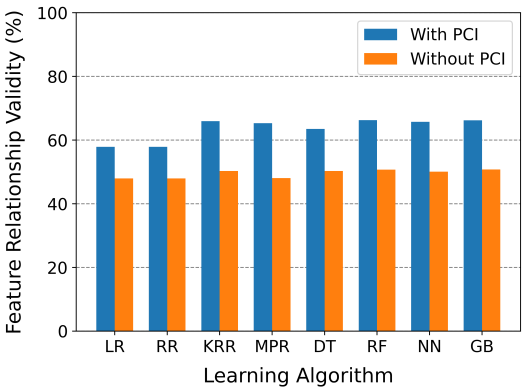

Figure 4.9: k-Fold Cross Validation of Combined Coexistence Data

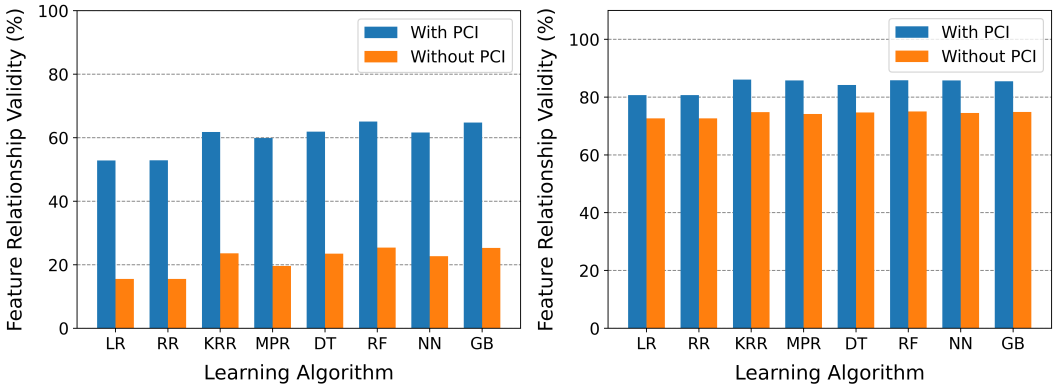

(a) Licensed Coexistence Data

(b) Unlicensed Coexistence Data

Figure 4.10: k-Fold Cross Validation of Licensed and Unlicensed Components

4.5.3 Validating the Role of Cell Selection

The observations made through multi-variate polynomial regression (MPR) are validated through the seven ML algorithms *viz.,* Linear regression (LR), Ridge Regression (RR), Kernel Ridge (RBF) Regression (KRR), Decision Tree (DT), Random Forest (RF), Gradient Boost (GB), and Feed Forward Neural Network (NN). The results for the combined LTE-LAA data are presented in Figure 4.9 and its Licensed and Unlicensed components in Figures 4.10 (a) and 4.10 (b), respectively. Observations are made on the following three themes.

4.5.3.1 Feature Relationship Model Validity

It can be discerned that the SINR-Capacity relationship validity of the LAA data varies with the component of the LTE-LAA system being analyzed. Thus, a comparison of the model Validities for the three data categories for "With PCI" and "Without PCI" scenarios is presented first.

With PCI Scenario: For the Combined LAA data the R-sq averaged over all learning algorithms is 63.61. Upon segregation, a visible difference between Licensed and Unlicensed components can be observed. Relationship Validity of Licensed data is slightly lower than Combined data for all algorithms and is 60.13 on average. SINR-Capacity feature relationship is the strongest in the Unlicensed spectrum, with a high R-sq of 84.30.

Without PCI Scenario: The trends observed in "With PCI" are seen here as well, with R-sq decreasing in the sequence: Unlicensed>Combined>Licensed. However, analysis of individual component data reveals an interesting finding. The validity of Unlicensed data models is still high (74.16 on average), while that of the Licensed data drops so low (21.40 on average) that the SINR-Capacity relationship appears to be very weak without cell association information.

4.5.3.2 Impact of PCI on Feature Relationships

Next, the impact of cell selection on each data category is analyzed by comparing the model Validities of "With PCI" and "Without PCI" for each category. Feature relationship analysis of Combined LAA operator data shows a clear impact of PCI on SINR-Capacity relationship (Figure 4.9). With PCI as a categorical parameter, the Validity of feature relationship models improves across all learning algorithms, with an average rise of 28.37%. Segregation of the LAA data into its Licensed and Unlicensed components offers even more valuable insights into the LTE-LAA coexistence system. For Licensed data (Figure 4.10 (a)), impact of PCI is far more pronounced than Combined and Unlicensed data. When PCI is considered while learning feature relationships, the average Validity for Licensed almost triples to 60.13. In sharp contrast, for the Unlicensed data, the average increase in R-sq is only about 13.65%. When seen together with the analysis presented in 4.5.3.1, these results seems intuitive. However, it is noteworthy that in terms of the absolute magnitude of relationship Validity, while the average value in "With PCI" scenario for Licensed data in itself is not high ($\approx$ 60 on average), the average increase from "Without PCI" scenario is a significant 38.73 points.

Further, the impact of PCI on feature relationships in the unlicensed spectrum is very likely to rise with greater penetration of LAA networks and a consequent rise in LAA device adoption. This can be inferred from the difference in the RB allocation to UEs in LTE and LAA, which were observed to be 41 RBs and 97 RBs, respectively, on average. Since LAA UEs currently enjoy a very high RB allocation, the impact of PCI on network feature relationships seems to be less significant as compared to the LTE component. Consequently, as the LAA UE density increases, RB allocation/device will decrease, and PCI will have a greater influence.

4.5.3.3 Choice of Learning Algorithms

A diverse set of supervised regression and learning algorithms is considered in this chapter. Based on the observed results, the only dominant factor that seems to affect the feature relationship Validity is the classification of algorithms as linear (Linear and Ridge Regression) and non-linear (remaining

six algorithms). An intra-class comparison of algorithms reveals almost identical performance. Thus, the standard deviation of model Validities for the two linear algorithms, for both, "With PCI" and "Without PCI" scenarios of all three data categories is almost zero. It is insignificant for the six non-linear algorithms as well.

In contrast, the inter-class difference (*i.e.,* linear vs. non-linear) is noticeable. Validities for linear algorithms are consistently lower than those of non-linear algorithms and the difference can be significant. For example, a comparison of Linear Regression and Gradient Boost, for the Licensed "Without PCI" scenario shows that the Validity is higher in the latter by 63.19%. A plausible reason is that theoretically, the SINR-Capacity relationship is considered to be non-linear [36]. Thus, non-linear learning algorithms seem to be more suited to fit the data and offer a better R-sq for the relationship than linear models.

However, there is a caveat. In "Without PCI" scenarios for Unlicensed and Combined data, the difference in Validities of linear and non-linear algorithms is 2.76% and 4.97% respectively, on average. Thus, for some scenarios, the non-linear SINR-Capacity relationship can be replaced by a simpler linear function, with a marginal loss of accuracy. This finding holds great relevance to time-critical dense network optimization as a linear SINR-Capacity constraint will offer a near-optimal solution with substantially reduced convergence times [13].

Although the performance of non-linear supervised learning algorithms is comparable, polynomial regression has two distinct advantages. First, it is computationally less expensive than other regression techniques such as DT and RF [111]. Secondly, it provides a feature relationship equation representing the curve along which the data is fit. These factors are relevant to the next stage of analysis, which is concerned with the performance at the level of an individual cell and leveraging cell quality in network optimization.

4.5.4 Inferences from the Analysis

Certain clear patterns emerge from the analysis presented above, which enable us to make reasonable inferences on the following aspects of an LTE-LAA system.

- **Feature Relationship Validity:** The SINR-Capacity relationship is the strongest for the Unlicensed coexistence data, followed by Combined, and Licensed data. The Licensed component in a coexistence network depends heavily on factors such as resource block allocation, which explains the low Validity of the models. In the Unlicensed component, the impact of interference from co-operating and alien Wi-Fi transmissions on the same channel is reflected in the high association of network capacity with SINR.

- **Cell Selection and Validity:** There is an undeniable impact of cell selection on SINR-Capacity validity regardless of the scenario. With PCI as the categorical parameter, feature relationships can be explained much better. In the Licensed component, the improvement with PCI is tremen-

dous ($\geq$ 155%), and the overall model Validity reaches a satisfactory level ($\geq$ 60 for non-linear algorithms). In the Unlicensed component, the accuracy of model Validity improves significantly with PCI, yielding accurate and reliable feature relationships ($\geq$ 84% for non-linear algorithms). Thus, a robust inference can be made that cell selection in coexistence networks plays a crucial role in network performance. Further, it has a substantial quantitative effect on both Licensed and Unlicensed components.

- **LTE-LAA Component Segregation:** For the Licensed data, the SINR-Capacity relationship is relatively weak, but the influence of PCI on this feature relationship is strong. In sharp contrast, for the Unlicensed component, SINR-Capacity is strong, and the impact of PCI is relatively low. The Combined data category obfuscates these differences between the two coexistence network components. Given the distinct feature relationship characteristics, it can be inferred that the operator data must be segregated into its Licensed and Unlicensed components for network analysis and optimization.

- **LTE-LAA Cell Selection:** The cell selection preferences should also be coexistence component-specific. Further, the variation in the impact upon Licensed and Unlicensed components also highlights that the LTE-LAA coexistence environment qualitatively differs from LTE HetNets.

- **Impact of Learning Algorithms:** Even though supervised learning and regression are ideal for learning feature relationships from real-world data, the choice of the algorithm may impact model Validity.

- **Nature of SINR-Capacity Relationship:** Although all learning models have shown it to be non-linear, in some scenarios, the linear models are almost as accurate and can be leveraged to accelerate network optimization.

4.6 Data-driven Cell Selection in Coexistence Networks

Having demonstrated the impact of cell selection and the significant role of PCI as a categorical parameter in the network feature relationships, this section focuses on the performance of individual cells. The analysis ahead only considers the scenario where both LTE and LAA are camped on the *same PCI*, which is the case 80% of the time.

4.6.1 LAA Performance at the Small Cell

Ten small cells are considered with adequate sample sizes. For each of these cells, the feature relationship model equation and Validity are presented in Table 4.2. It can be discerned that the model Validity of the small cells varies drastically. This implies that the cell selection in LTE-LAA coexistence plays a crucial role in determining the end-user experience.

Table 4.2: Feature Relationship Models at the PCI level

PCI	**Unlicensed Coexistence Data**		**Licensed Coexistence Data**	
	Model Equation	Validity	Model Equation	Validity
163	Y = -04.7015 + 2.9321X + -0.0065X^2	30.57	Y = -12.6541 + 10.491X + -0.3854X^2	48.85
059	Y = 25.7038 + -1.9219X + 0.2021X^2	67.90	Y = 6.9259 + -0.129X + 0.0599X^2	11.97
038	Y = 17.3392 + 1.5234X + 0.0092X^2	17.79	Y = 57.36 + -5.6447X + 0.4109X^2	15.54
470	Y = 04.6871 + 1.9025X + 0.0458X^2	69.06	Y = 6.3895 + 0.4035X + 0.0816X^2	18.91
110	Y = 12.6426 + 2.6063X + -0.0102X^2	53.56	Y = 27.4799 + -0.5368X + 0.0793X^2	34.45
394	Y = 05.2298 + 1.5573X + 0.0871X^2	57.16	Y = 22.0641 + 2.6662X + 0.0447X^2	61.22
258	Y = 11.4145 + 2.3327X + 0.0514X^2	71.40	Y = 16.262 + 2.3345X + 0.0051X^2	25.16
261	Y = -07.7242 + 5.0802X + -0.1139X^2	13.70	Y = 47.3413 + -0.6971X + 0.1068X^2	21.30
224	Y = 07.9043 + 0.2954X + 0.0551X^2	37.59	Y = 8.0361 + -0.572X + 0.1536X^2	19.45
201	Y = 58.5143 + -8.2243X + 0.4999X^2	75.60	Y = 8.1803 + 1.4577X + 0.0568X^2	61.39

Validity: R^2 of the model, X: SINR, Y: Network Capacity

Let us consider the *Validity* of a feature relationship model to be the *measure of cell quality* and its ability to meet QoS guarantees. It then follows that cell selection in the coexistence networks is far from desirable despite current best practices. Further, the same PCI value may lead to starkly different network performance in LTE (Licensed) and LAA (Unlicensed) components, *e.g.,* PCI 059. Studying this variation may shine a light on the factors that influence ideal cell selection preferences for the two components, which will likely differ. It also calls for a deeper analysis of the specific PCI scenarios characteristic of the current LTE-LAA coexistence deployment architecture.

4.6.2 Cell Selection through Data Learning

Taking a cue from these inferences, the coexistence operator data is used to derive an approximate measure of the cell quality. The proposed solution considers the **Validity** of the network feature relationship model (SINR-Capacity relationship in this instance) for each cell as a measure of its *quality*. Consequently, a cell with a higher magnitude of SINR-Capacity Validity denotes better cell quality, and should result in lower *Association Time* (AT) and offer high throughput to the UE. This hypothesis will hold if the considered cell quality metric exhibits a direct correlation with cell association time and network performance. To validate this hypothesis, a two-tiered approach is adopted.

First, two state-of-the-art solutions to cell selection and resource allocation in LTE HetNets [19,20] are implemented. Next, a network optimization model based on a 3GPP prescribed bare-bones cell selection approach is implemented. Finally, this thesis proposes a cell-quality-based cell selection optimization model as a Proof-of-Concept (PoC) and compares its performance with the two state-

of-the-art works and the baseline optimization model. Second, the accuracy of PCI-specific Validity as a cell-quality metric is evaluated. This is done by using the network feature relationships corresponding to the metric value as a constraint in the two optimization formulations. The output for the feature relationship models for the ten small cells (Table 4.2) is observed and the thesis ascertains if a correlation between Validity and network performance exists.

Table 4.3: GAMS Simulation Parameters

Parameter	**Value**
LAA Unlicensed transmission power	23 dBm
LTE Licensed transmission power	46 dBm
Operating Frequency LAA	5 GHz
Operating Frequency LTE	Band 66 for Verizon & T-Mobile, Band 2 for AT&T
Bandwidth	20 MHz
LTE Control and Data channels	PUCCH and PDCCH
SINR threshold for cell attachment	-2 dB

*PUCCH- Physical Uplink Control Channel, PDCCH- Physical Downlink Control Channel

4.6.3 Implementation Details

4.6.3.1 State-of-the-art and Proof-of-Concept Implementation

This chapter considers two recent works that seek to optimize the user association, cell selection, and radio resource allocation in LTE HetNets. The first solution achieves these goals by optimizing transmission power and *cell individual offset* and is denoted as OM_1 [19]. The second work (denoted as OM_2) proposes a queuing theory based comparative framework for different cell selection and resource allocation combinations, and then formulates a joint optimization model for user association and resource sharing [20]. Further, an optimization model is implemented for proof-of-concept evaluation. Its objective is to maximize the network capacity by considering the user association and resource allocation split on Licensed and Unlicensed components. While the model architecture is somewhat similar to OM_1, this thesis employs a network data learning-based cell selection approach by considering the SINR-Capacity relationship as the primary constraint. It is referred to as *PoC* henceforth. In addition, a bare-bones LTE cell attachment model based on 3GPP prescribed procedures is also implemented and referred to as *BCM*.

4.6.3.2 Bare-bones Cell Selection Implementation

The bare-bones LTE cell attachment model is based on 3GPP prescribed procedures and is referred to as *BCM*. The UE sends the measurement report every 80 ms to the serving BS. The BS measures

the serving BS as well as the adjacent cell, and based on the outcome, UE will continue to camp on the current BS or perform cell re-selection and camp on the neighboring cell. After a successful attachment, the model allocates the radio resources based on the classical proportional fair scheduling algorithm.

4.6.3.3 Metrics and Methodology

A *regression-inspired optimization* methodology is adopted for evaluation [7, 8, 13, 76, 112, 113]. Consequently, in each cell association optimization model, the resource-heavy constraints pertaining to signal strength and network capacity are replaced with the network feature relationship equations present in Table 4.2. For example, equation (6) in OM_1 and equation 4(b) in OM_2 are replaced by the SINR-Capacity regression equations. The cell selection models are implemented on GAMS [85] based on the simulation parameters in Table 4.3. For each PCI, they generate optimal values for two metrics, *viz., Association Time* (AT) and *Network Capacity* (Capacity).

Table 4.4: Baseline Values for BCM, OM_1, and OM_2

Optimization	**Unlicensed**		**Licensed**	
Model	*AT (s)*	*Capacity (Mbps)*	*AT (s)*	*Capacity (Mbps)*
BCM	5.6	35	5.1	39
OM_1	4.6	26	4.9	28
OM_2	4.8	20	5.1	23

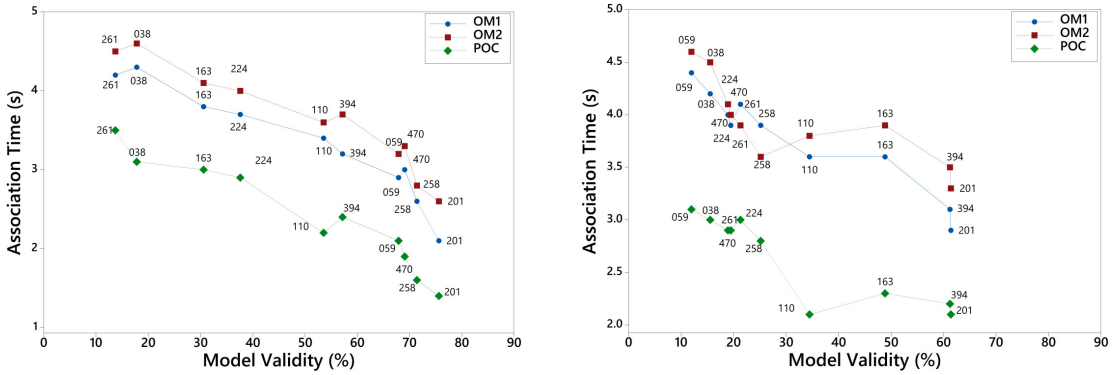

(a) Unlicensed Association Time

(b) Licensed Association Time

Figure 4.11: data-driven cell selection: Association Time Evaluation

4.6.4 Hypothesis Validation: Results & Analysis

A comparative analysis of the three models, *viz.,* OM_1, OM_2, and POC, is presented in Figure 4.11 & Figure 4.12, for Association Time and Network Capacity, respectively. Further, the baseline values

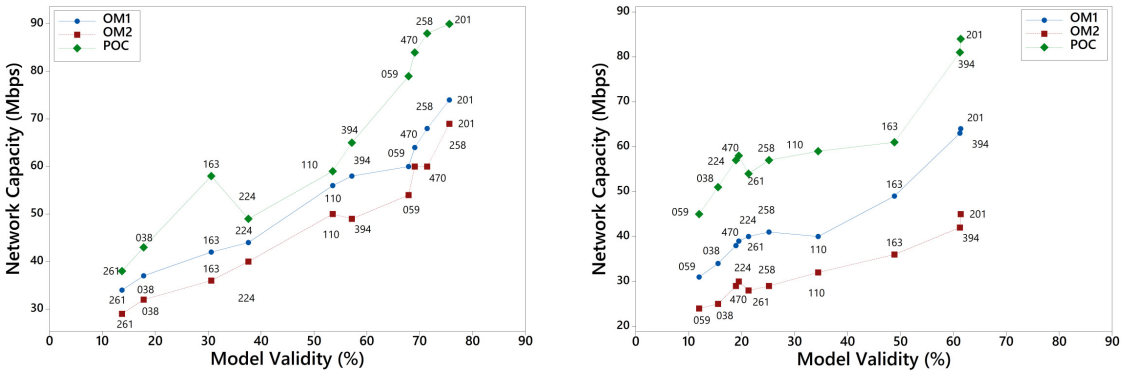

(a) Unlicensed Network Capacity

(b) Licensed Network Capacity

Figure 4.12: data-driven cell selection: Network Capacity Evaluation

for the bare-bones BCM are presented in Table 4.4.

It can be discerned from Figure 4.11 & Figure 4.12 that there is a definitive correlation between model Validity and the two parameters. The time taken for cell attachment should be low when cell quality is high and vice-versa, and this is the trend that can be observed in the results. Network capacity also has an upward graph with rising values of model Validity. The performance of the PoC model is unarguably better than the regression optimized variants of OM_1 and OM_2. The PoC model also outperforms the baseline models in Table 4.4.

POC outperforms OM_1 and OM_2 by 28.35% and 34.89%, respectively, in terms of Unlicensed AT and, 30.68% and 32.72%, respectively, in terms of Licensed AT, on average. Thus association time reduction by PoC is comparable for both components. However, in terms of network capacity, PoC improves predicted Licensed optimal Capacity by 90.41% on average for OM_2 compared to 32.72% average improvement in the Unlicensed Capacity. For, OM_1 however, average Capacity improvement by PoC is comparable for Licensed (39.97%) and Unlicensed (30.06%). Clearly, pivoting the cell selection decision on a cell quality metric derived from network data feature relationship has led to a much reduced cell attachment time.

With respect to the correlation between Validity (as the cell-quality metric) and network performance metrics, *viz.,* AT and Capacity, Unlicensed coexistence component fares better than Licensed. An explanation can be found in the inferences made in Subsection 4.5.4. The multi-variate feature relationship Validity of Licensed data is lower than Unlicensed data. This explains why only one Unlicensed PCI fails to observe the expected trend in Figures 4.11 (a) and 4.12 (a) as compared to two anomalous small cells in the Licensed component illustrated in Figures 4.11 (b) and 4.12 (b). Nevertheless, a direct correlation between Validity and network performance exists for both components.

4.7 Data-reduction and Feature Relationship Validity

The complexity of regression and learning algorithms such as Ridge regression and Neural Networks depends on the number of training points. While a large amount of training data is typically good, it may not be desirable when the model has to be trained within a time budget. This is especially true of dense and ultra-dense LTE-LAA networks where cell selection and handover is time-critical [13]. As we advance to 5G New Radio Unlicensed (NR-U) and with the allocation of 1200 MHz of unlicensed spectrum for coexistence operation in the 6 GHz band by the Federal Communications Commission of USA (FCC), coexistence deployments will only become denser. Thus, learning from large volumes of operator data may have enormous computational overheads that will cause cell selection delays, leading to sub-optimal network performance.

Instance pruning through data numerosity reduction is a probable solution to minimize delays in learning-based cell selection in dense LAA and future NR-U coexistence deployments. Data numerosity reduction algorithms [114] select a subset of data that can be used as a good proxy for the original dataset for learning the LTE-LAA feature relationship. It usually involves sampling a sub-set of training data while keeping test data the same [115]. Numerosity reduction can be accomplished by both parametric and non-parametric techniques, and kCV is usually used for validation.

It is possible to achieve only a marginal drop in model accuracy despite a significant reduction in data size. For example, authors in [115], restrict the loss in model accuracy to 0.5% while reducing the dataset size by 85% on average. However, instance pruning through numerosity reduction is not without its pitfalls. The performance of data reduction is context-specific and depends upon several conditions, including the type of data and weight of attributes. Even more complex are the twin challenges of not removing instances that can help generalize the model and identifying irrelevant attributes [115].

Therefore, to perform reliable instance pruning for cell selection in LAA/NR-U coexistence deployments, the first step is to evaluate popular numerosity reduction techniques through the gathered operator data. The objective is to study the behavior of feature relationship validity as the dataset is pruned for both Licensed and Unlicensed components.

4.7.1 Data Reduction Techniques

In line with our methodology, two non-parametric solutions were deployed *viz.,* random sampling and k-medoids clustering. Thus the data instances can be sampled either "randomly" or by collapsing "similar" training instances into clusters. They are validated through kCV, where $k = 5$. The two techniques are discussed below.

- *Random Sampling:* This strategy assumes that the dataset is independent and identically distributed. Each training instance is sampled with probability p in order to create the smaller training set. Note that $p = K/N$, where K is the size of training subset that is sampled.

- *k-medoids Clustering:* Alternatively, one may choose to reduce the training set size by collapsing similar training instances into a single training instance. In particular, the k-medoids algorithm [116] is deployed to cluster the training points into k clusters. k-medoids is more suited to partition operator data than k-means because it designates actual data points as the center of each cluster. Cosine metric is used to determine the similarity between a pair of data points to arrive at the "medoid" for each cluster, which has the least average dissimilarity to other points in the cluster. The medoid is chosen as the single representative for each cluster, resulting in a new/sampled dataset with the reduced size of k/N where N is the total number of training points in the original dataset.

Please note that sophisticated algorithms including *local density-based instance selection* (LDIS) [117] can also be deployed. However, random sampling and k-medoids Clustering were chosen because an instance pruning algorithm ought to have a minimal computational footprint so as to ensure optimal performance in the downstream task (*e.g.,* learning a mapping between SINR and Throughput)[2].

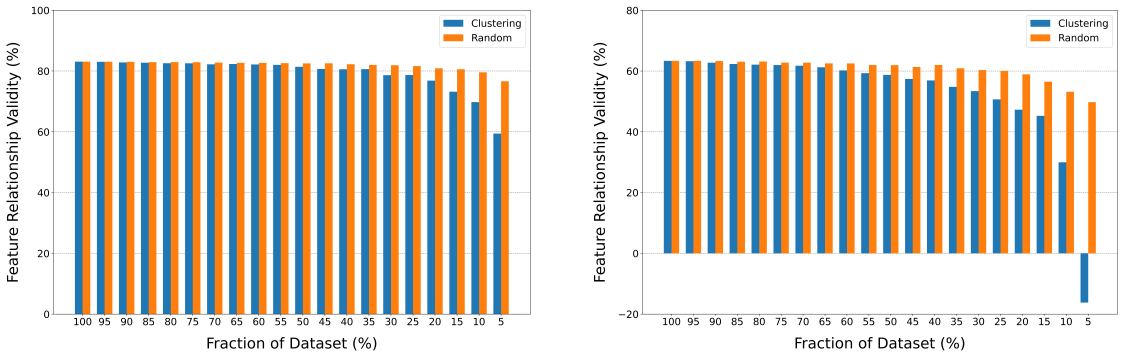

(a) Unlicensed Data Capacity

(b) Licensed Data Capacity

Figure 4.13: Impact of Numerosity Reduction on Feature Relationship Validity

4.7.2 Results and Analysis

Since it is more meaningful to segregate coexistence data, Licensed and Unlicensed datasets were separately subjected to both numerosity reduction techniques. Please note that the data considered is from the scenario where both components are camped on the same PCI. Results are presented in Figures 4.13 (a) 4.13 (b), respectively. The impact on model validity can be analyzed across the following two dimensions.

- *Choice of Pruning Technique*: Surprisingly enough, random sampling performs better than clustering for both Licensed and Unlicensed data. Model Validity reduces at a much lower rate for random sampling than it does for clustering. Further, for both Licensed and Unlicensed, even at

[2]A detailed discussion and analysis of popular instance pruning algorithms can be found in [115] and [117].

5% volume of the original data, the R-sq of random sampling is 49.8 and 76.6, respectively. In comparison, k-medoids clustering leads to a negative Validity of -16.2 at 5% volume of Licensed data exhibiting non-existing feature relationship. The most significant accuracy drop occurs when the data is reduced from 10% to 5%. If Licensed data is considered, this drop is a staggering 154% for clustering as compared to just a 6% accuracy drop in random sampling. Clearly, random sampling outperforms clustering. There are several plausible reasons for this occurrence. First, imbalanced clusters may lead to a skewed distribution of data. Thus, the sampled data may not be independent and identically distributed, resulting in a greater loss in accuracy for the clustering-based sampling. Note that the learning algorithms assume that data points are independent and identically distributed. Second, clustering may require the inclusion of additional relevant system variables such as resource block allocation, channel quality indicator, *etc.*, for the results to be accurate. Therefore, random sampling seems to offer a more reliable means of instance pruning for the SINR-Capacity feature relationship in coexistence deployments.

- *Type of LAA Data*: There are two significant differences between the Licensed and Unlicensed components. First is the magnitude of model accuracy for different fractions of training data. As compared to Licensed, Unlicensed model accuracy is significantly higher for both random sampling and k-medoids clustering at each instance of data reduction. Second, the relative drop in Validity at each instance of data reduction as compared to the earlier instance is also lower for Unlicensed data. This implies that data reduction is more effective in learning the SINR-Capacity feature relationship in the Unlicensed component.

It is worth highlighting that the theoretical computational complexities of the algorithms, *viz.,* random sampling and k-medoids Clustering, are $\mathcal{O}(N)$ and $\mathcal{O}(kN^2T)$, respectively, in the worst case. Here, N is number of instances, k is the number of clusters, and T is the number of iterations. However, empirically, the computational overhead is much lower, especially for random sampling, the better performing of the two. Further, the algorithms under study will fit within the LTE-LAA performance constraints, typically in the order of milliseconds, for the following reasons:

(1) The data pruning algorithms need to be run only once for a particular time epoch.

(2) They can be run separately from the active cell selection process.

(3) In the scenario that they need to be run during the cell selection process (e.g., A UE initiated cell-selection/handover), a typical run-time for a dataset of 680 records, when reduced by 50-90%, is 0.08–0.15 seconds.

Thus, it can be inferred that instance pruning is an effective tool to learn feature relationships in LTE-LAA/NR-U coexistence networks accurately and with lower computational overheads. A more detailed analysis at the PCI level with additional attributes such as resource block allocation is the logical next step in cell selection with numerosity reduction.

4.8 Conclusions

Drawing from the observations of the real-world deployments and the analysis of a large dataset from three major LTE-LAA coexistence service providers, some explanations on the impact of PCI or cell selection in these networks are put forward. The differences in Licensed and Unlicensed components can be attributed to factors such as operator deployment architecture, the impact of cooperating and rogue Wi-Fi transmissions in the unlicensed band, and resource block allocation. Numerosity reduction exercise also highlights these differences, such as the poor performance of clustering compared to sampling and that of the Licensed component compared to the Unlicensed. It indicates that additional network variables may affect the SINR-Capacity relationship, especially in the Licensed spectrum. Resource Block is a likely candidate. Its allocation in the Licensed and Unlicensed components may differ significantly because the number of competing for LAA-capable devices in the Unlicensed spectrum is currently far lesser than LTE devices in the Licensed band. Further, the scope of this chapter is limited to studying the role of PCI when LTE and LAA components are camped on the same cell. Network performance and feature relationships may be different when they are latched onto different cells.

It is reasonable to summarize that feature combination analysis of network data can yield reliable metrics for cell-quality estimation. Further, cell quality has a direct correlation with network performance and cell association guided by cell-quality estimates derived from operator data can greatly enhance the end-user experience in LTE-LAA coexistence networks. As coexistence network densification continues and the number of small cells increases, the convergence time required for network optimization will increase significantly as well. Thus, Association Time will become a major impediment to QoS delivery to the end user, and a cell-quality-based selection approach will prove to be highly beneficial in alleviating this problem. To conclude, this chapter paves the way for cell selection solutions driven by operator data that will enhance the performance of current LTE-LAA deployments as well as upcoming NR-U coexistence networks.

Chapter 5

A New Cell Selection Phenomenon in Unlicensed Networks

5.1 Introduction

LTE-LAA deployments have proliferated rapidly around the world, with 38 operators offering or planning to deploy LAA services in 21 countries [4]. As defined by 3GPP, "Carrier aggregation with at least one Secondary Cell (Scell) operating in the unlicensed spectrum is referred to as Licensed-Assisted Access (LAA)" [53]. Buoyed by the quick adoption and success of LAA coexistence deployments, 5G New Radio Unlicensed (NR-U) has been introduced as an evolutionary enhancement of LTE-LAA, under the 3GPP release 16 specifications. Furthermore, the Federal Communications Commission and the European Commission have both proposed rules for unlicensed coexistence in the 6 GHz (5925 MHz-7125 MHz) band for NR-U operation [52, 118].

The improved network performance offered by LTE-LAA depends on efficient cell selection by its Licensed and Unlicensed carrier components. Being a novel coexistence framework, LTE-LAA is characteristically different from traditional LTE heterogeneous networks (HetNets) in terms of deployment architecture, backhaul connectivity, and impact of external co-channel interference from Wi-Fi transmissions [64, 119].

Despite the attention that LTE-LAA has received from industry and academia, a peculiar aspect of the current LAA deployment architecture is overlooked in the LAA literature. Cellular providers aim to minimize feedback delay from user equipment (UE) and carrier aggregation (dual connectivity) while planning coexistence deployments. Hence, macro and small cells are usually placed in close proximity, and may often be co-located on the same physical structure, such as a street lamp/electricity pole. Thus, the LTE (Licensed) and LAA (Unlicensed) components of the network may share the same Physical Cell ID (PCI). But operator data reveals that the Licensed and Unlicensed carriers of a UE may also be camped on different cells or cells with different physical locations. This creates a different PCI scenario, as shown in Figure 5.1. The existence of these PCI scenarios, *viz.,* "Same PCI" and

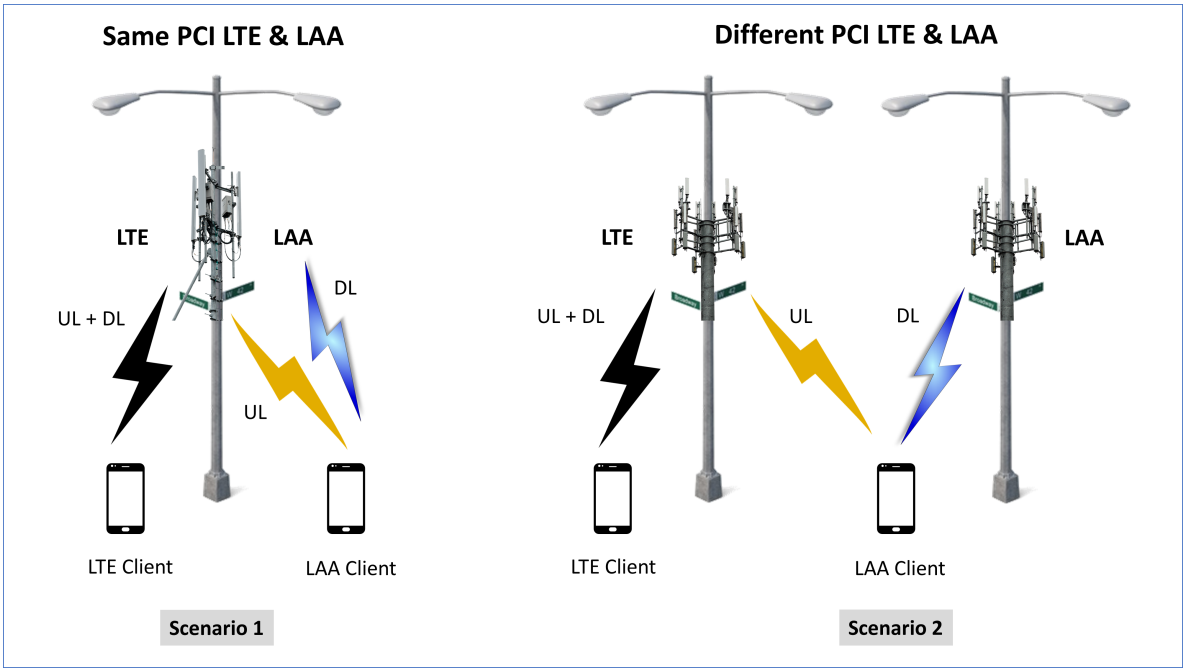

Figure 5.1: Coexistence PCI Scenarios - A new phenomenon

"Different PCI," is a novel phenomenon that is unique to the LTE-WiFi coexistence environment.

The two PCI scenarios differ in several respects, especially network performance. While LAA supports only Carrier Aggregation, NR-U will also support Dual Connectivity and Standalone unlicensed modes. Thus, this phenomenon is bound to intensify in NR-U deployments with respect to the frequency of occurrence and the multitude of PCI scenarios. Moreover, the amount of spectrum available at 6 GHz is higher compared to 5 GHz, and a higher rate of carrier aggregation per UE is possible in the 5G NR-U system. Consequently, the impact of unlicensed PCI scenarios in 5G NR-U will also be much greater than in LAA. Thus, their analysis is important not only from the perspective of optimizing existing LAA performance but also for the upcoming NR-U deployments.

From a Radio Resource Management (RRM) perspective, it is pertinent to study how the performance of the coexistence system varies when the Licensed and Unlicensed network components are attached to the same or different PCIs.

Thus, cellular operator data needs to be analyzed to study the frequency of occurrence of the two scenarios and the distribution of important network variables in them. Data analysis is necessary to understand how the relationships between network variables differ in the two scenarios. More importantly, the variation in network performance and the ability to accurately predict expected capacity is of great interest. These tasks can typically be performed through machine learning (ML) algorithms. The PCI scenarios should also be investigated for other differences they cause in the network environment. The performance of data reduction mechanisms that are often used to help

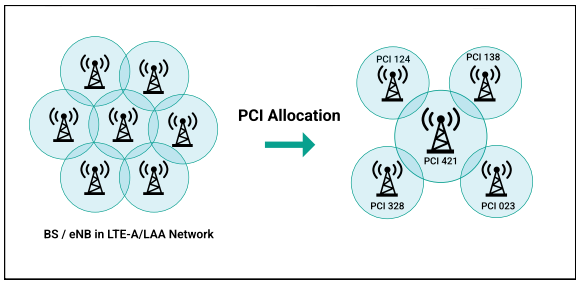

(a) PCI Allocation in LTE-A/LAA

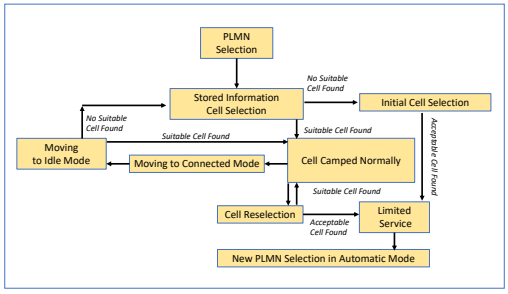

(b) Cell Selection Process in LTE-A/LAA

Figure 5.2: PCI Allocation and Cell Selection Process in LTE-A/LAA

expedite data-driven cell selection by the cellular operator is one such example.

Additionally, differences in network performance should also be investigated through on-site measurements, i.e., by monitoring the LTE, LAA, and Wi-Fi networks in the two scenarios. Network performance may also vary depending on the type of traffic requested by the UE, QoS constraints, and interference from coexisting Wi-Fi access points (APs) in the unlicensed spectrum. The effect of PCI scenarios on network performance ought to be validated through real-time experiments, on both the cellular (Licensed and Unlicensed) and Wi-Fi side. It is relevant to see how Wi-Fi performance varies when coexisting with the same PCI and different PCI LAA configurations. Moreover, on-site experiments should ideally consider multiple types of traffic for a comprehensive evaluation.

Equally important is the awareness of the PCI scenarios at the UE, as they are intricately associated with the cell selection decisions of the Licensed and Unlicensed components. Having an awareness of the PCI scenario will help an end-user device make informed cell selection decisions. The first step in that direction would be to accurately identify and differentiate between the two coexistence scenarios with a minimal feature vector. This is a challenging problem, given the inherent imbalance in the occurrence of the two scenarios in current LAA deployments.

These challenges must be addressed, as LAA deployments serve as a precursor to future NR-U deployments, where a lot more complex configurations are possible. For example, it is possible that NR-Licensed, NR-U, LTE, and LAA small cells are located on adjacent poles, leading to far more complex PCI scenarios. Thus, cell selection decisions resulting from the awareness of PCI scenarios will ensure better network performance for the end user.

However, the current LAA deployments have not been studied for the phenomenon of multiple PCI scenarios and the challenges they present.

5.1.1 Contributions

The proposed work analyzes LTE-LAA deployments through field experiments, measurements, and machine learning-based operator data modeling, with the vision to find solutions for upcoming NR-U

deployments. The major research contributions are elucidated below.

- **Impact Assessment of PCI Scenarios** A PCI scenario specific distribution analysis of important network variables such as Throughput and SINR is performed. Further, the effect of PCI scenarios on network performance prediction and data reduction techniques in Licensed and Unlicensed components is explored and insightful inferences are drawn. This is done by analyzing the SINR-Capacity relationship through eight regression and supervised machine learning algorithms, and two popular numerosity reduction algorithms.

- **On-site Experiments**: Operator sites with the Same and Different PCI configurations are identified using the Network Signal Guru (NSG) tool. Then, on-site experiments are conducted using multiple coexisting Wi-Fi hotspots. Variation in network performance is observed for both PCI scenarios by varying the type of traffic, the number of interfering Wi-Fi hotspots, the distance *etc.* Further, the role of QoS constraints in LTE-LAA performance is explored through delay critical data traffic. Metrics such as Throughput, Signal Strength, Resource Block allocation, and Latency are measured. Experiments are conducted for both cellular (LTE/LAA) and Wi-Fi sub-systems.

- **Predicting PCI Scenarios** A binary classification model is designed that predicts the PCI scenario with high accuracy, in both the Licensed and Unlicensed components. The proposed classification model requires a minimalist two-variable feature set and overcomes the challenge of data imbalance between the two scenarios.

Finally, open research problems related to the PCI scenarios in the unlicensed coexistence networks are identified and outlined.

5.2 Unique PCI Phenomenon in LAA Deployments

In the current coexistence deployments, the uplink transmissions are generally performed on the licensed spectrum and downlink transmissions on the LAA unlicensed spectrum. The strategy is designed to meet QoS requirements, reduce delay in ACK packets, and maximize power and spectral efficiency. In contrast, if the client is LTE-only, both uplink and downlink occur on the licensed LTE BS. However, cell selection in LTE-LAA coexistence networks involves additional technical nuances due to the system architecture.

5.2.1 The Two PCI Scenarios

Data collected from coexistence deployments of the three operators in Chicago, *viz.,* AT&T, Verizon, and T-Mobile reveals that a typical LTE-LAA coexistence deployment may be broadly categorized into two PCI scenarios, depicted in Figure 5.3. "Same PCI" represents the coexistence network architecture with Licensed (LTE) and Unlicensed (LAA) clients camped on the same cell, while "Different PCI"

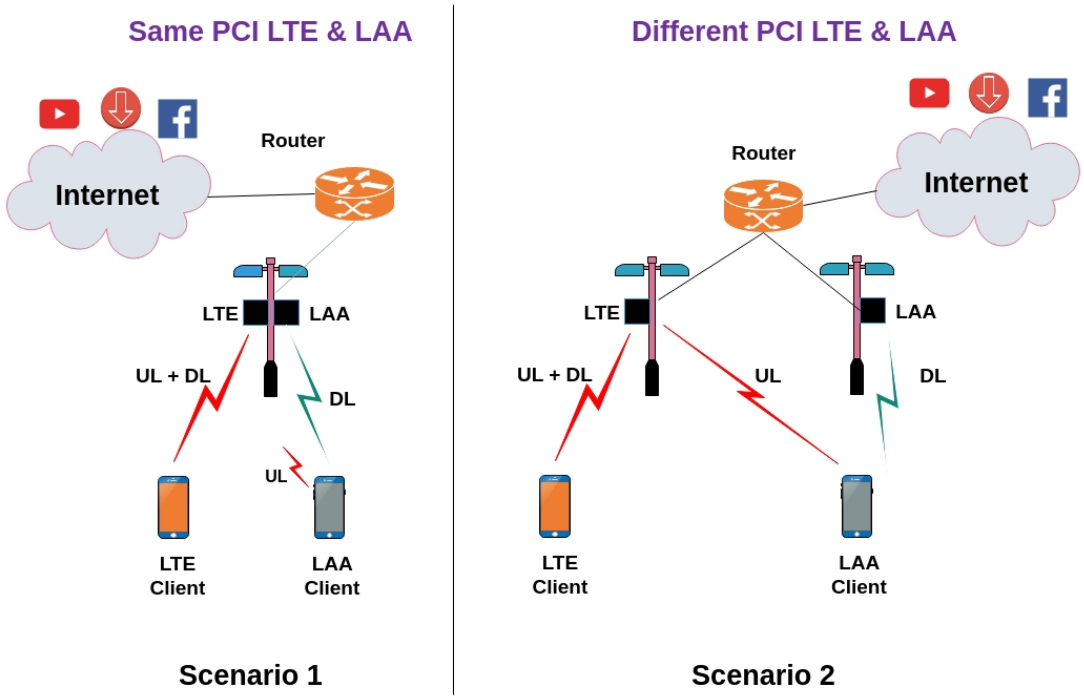

Figure 5.3: PCI Scenarios in Unlicensed Networks

depicts the case when they are latched on to different cells with different PCIs. An architectural representation of the two scenarios is shown in Figure 5.3. Same PCI is the dominant scenario and is observed in over 80% of the sample space.

It also seems to be the preferred scenario for maximal network throughput, which is why cell selection solutions often focus on it [7, 8]. However, the occurrence of Different PCI scenarios in LAA operator data is significant (18%) and cannot be overlooked [7]. Further, to the best of our knowledge, this is a hitherto unobserved phenomenon and unique to the coexistence paradigm. With the commencement of 5G-NRU operation in the 5GHz and 6GHz spectrum, taking the PCI scenarios into consideration will enhance coexistence network performance [64, 120].

These scenarios are the result of three network design factors, *viz.,* availability of space/structures for cell installation, availability of fiber optic-equipped backhaul connectivity, and operator deployment strategy. The LTE-LAA coexistence networks in the Chicago region have been deployed in both semi-indoor and outdoor environments. The operator data has been gathered for an outdoor setting, where the LTE-LAA cells have been installed on the street lights/electricity poles. The deployment plan is shaped not only by the availability of these poles but also by their type. Only some of these poles are

structurally capable of providing a high-speed fiber optic connection to the backhaul. From the network planning perspective, this is an important consideration, because the Unlicensed carrier bandwidth is 3X that of the Licensed carrier, and the next-generation millimeter-wave networks offer up to 400 MHz bandwidth, which is 10X that of the current 5 GHz unlicensed bands [64]. Such speeds can only be serviced by a fiber optic connection to the backhaul. CapEx-QoS trade-off is another major consideration, as fiber optic cabling is expensive and is set to cost the 5G industry over $130 Billion in installation. These factors, coupled with market penetration of LAA-equipped devices and subscriber density, determine operator deployment strategy and create the two PCI scenarios.

Preliminary on-site measurements indicated that LAA performance in the two scenarios is likely to be different. When LTE and LAA have the same PCI, they share the backhaul, which facilitates efficient resource splitting and packet aggregation. Consequently, the LTE-LAA network performance analysis is usually limited to the Same PCI scenario [7,8]. However, the two PCI scenarios may impact LAA and Wi-Fi network performance differently.

Furthermore, the performance of the LAA uplink (UL) and the LAA downlink (DL) is likely to differ. This becomes important due to LAA mechanisms such as subframe and carrier (pool-based) resource allocation schemes and group UL grant. The two PCI scenarios may influence the use of Group ID or PCI for multiplexed transmissions on the subframe [53, 61]. Thus, Same PCI and Different PCI configurations will affect LAA UL and DL mechanisms as well. Similarly, these PCI scenarios will affect the network throughput, resource allocation, and latency for different types of data traffic depending on the respective Channel Access Priority Class. Equally importantly, the impact of LAA on the performance of coexisting Wi-Fi networks will also vary depending on the type of coexistence PCI scenario. In this thesis, these aspects are explored through a PCI scenario-specific analysis of LAA deployment data.

5.2.2 Relevance to 5G NR-U

LAA is the evolutionary antecedent of NR-U and the first commercially successful cellular-WiFi co-existence standard. As such, the unresolved challenges encountered in LAA will assume a different dimension and scale in NR-U. This is especially true for the phenomenon of PCI scenarios that has come to attention only through the analysis of LAA operator data.

NR-U deployments will support three modes, viz., Carrier Aggregation, Dual Connectivity, and Standalone [121]. Apart from the fully unlicensed Standalone operation, the other two modes will operate in the 5GHz spectrum. This implies that the following can be present/co-located on a physical installation such as a pole or a lamppost:

- NR-U and NR Licensed
- NR-U alone in Standalone mode
- NR Licensed and LAA Unlicensed

- NR Licensed, NR-U and LAA
- LTE Licensed, NR Licensed, NR-U and LAA

Compared to the LAA deployment scenarios shown in Figure 5.3, the above small cell combinations present in physical installations close to each other can lead to more complex PCI scenarios than LAA. Thus, the analysis and solutions presented in this chapter will certainly guide solutions for cell selection and network optimization in NR-U.

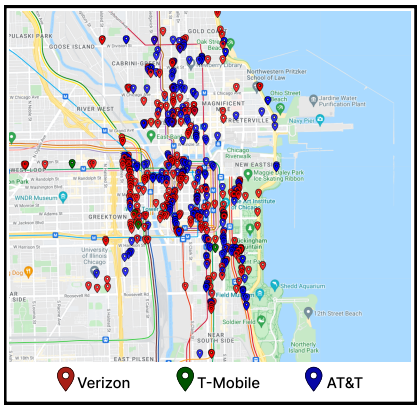

(a) LAA Sites in Downtown Chicago

Figure 5.4: LAA deployment sites

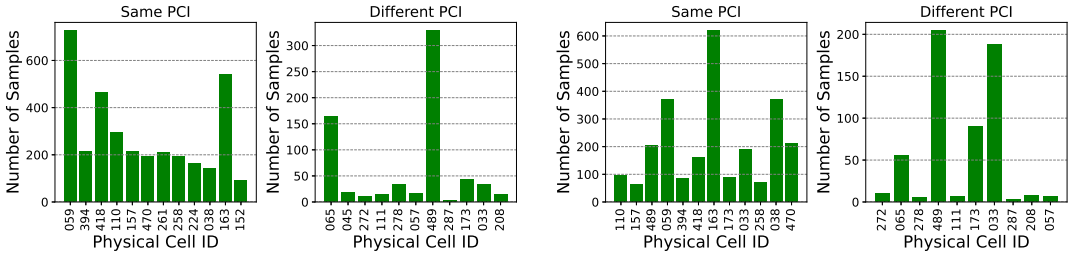

(a) Unlicensed Data

(b) Licensed Data

Figure 5.5: Sample Sizes for the Same PCI and Different PCI Scenarios

5.3 Exploratory Data Analysis

Having discussed the new-found phenomenon, this section presents the data distribution analysis. Real-time LAA network data for three operators, *viz.,* AT&T, T-Mobile, and Verizon is gathered from downtown Chicago, as depicted in Figure 5.4(a). Close to 7500 samples were successfully extracted

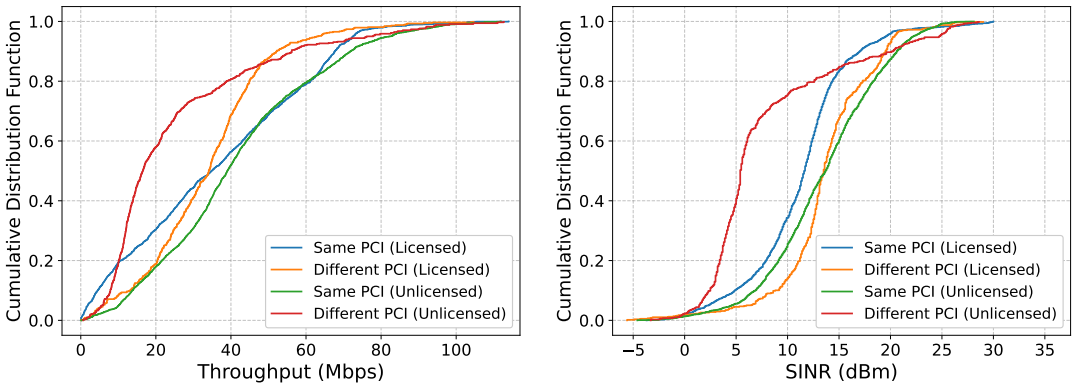

(a) Network Capacity Distribution

(b) Signal Strength Distribution

Figure 5.6: Distribution of Network Variables in the Two PCI Scenarios

and analyzed in this chapter. For a detailed description on data gathering and extraction, please refer to Chapter chapter 4.

5.3.1 Exploratory Data Analysis

5.3.1.1 Sample Size Distribution

The PCI-specific distribution[1] of extracted samples in the Same PCI and Different PCI scenarios, for Licensed and Unlicensed components is presented in Figure 5.5. As discussed earlier, Same PCI has a much higher proportion of samples in both LTE and LAA components. However, there is another dimension to this imbalance. Since the Different PCI LAA sites are less in number, the probability of encountering them also reduces. Consequently, the samples are also concentrated within a few small cells, leading to an internal pattern imbalance in the feature set of the Different PCI sample space. These challenges add complexity to the intended objective of accurately identifying PCI scenarios, through imbalanced classification with a small feature set.

5.3.1.2 Density Distribution

The cumulative distribution plots of Throughput and SINR values in the operator data are presented in Figures 5.6(a) & 5.6(b), respectively. Both distributions exhibit the impact of the coexistence component and the PCI scenario within the component.

Beginning with component-specific analysis, for more than 85% Different PCI Throughput samples, the Unlicensed component has a lower magnitude, but this trend reverses for the last 15% samples. Consequently, 80% users in the Unlicensed Different PCI environment are likely to receive 10 Mbps less Throughout than Licensed Different PCI users. In contrast, Licensed Same PCI performs worse

[1]Due to a large number of PCIs, only those with significant sample-sizes are displayed here.

than Unlicensed Different PCI for 80% users, but the performance of both is comparable for 20% users in the Throughput range of 45 Mbps–63 Mbps. The SINR trend for Licensed and Unlicensed Different PCI conforms to the Throughput trend. However, the SINR trend for the Same PCI does not correspond to the Throughput trend in its entirety, and Unlicensed performance remains better than Licensed throughout. This shows a clear impact of PCI configurations on the performance of unlicensed network components. The allocation of radio resources and their availability plays a key role in network performance. There seems to be better resource allocation in Licensed Same PCI that enables it to match up to Unlicensed Same PCI, despite lower SINR.

A PCI scenario-specific analysis also highlights a difference in resource allocation in the two scenarios. For example, Licensed Same PCI performs better than Licensed Different PCI in terms of Throughput, in 50% samples where Throughput is higher than 35 Mbps. However, the cumulative Licensed Same PCI SINR distribution remains consistently higher than the Licensed Different PCI SINR. This indicates that the variation in Throughput is a result of other network-related factors that differ in the two scenarios. In the Unlicensed component, the Same PCI Throughput is always better than the Different PCI Throughput. This is despite the fact that the cumulative distribution of Unlicensed SINR is not always better in Same PCI, and Different PCI performs better at higher SINRs ($\gtrsim 21.5dBm$).

Overall, both Licensed and Unlicensed Same PCI network capacity seems to be better than the corresponding Different PCI. This could be attributed to more efficient cell selection and backhaul.

5.4 Network Performance Analysis

The objective of the analysis presented in this section is to infer how network performance in the Licensed and Unlicensed components of the coexistence system varies in each PCI scenario. The discussion seeks to (a) highlight the relevance of PCI scenario-specific network analysis, (b) investigate the impact of PCI scenarios on the network performance in Licensed and Unlicensed components, and (c) examine the performance of data reduction techniques in both scenarios.

5.4.1 Methodology and Machine Learning Algorithms

5.4.1.1 Methodology

To study the variation in network performance in the two PCI scenarios, a data-driven approach leveraging machine learning algorithms is ideal [9,122]. Thus, the prediction of network performance is done using feature relationship modeling. Operator data is subjected to eight supervised machine learning algorithms to determine the relationship between network feature points of primary importance, *viz.*, Signal and Interference plus Noise Ratio (SINR), network throughput (Capacity), and cell allocation (PCI). It is a good practice to employ a broad set of machine learning algorithms consisting of different types *e.g.,* deterministic and stochastic, to ensure a robust coexistence performance prediction and

feature relationship analysis through cross-verification of results. Further, for both PCI scenarios, *i.e.,* Same PCI and Different PCI, a fine-grained SINR-Capacity feature relationship analysis is presented by comparing models that consider PCI as a categorical parameter (With PCI) with models that do not consider PCI as a categorical parameter (Without PCI). Since the analysis of the combined coexistence network data is shown to obfuscate the findings [7, 8], operator data is segregated into its Licensed and Unlicensed components. Finally, the R-sq of a model reflects the strength of the relationship between the network feature points. In this chapter, a multivariate relationship analysis is performed to determine the explanability of network throughput. Thus, the model R-sq is denoted as "**Throughput$_{\mathbf{Exp}}$**" in this chapter. Throughput$_{\text{Exp}}$ serves as a metric for a comparative analysis of network performance prediction and feature relationship strength. A higher Throughput$_{\text{Exp}}$ implies a strong feature relationship and consequently, a greater confidence in the model to predict the response variable, i.e., network throughput.

5.4.1.2 Machine Learning Algorithms

Let N be the number of training points and D be the dimensionality of the feature vector. Then the LTE-LAA network data can be represented as $\{\mathbf{x}_i, y_i\}_{i=1}^{N}$, where $\mathbf{x}_i \in \mathbb{R}^D$ is the feature vector and $y_i \in \mathbb{R}$ is the ground truth value for the i^{th} training point. The objective is to learn a mapping $f : \mathbf{x}_i \rightarrow y_i$ where x_i is the feature vector constructed using Signal & Interference plus Noise Ratio (SINR) and cell-allocation (PCI) and y_i is the target value, *i.e.,* network throughput (Capacity). A diverse set of regression algorithms are considered, which are discussed below:

(i) *Linear Regression*: This family of algorithms [77] aims to learn a linear mapping by solving, $\arg\min_{\mathbf{w},b} \sum_{i=1}^{N} ||(\mathbf{w}^\top \mathbf{x}_i + b) - y_i||_2^2 + \alpha \mathbf{w}^\top \mathbf{w}$. Here, $\mathbf{w} \in \mathbb{R}^D$ is the weight vector and $b \in \mathbb{R}$ is the bias term. Moreover, α is a hyperparameter used to control the importance/weightage of the l_2-regularization term. α is set as zero in the case of Ordinary Least Squares Linear Regression (OLS), whereas it is set via k-fold cross-validation (kCV) in the case of Ridge Regression (RR).

(ii) *Kernel Regression*: Kernel Ridge Regression algorithms [77] learn a non-linear mapping through a kernel function $K(a, b)$. The goal is to solve $\arg\min_{\mathbf{w},b} \sum_{i=1}^{N} ||K(\mathbf{w}, \mathbf{x}_i) + b - y_i||_2^2 + \alpha \mathbf{w}^\top \mathbf{w}$. Here, $\mathbf{w} \in \mathbb{R}^D$ is the weight vector, $b \in \mathbb{R}$ is the bias term, and α is a hyperparameter as defined earlier. Varying the kernel function as Radial Basic Function and Polynomial leads to Kernel RBF Regression (RBF) and Multi-variate Polynomial Regression (MPR), respectively. In MPR, 2–4 degree polynomials were considered and the optimal degree was chosen based on the value of R-sq via kCV.

(iii) *Neural networks (NN)*: This family of algorithms learns a non-linear mapping via a sequence of feed-forward layers in contrast to hand-crafted kernel functions used by Kernel Ridge Regression [77]. A wide range of neural networks were considered with 1–2 hidden layers, 5–50 neurons per hidden layer, and ReLU, logistic & Tanh activation functions. The optimal configuration and hyperparameters were chosen on the basis of the R-sq metric via kCV.

(iv) *Decision Tree Regressor*: Decision Trees (DT) recursively partition the data points to min-

imize the mean squared error at each node [77]. Trees of depth 5–20 were experimented with, and the optimal depth was determined via kCV. The Minimal Cost-Complexity Pruning algorithm was implemented to prune the learned tree and avoid overfitting [77]. Ensembles with 3–100 base learners were considered, and the optimal number was determined by kCV. In particular, an ensemble of 25 decision tree regressors yielded the best R-sq value for both Random Forest Regressor (RF) and Gradient Boosting (GB) in the experiments.

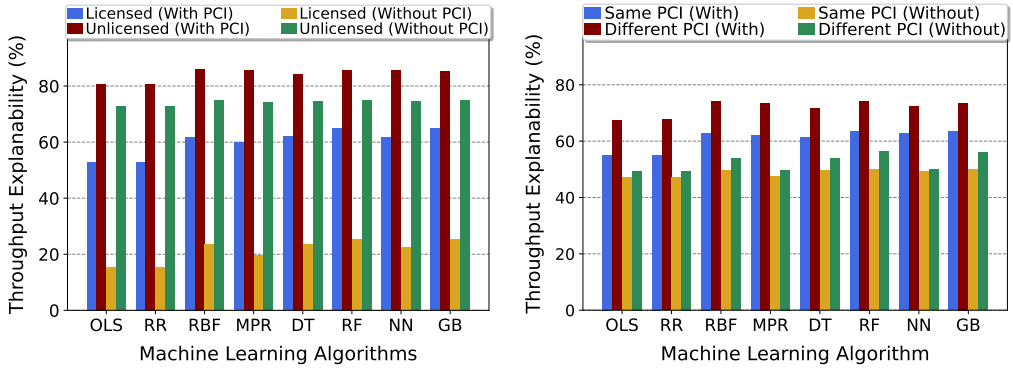

(a) Coexistence Component Only

(b) PCI Scenario Only

Figure 5.7: Data Segregation for Performance Prediction through Feature Relationship Analysis

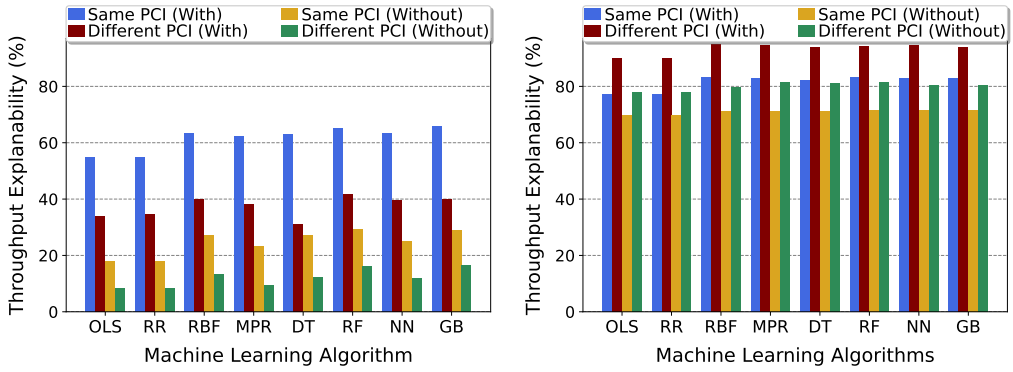

(a) Licensed Component

(b) Unlicensed Component

Figure 5.8: LAA PCI Scenarios and Network Performance Prediction

5.4.2 PCI Scenarios and LTE-LAA Performance

SINR-Capacity feature relationship analysis is performed on LTE-LAA operator data. It is worth mentioning that for Licensed and Unlicensed, 18.61% and 16.04% data belongs to the Same PCI scenario, respectively. The rest falls under the Different PCI scenario. Linear algorithms (Linear and

Ridge Regression), generate models with lower $\text{Throughput}_{\text{Exp}}$ than non-linear algorithms (remaining six algorithms). The latter seem to be more suited to fit the SINR-Capacity (and PCI) data which is also considered to be non-linear [7,8]. However, the trend of predictive performance is fairly consistent across all algorithms. Hence, the discussion ahead focuses on network feature relationship patterns as a whole and not on the results of individual algorithms.

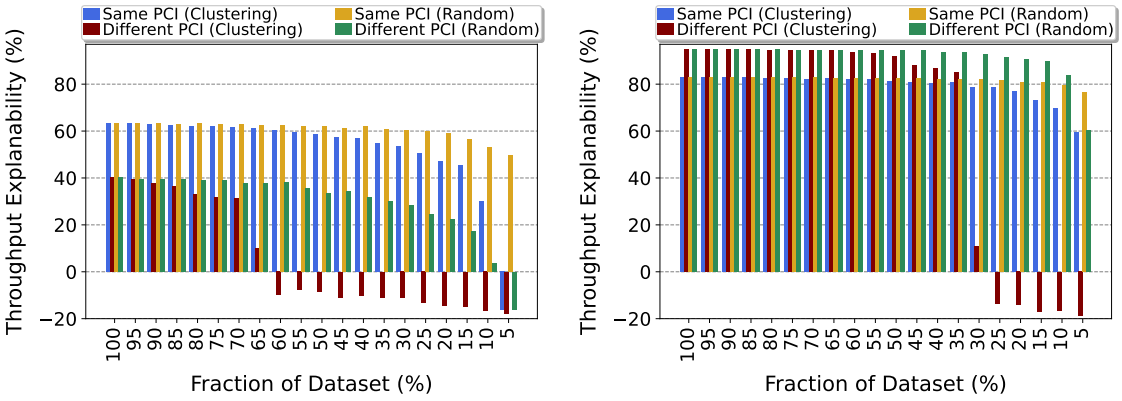

(a) Licensed (b) Unlicensed

Figure 5.9: Impact of PCI Architecture on Numerosity Reduction

The results of data analysis are distilled in the form of inferences presented below along with the explanations.

(i) *Component and PCI scenario-specific data segregation seems to be a pre-condition for accurate co-existence network performance prediction.* Although the need for component-specific data segregation has been highlighted earlier [7, 8], for reliable modeling of feature relationships, component-specific data segregation alone is not sufficient. Figure 5.7(a), presents the relationship analysis for data segregated based on LTE-LAA network components, with and without PCI as a categorical parameter. It shows that the SINR-Capacity $\text{Throughput}_{\text{Exp}}$ for Licensed data models is always lower than the corresponding Unlicensed models. However, it will be demonstrated ahead that this is not the case. Similarly, segregating data based on the PCI scenario alone does not yield an accurate network performance prediction. For example, Figure 5.7(b), shows that the $\text{Throughput}_{\text{Exp}}$ of the Same PCI models is invariably lower than that of the different PCI models. Again, it is now known to be not true.

Thus, for reliable network prediction models, coexistence network data should be segregated based on both *network component* (Licensed/Unlicensed) and *PCI scenario* (Same/Different).

(ii) *Current LAA deployment architecture may not facilitate efficient Licensed operation in both PCI scenarios.* It is evident from Figure 5.8(a), that the Licensed Same PCI model $\text{Throughput}_{\text{Exp}}$ is significantly higher than the corresponding Different PCI model $\text{Throughput}_{\text{Exp}}$. This implies that predicting network performance (e.g., network capacity) is more reliable in the former case. The

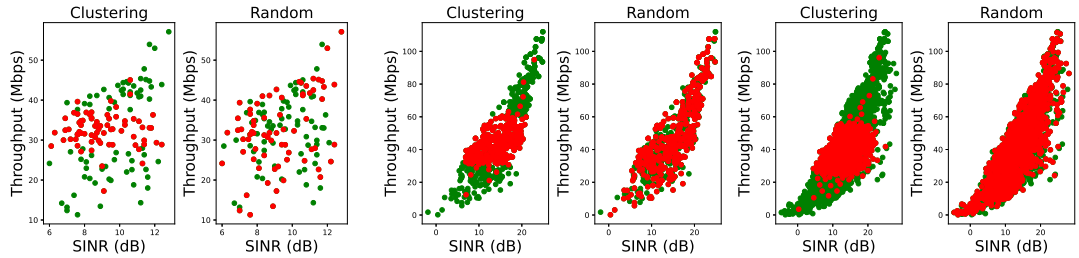

(a) Same PCI (038) (b) Same PCI (059) (c) Same PCI (470)

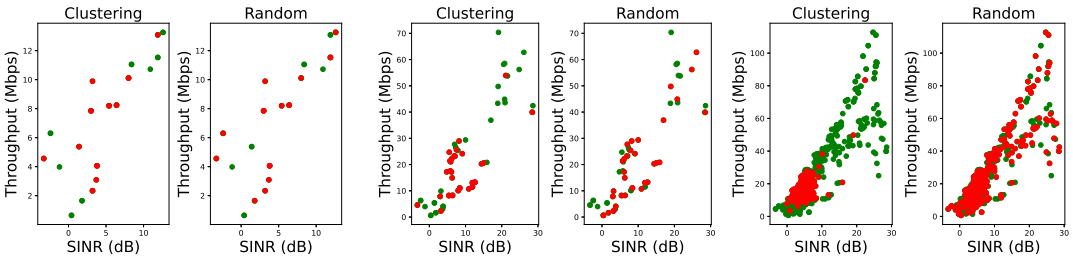

(d) Different PCI (033) (e) Different PCI (057) (f) Different PCI (489)

Figure 5.10: Cell-specific Numerosity Reduction for Unlicensed PCIs

trend holds for all regression and learning algorithms, regardless of whether PCI is considered a categorical parameter. However, without PCI as a categorical parameter, the difference in the model $\text{Throughput}_{\text{Exp}}$ for the two scenarios is exaggerated (109.72% on average) compared to when PCI is a categorical parameter (65.52% on average). Thus, the "Without PCI" modeling should be avoided for a reliable representation of the feature relationships. The more important inference is that for the Licensed component, feature relationships are rather poor in the Different PCI scenario. This implies that network performance cannot be predicted with confidence.

Thus, the current coexistence deployment architecture appears to be creating performance bottlenecks in the Different PCI configuration and may not facilitate optimal network performance in the Licensed component.

(iii) *Current LAA deployment architecture favors Unlicensed operation.* $\text{Throughput}_{\text{Exp}}$ of Unlicensed models demonstrates a trend exactly opposite to that observed in the Licensed component. Different PCI scenario models, across all machine learning algorithms, perform better than Same PCI scenarios. Further, there are three more points of difference when compared to the Licensed performance prediction patterns. First, the difference in $\text{Throughput}_{\text{Exp}}$ for the two Unlicensed PCI scenarios is not as pronounced as it was in the Licensed (only 14.68% on average for "With PCI"). Second, the absolute magnitude of $\text{Throughput}_{\text{Exp}}$ for Unlicensed models, for both Same and Different PCI scenarios, is much higher than that of Licensed models. For example, the average Different PCI $\text{Throughput}_{\text{Exp}}$ for "With PCI" models is 37.39 for Licensed and 93.31 for Unlicensed. Third, not using PCI as a

categorical parameter does not affect the relative difference in model $\text{Throughput}_{\text{Exp}}$ for the two PCI scenarios, unlike Licensed models, although the absolute values decrease as expected in the case of "Without PCI" [7, 8].

The main takeaway is that the network feature relationships and performance prediction in the Unlicensed component are largely consistent in both PCI scenarios. This implies that the LTE-LAA site architecture leads to a relatively more efficient Unlicensed operation.

5.4.3 PCI Scenarios and Numerosity Reduction

Numerosity reduction is a crucial tool for reducing the computational overhead of network data-driven cell selection and handover [123]. Sampling and clustering are two popular approaches to numerosity reduction [122]. The efficiency of these techniques depends on the selection of a smaller sample that resembles the characteristics and distribution of the original dataset. However, the nature and distribution of the data may vary in the two PCI scenarios, thus affecting the performance of the numerosity reduction techniques.

This problem is investigated by observing the performance of two nonparametric techniques *viz.,* Random Sampling and k-mediods Clustering, validated through kCV, for k=5 [122, 123].

5.4.3.1 Macro Level Analysis

It can be discerned from Figures 5.9 (a) & 5.9 (b), that for both Licensed and Unlicensed, for all subsets of the original dataset, the $\text{Throughput}_{\text{Exp}}$ trends are as observed earlier. Further, Random Sampling seems to be a better numerosity reduction technique than k-mediods Clustering for both PCI scenarios in both the coexistence components. Two differences are evident between the PCI scenarios. First, the Different PCI dataset is less than one-fourth of the Same PCI, which implies that as the reduced dataset gets smaller, the ability to predict the response variable will decrease at a faster rate in the Different PCI models than in the Same PCI models. For example, consider the average decrease in $\text{Throughput}_{\text{Exp}}$ for randomly sampled models in the Unlicensed component for both scenarios. In the Same PCI scenario, for data subsets ranging from 30% to 10% size of the original, the average decrease is six times that of subsets ranging from 100% to 30% of the original. In Different PCI, a similar comparison yields an 18-fold gap. Thus, for the Different PCI scenario, numerosity reduction techniques should be applied only if the original dataset has a large number of sample points. Second, PCI scenarios respond differently to the data reduction algorithms. The performance of both sampling and clustering on the Same PCI data is consistent up to a 10% fraction of the original dataset for both Licensed and Unlicensed. However, for the Different PCI scenario, k-mediods Clustering does not seem to be a good choice. For Licensed, the Different PCI clustering models show negative $\text{Throughput}_{\text{Exp}}$ 60% fraction onward, while for Unlicensed, the $\text{Throughput}_{\text{Exp}}$ is negative after the 25% fraction. *This occurrence cannot be attributed to a smaller sample space of Different PCI data* as Random Sampling performs significantly better for subsets of identical sizes, and the model $\text{Throughput}_{\text{Exp}}$ is never

negative even in the 10% subset.

5.4.3.2 PCI Level Micro Analysis

At the level of individual PCIs, the impact of numerosity reduction techniques becomes more visible. Data from three different cells, with a low, medium, and large number of samples, is subjected to Clustering and Random Sampling. The results are presented in Figures 5.10(a), (b) and (c) for the Same PCI cells, and Figures 5.10(d), (e) and (f) for the Different PCI cells. Random Sampling seems to perform better since, at each stage, the selected samples are more evenly distributed. When the data distribution is dispersed, as in Same PCI 038, Figure 5.10(a), both the algorithms yield similar results after distribution. Else, Clustering tends to capture only a subset of the overall distribution, especially for Different PCI. This changes the characteristics of the reduced sample vis-à-vis the baseline sample, leading to poor prediction performance.

Therefore, it is safe to conclude that k-mediods Clustering should be avoided in the Different PCI scenario. This is an interesting finding, as clustering algorithms are often used during the preprocessing phase of cell allocation and categorization [122]. It is worth noting that while the Same PCI scenario seems unaffected by the choice of data reduction approach, our evaluation is limited to two popular techniques, and a wider set of algorithms may yield a different view. More sophisticated algorithms including *local density-based instance selection* (LDIS) [117] can also be implemented. However, random sampling and k-mediods Clustering were chosen because an instance pruning algorithm should have a minimal computational footprint to ensure optimal performance in the downstream task (*e.g.,* learning a mapping between SINR and Throughput). A detailed discussion and analysis of popular instance pruning algorithms can be found in [115] and [117].

Nevertheless, it can be inferred from the findings that the PCI scenario influences the choice of numerosity reduction technique.

5.5 On-site Experiments, Results, and Analysis

Next, a measurement-based analysis of real-time network performance is carried out for the two PCI scenarios. The onsite experiments and measurements involve several challenges, such as the identification of the two PCI scenarios in operator deployments, and creating a controlled LTE-WiFi coexistence environment. Where applicable, inferences drawn from operator data analysis are compared with measurement-based observations.

5.5.1 Experiment Setup and Site Selection

An increasingly large number of Release 13 compliant LAA Base Stations (BS) are being deployed in downtown Chicago. Further, up to three Wi-Fi channels can be aggregated by an LAA BS in the U-NII 1 band (Channels 36, 40, & 44) or the U-NII 3 band (Channels 149, 153, & 157). It is capable of 2×2

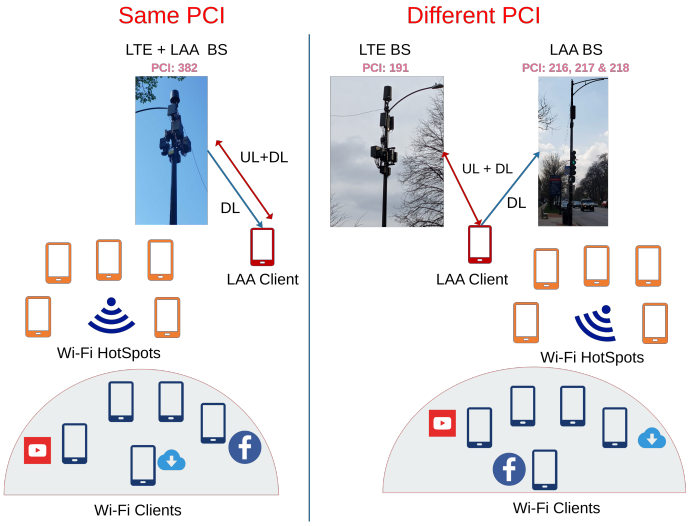

Figure 5.11: Illustration of the On-site Experiment Setup

MIMO transmissions with a maximum modulation coding scheme (MCS) of 256 QAM. Consequently, PCI scenario-specific site determination is a challenging task. The first step involves identifying the sites where the LAA & LTE BS are mounted on the same pole (Same PCI) and where the LAA & LTE BS are mounted on different poles (Different PCI), as shown in Figure 5.11. This is done using the NSG app, by monitoring the PCI assigned to the LTE and LAA components. Thereafter, the signal strengths (e.g., SINR and RSRP) are monitored and compared to verify the sources.

5.5.2 Methodology

The variation in real-time network performance in the two PCI scenarios is observed and compared to the findings of the data analysis. The traffic type and the LTE-WiFi coexistence environment are varied for a comprehensive evaluation of the impact on network performance. NSG app, with root permission, was used to observe performance metrics such as SINR, Throughput, Resource Block (RB) allocation for each channel, TXOP, *etc.* The observations were made at 15-minute intervals (on the ground, not point-to-point) up to a distance of 150m from the LAA small cell.

5.5.2.1 Traffic Types and Quality of Service

Several realistic traffic scenarios are considered, as LAA categorizes different types of data traffic into different *access classes*. Further, the Listen Before Talk (LBT) mechanism prescribes different duration of transmission opportunity (TXOP) to different traffic access classes, presented in Table 2.1. For example, background data (Access Class = 4) is offered a TXOP of 8ms, the maximum for any type of traffic, to maximize network capacity. Likewise, Wi-Fi defines specific *access categories* for

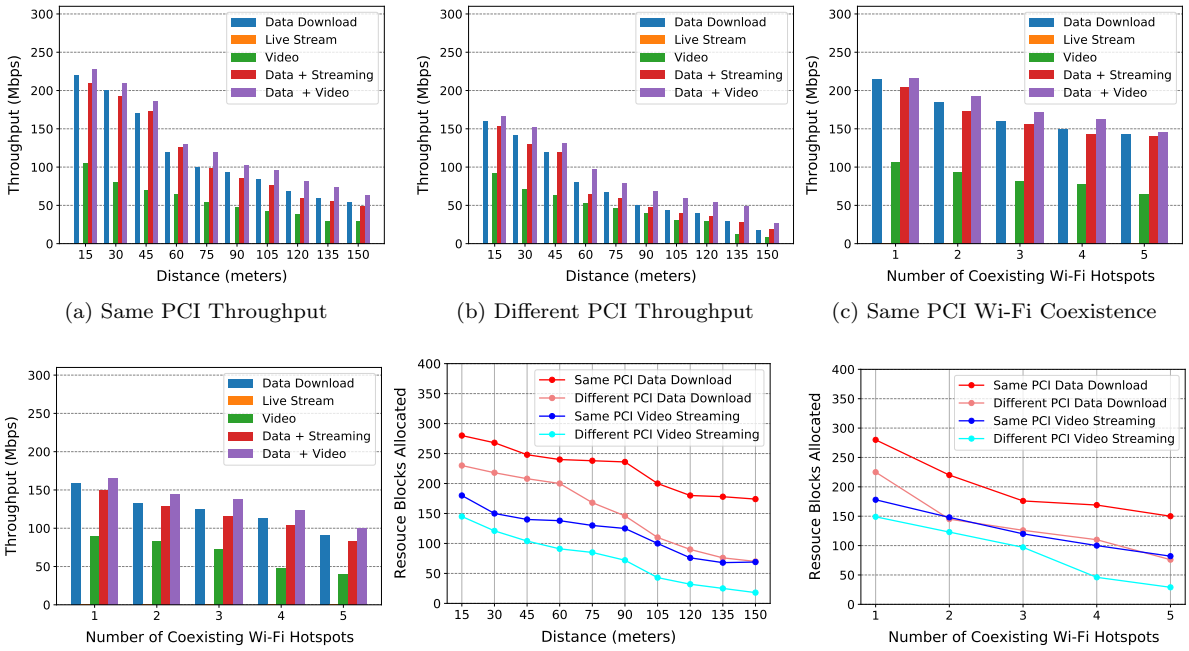

(a) Same PCI Throughput (b) Different PCI Throughput (c) Same PCI Wi-Fi Coexistence

(d) Different PCI Wi-Fi Coexistence (e) Resource Block Allocation (f) Resource Blocks vs Wi-Fi AP

Figure 5.12: Unlicensed On-site Measurements

different types of traffic, presented in Table 2.2. The Wi-Fi TXOP duration is smaller (2.528ms for background data), which implies that LAA can occupy the transmission channel for a longer duration on average. Most importantly, categorizing traffic is vital to meet QoS guarantees and is done through a QoS Class Identifier (QCI) which assigns a maximum packet delay threshold to each traffic class. The permitted delay determines which component (Licensed or Unlicensed) the traffic pipeline will be assigned to. The traffic types considered in the evaluation are:

- Data download: A fully bufferable large (>10 GB) YUV datafile from Derf Test Media Collection [124].
- Video: A 1920×1080 resolution Youtube video with a 12 Mbps bit-rate.
- Live Streaming: A 1280×720 resolution, 7.5 Mbps bitrate live stream on Youtube.
- Data & Video, Data & Streaming traffic combinations.

5.5.2.2 Controlled Coexistence Environment

LTE-LAA sites were identified where no interfering Wi-Fi signals were detected at the time of conducting the experiments. It was also verified (using NSG) that more than 95% of the available LAA RBs were allocated to the LAA client device. This can be attributed to fewer active users due to

COVID-19, and the availability of a limited number of LAA devices in the market which are also quite expensive. These factors helped us create a controlled coexistence environment. Measurements for Same PCI and Different PCI scenarios in Licensed and Unlicensed components were done with one active Wi-Fi hotspot to ensure true LTE-WiFi coexistence. Thereafter, different coexistence scenarios were created by incrementally introducing up to five mobile Wi-Fi hotspots. All Wi-Fi hotspots were operational on the same channel as LAA. Ten mobile devices including Google Pixel (2, 3, & 5), Motorola Edge+, and Samsung Galaxy S9 were used; five to create Wi-Fi hotspots and the remaining five to act as clients. A Google Pixel 5 served as the LTE-LAA client. For maximal impact, a dense network scenario was created with all Wi-Fi hotspots within a 10m range of each other and the target UE.

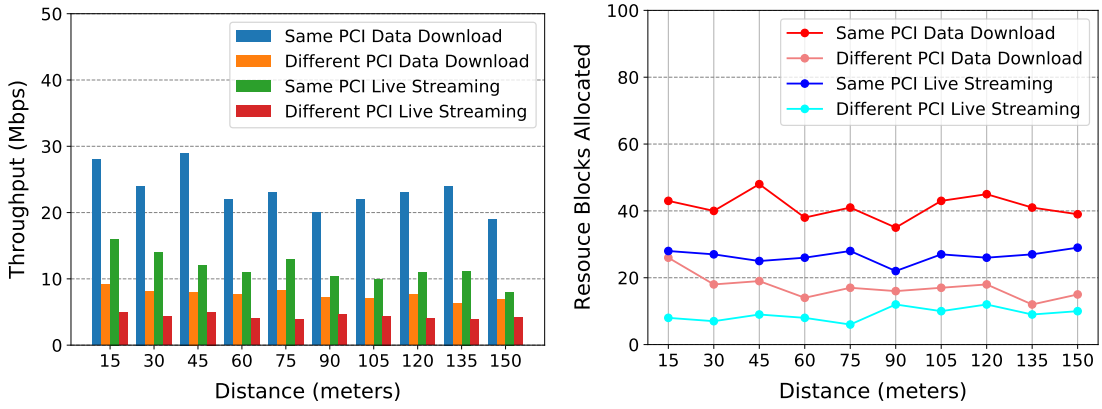

(a) Throughput

(b) RB Allocation

Figure 5.13: Licensed On-site Experiments

5.5.3 Results and Analysis

5.5.3.1 Unlicensed Component

The variation in Throughput with distance for five types of traffic and one coexisting Wi-Fi hotspot is shown in Figures 5.12(a) & 5.12(b). It is evident that the network performance in the Same PCI scenario far exceeds that in the Different PCI scenario (by 76.93% on average for background data). As expected, the Throughput for all types of traffic decreases with distance, due to the corresponding decrease in SINR. Likewise, with the incremental introduction of Wi-Fi hotspots (*i.e.,* Co-channel interference), the network Throughput consistently decreases, which is evident from Figures 5.12(c) & 5.12(d). This can be attributed to the combined decrease in SINR and RB allocation, which will be discussed later. The following findings are noteworthy.

- *Correlating Throughput$_{Exp}$ with network performance*: Although the Throughput$_{\text{Exp}}$ of SINR-Capacity model for the Different PCI scenarios are higher than those of the Same PCI, the reverse

is true for performance in terms of actual network Throughput. This cannot be attributed to a variation in SINR, which is comparable for both scenarios. From a network monitoring standpoint, it can be discerned from Figure 5.12(e) that RB allocation for data download and video streaming in Same PCI is higher than the corresponding Different PCI functions by 65.19% and 98.63%, respectively. With similar levels of SINR, a higher RB allocation explains the greater Throughput in Same PCI despite low model $\text{Throughput}_{\text{Exp}}$. However, from a data analysis perspective, the opposing trends imply that in Same PCI scenarios network variables other than SINR, Capacity, and PCI (e.g., RB allocated, QCI, etc.) play a more significant role in the network model. Including these variables in the prediction of network performance may offer trends consistent with measurement analysis [7, 8]. They may also yield more robust network models with higher $\text{Throughput}_{\text{Exp}}$ and reliable feature relationship equations for use in network optimization [8, 13]. However, adding more network features will increase the computational overhead of training ML models.

- *Impact of coexisting Wi-Fi APs*: Figure 5.12(f) shows that increasing the coexisting Wi-Fi hotspots from one to five not only degrades the SINR due to increased interference but also reduces the RB allocation due to increased contention for channel access.

5.5.3.2 Licensed Component

Throughput and RB allocation results for the Licensed on-site experiments are presented in Figures 5.13(a) & 5.13(b), respectively. The Same PCI and Different PCI performance trends in the Licensed component are similar for both operator data analysis and network experiments. The Same PCI scenario outperforms the Different PCI, in terms of network performance prediction, network throughput, and RB allocation, for comparable levels of SINR. Compared to the Same PCI scenarios, the network performance drop (*e.g.,* Throughput & RB) in Different PCI conforms to the significantly lower model $\text{Throughput}_{\text{Exp}}$. As inferred earlier from the data analysis, Licensed operation in the current LTE-LAA deployments is not efficient in the Different PCI scenario.

5.5.3.3 PCI Scenarios and QoS

An insightful observation on the LTE-LAA operation can be made by monitoring network performance metrics when Live Stream traffic is active. It can be discerned from Figure 5.12 that the Unlicensed component does not register any Throughput for Live Stream, in both Same PCI and Different PCI scenarios. Likewise, in both the Unlicensed scenarios, no RB is allocated to Live Stream.

Live Stream falls in QCI class 7, along with other delay-critical and data-intensive services as online interactive gaming. The maximum permitted Packet Delay and Packet Loss Rate for QCI 7 are 100ms and $10^{-}3$, respectively. Live stream traffic is not assigned to the LAA component despite high RB availability and little contention from coexisting Wi-Fi APs, as the cellular operator cannot guarantee the QoS requirements in the Unlicensed spectrum. Consequently, as illustrated in Figure 5.13, the

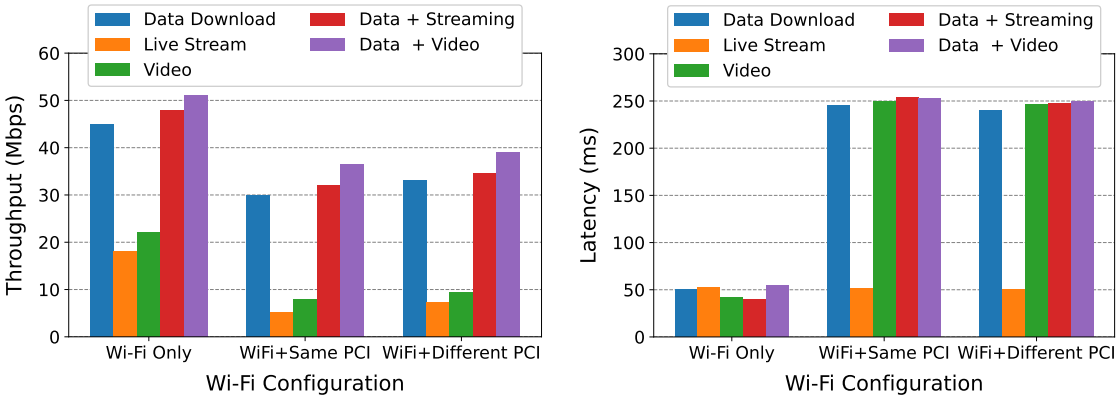

(a) Throughput

(b) Latency

Figure 5.14: Wi-Fi On-site Measurements

Licensed LTE component carries Live Stream traffic, for both the Same PCI and different PCI scenarios. Thus, with respect to QoS guarantees, PCI Scenarios do not seem to have any bearing on the operator's decision of assigning particular traffic pipelines to LTE or LAA interfaces.

5.5.3.4 Resource Blocks and LTE-LAA Performance

A detailed comparison of Licensed and Unlicensed feature relationships is presented in [7,8]. However, the feature combination is limited to SINR, Capacity, and PCI. Measurement results reveal that RB allocation may significantly influence feature relationships and enhance network performance prediction. In general, the Same PCI RB allocation is higher than the Different PCI. However, this difference is more pronounced in the Licensed spectrum as compared to the Unlicensed. Further, despite the factors of resource sharing, contention, and back-off mechanisms in the Unlicensed spectrum, the observed RB allocation is much higher than the Licensed. This is because three 20MHz channels are available in the Unlicensed spectrum, leading up to a maximal RB allocation of 300. However, as user density increases, the high availability of resource blocks may not be possible. Finally, Figure 5.12(e) shows that the RB allocation in the Unlicensed spectrum is adversely affected by distance, while there seems to be no evident pattern in the Licensed spectrum, as seen in Figure 5.13(b). However, the existence of a correlation can only be ascertained through feature relationship analysis.

5.5.3.5 Impact on Wi-Fi Performance

In this experiment, Wi-Fi AP 802.11 ac is made to coexist with LAA BS for the five different traffic flows. The closed authentication method is used so that outside Wi-Fi clients are not connected to the AP. The Wi-Fi performance is measured using Wireshark, which runs on a laptop in monitor mode so that it can capture all packets in the air corresponding to the locked channel. The Throughput

and Latency for Wi-Fi baseline and coexistence scenarios is computed, and the results are presented in Figures 5.14(a) & 5.14(b). Wi-Fi performance is better for both scenarios when there is no LAA transmission. Upon activating LAA clients and initiating data traffic, it was observed that there is an immense adverse impact on Wi-Fi performance. While Throughput drops to half as compared to the baseline scenario, Latency increases by as much as four times for most traffic flows. Between the Same PCI and Different PCI, the latter seems to coexist better with Wi-Fi, offering relatively better performance than the Same PCI scenario. This conforms to the LAA-side observations, as a better performance of the Same PCI LAA, leads to greater contention with Wi-Fi, degrading Throughput, and increasing Latency, more than the Different PCI LAA.

The on-site experiments at LAA sites demonstrate the impact of coexistence PCI scenarios on both LAA and Wi-Fi sub-systems. The next section attempts to solve the important problem of recognizing the PCI scenario by analyzing the operator data.

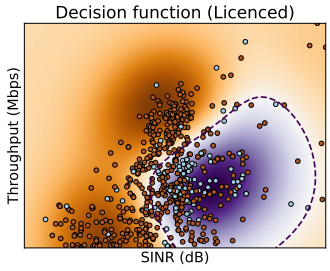

(a) Licensed

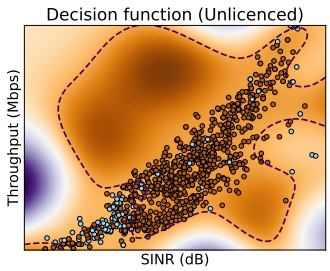

(b) Unlicensed

Figure 5.15: Decision Boundaries

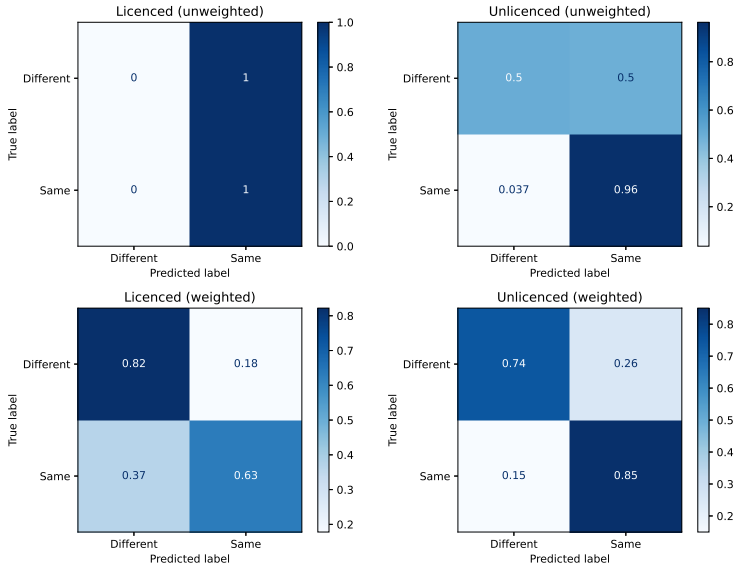

Figure 5.16: Confusion Matrix

5.6 Predictive Modeling of PCI Scenarios

Unlicensed network performance is influenced by the PCI scenario to which a UE belongs. Thus, awareness of PCI scenarios at the UE will be instrumental in implementing UE-initiated cellular operations such as cell selection, handover, broadcasts, etc. [125, 126]. A reliable solution will also be

beneficial during vertical handovers in emerging 5G heterogeneous networks [127]. Thus, identification of the PCI Scenario at the UE will further improve its decision-making process while performing these operations for enhanced end-user QoS.

However, there are two factors that make this task extremely challenging. First, there is the problem of power costs in UE-driven procedures, because battery drain is a major constraint in mobile devices. UE-driven cell selection and handover mechanisms must be *light-weight* with low power costs to avoid battery drain [125]. Traditionally, advanced power-saving mechanisms, such as "sleep modes" are implemented to reduce battery drain [126]. Since the PCI Scenario identification requires ML-based classification models that are inherently computationally expensive, the simplest feature vector conceivable in a wireless network comprising only SINR and throughput is considered in the proposed solution. The rationale is that the cell selection mechanism in LTE/LTE-A/LAA relies heavily on some measure of signal strength such as SINR or RSRP [59]. Furthermore, from the perspective of QoS guarantees, network throughput is the metric of primary interest. Learning the PCI scenario from a simple two-variable feature vector is particularly useful as it minimizes the energy budget of the computational requirements for classification, especially if it is being performed on a mobile device. However, it significantly increases the difficulty in achieving high prediction accuracy, an obstacle that the proposed solution overcomes.

Second, the inherent imbalance in the PCI scenario distribution (¿80% LAA sites are Same PCI), is reflected in the network data, rendering the minority class to be a mere 16% in our data set. Together, the minimalist feature vector and extreme data imbalance make PCI scenario detection a difficult problem to solve.

5.6.1 Problem setup

The identification of two PCI scenarios, i.e., Same or Different can be posed as a binary classification problem. In particular, the task is to learn a mapping $h : \mathbf{x}_i \rightarrow t_i$, where $\mathbf{x}_i$ is the feature vector with attributes SINR (dBm) & Throughput (Mbps). Further, t_i is 1 when the data point belongs to the Same PCI scenario and 0, otherwise.

5.6.2 Learning the decision function (h)

The Support Vector Machine (SVM) algorithm was deployed to learn h. In principle, other machine learning algorithms, including logistic regression, neural networks, and decision trees, can also be used with varying trade-offs in accuracy and compute time. Suppose that the data set has N training points, *i.e.,* $\{(\mathbf{x}_i, t_i)\}_{i=1}^{N}$, then the SVM algorithm aims to solve the following optimization problem:

$$\arg\min_{\mathbf{w},b} \frac{1}{2}\mathbf{w}^\top \mathbf{w} + C\sum_{i=1}^{N}\zeta_i \tag{5.1}$$
$$\text{s.t. } t_i(\mathbf{w}^\top \phi(\mathbf{x}_i) + b) \geq 1 - \zeta_i, \forall i$$
$$\zeta_i \geq 0, \forall i$$

where $\mathbf{w}$ and b are the weight vector and bias, respectively. C is a hyperparameter that is set through cross-validation. Moreover, ϕ is a function that allows us to learn non-linear boundaries. Figure 5.15 indicates that the data is not linearly separable. Thus, a non-linear decision function could help us make more accurate predictions as compared to a linear decision function. In Figure 5.15, the decision boundaries for both Unlicensed and Licensed data are presented. In the figure, 'orange' points refer to points belonging to the Same PCI scenario, whereas 'navy' points signify the Different PCI scenario. The SVM algorithm was used with the RBF kernel to learn the decision boundaries.

Table 5.1: Macro f-scores of PCI Scenario Classification

Network Component	**Linear**	**Polynomial**	**RBF**
Unlicenced	66.4	74.81	**75.0**
Licenced	59.0	56.2	**59.20**

The variation of Macro f-scores for the task of PCI scenario classifications with different kernel functions used by the SVM algorithm is presented in Table 5.1. The scores are computed via k-fold cross-validation, where $k = 5$. The Radial Basis Function (RBF) yields the best accuracy in both settings.

5.6.3 Data imbalance

Data analysis reveals that the data is imbalanced in favor of the Same PCI scenario – 83.51% data points are from the Same PCI scenario, whereas 16.49% data points are from different PCI. It is important that a classification model performs well in both classes and not just on the majority class. If this is not ensured, the Same PCI scenario will be detected with high accuracy, but a Different PCI sample may also be misjudged as the Same PCI. From the perspective of UE-initiated cell selection or handover, when a UE wishes to camp on a small cell with Different PCI architecture (e.g., to experience better Wi-Fi performance), it is very likely to erroneously camp on the Same PCI cell. Figure 5.16 shows that the standard classifier performs well only on the majority class. Therefore, it becomes crucial to explicitly handle the issue of data imbalance. Popular approaches handle data imbalance by introducing class weights or by down-sampling the majority class [128]. In particular, the inverse frequency was used as the class weight for both Unlicenced and Licenced data. In practice, class weights can be readily incorporated into eq. 5.1. The class imbalance requires us to adapt the evaluation metric in addition to the training pipeline as discussed below.

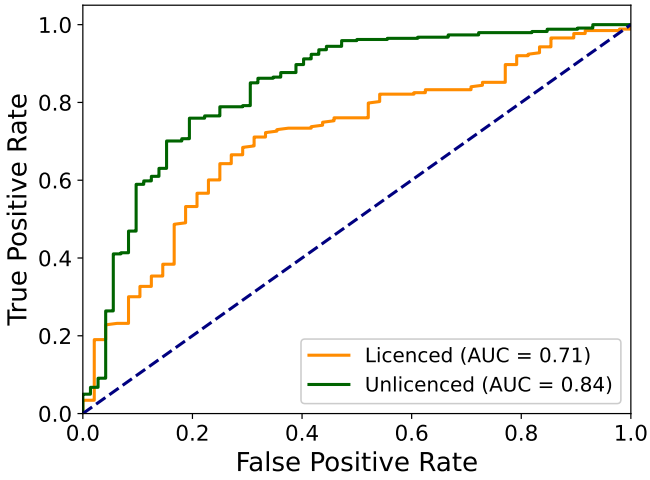

Figure 5.17: ROC Curve for PCI Scenario Classification

5.6.4 Results and analysis

A trivial algorithm that always predicts the majority class can lead to 83.51% accuracy on the classification task. Note that, accuracy is defined as the percentage of points that were correctly classified by the model. However, such a model would be clearly undesirable, as it does well only on the majority class. Hence, it becomes important to look at the f-score, confusion matrix, and receiver operating characteristic (ROC) curve for an exhaustive evaluation of the classification model.

The confusion matrices in Figure 5.16 demonstrate that class weights allow for more balanced predictions on both classes, compared to the standard classifier. Learning a classifier with class weights (second row) leads to accurate predictions on both classes, whereas the standard classifier (first row) performs well only on one class. In particular, the unweighted predictor yields 100% and 96% accuracy for the same PCI class for Licenced and Unlicenced data, respectively. However, the accuracy drops down to 0% and 50% on the Different PCI class for Licenced and Unlicenced data, respectively. On the other hand, the weighted predictor yields 82% and 74% accuracies on the Different PCI class for Licenced and Unlicenced data, respectively

Moreover, the ROC curve in Figure 5.17 presents the relationship between True Positive Rate (TPR) and False Positive Rate (FPR). Getting high TPR might be more important for certain applications, whereas a low FPR might be more important for others. So, the end-user may choose the configuration depending on the application based on the ROC curve. For example, when a user is mobile and needs higher performance in the Unlicensed spectrum by camping on the Same PCI cell, it is highly desirable to have a high TPR. Likewise, in an indoor setting, where the user needs higher Wi-Fi bandwidth for traffic such as Live-streams, it may be important to ensure a low FPR, for reliable identification of Different PCI Scenario. At times ensuring both high TPR and low FPR may also be necessary for

latency-critical services such as augmented reality applications on the Licensed/Unlicensed component or live streams on the Licensed component.

The proposed PCI scenario classification solution is highly suitable for UE-driven procedures, especially in Unlicensed networks where its prediction performance is high (AUC=0.84). It is worth noting that the high accuracy is despite the use of a minimal feature set comprising only SINR and Throughput. Thus, the proposed solution offers a strong prediction of the PCI scenario while ensuring energy savings at the UE, which is a prerequisite for UE-initiated handovers and cell attachments [126].

It is important to add that for UE-driven cell selection, the distinction in the performance of the Same PCI and Different PCI scenarios will raise questions of fairness in resource allocation. In the recent past, game theory approaches have been shown to be particularly useful in solving problems of fair coexistence [129]. Thus, to decide when a UE can attach to the Same PCI or Different PCI cell, a solution from game theory may be quite effective.

5.7 Conclusions and Way Forward

Unlicensed coexistence deployments are currently in a nascent stage and the two important factors that determine network characteristics and performance are deployment architecture and fiber optic backhaul availability. From the observations made at the LAA sites and the analysis of the dataset gathered from three major LTE-LAA coexistence service providers, this chapter put forward some explanations and discussed a few open challenges with regard to the PCI Scenarios. First, the Same PCI for LTE and LAA components implies that the deployment has a common backhaul connectivity, which facilitates the efficient splitting of Licensed and Unlicensed data. In this scenario, packet aggregation is likely to be more seamless and efficient. Consequently, the performance at the transport layer will improve, offering improved QoS to the end user. Second, the impact of PCI as a categorical parameter when LTE and LAA components are camped on different cells is different from the Same PCI scenario. Third, resource block allocation not only differs in the Licensed and Unlicensed spectrum but is also different for the two PCI scenarios within the same LTE-LAA component. Finally, successfully solving the PCI scenario identification problem with the minimal feature set will facilitate greater choice in the UE during the cell selection or handover process. These findings are extremely important in light of the upcoming 5G-NR Unlicensed coexistence deployments and the allocation of additional 1200MHz of Unlicensed spectrum in the 6 GHz band by the Federal Communications Commission.

Network performance measurements indicate that RB allocation is an important network feature point and considering it in the feature combination may explain the contrasting findings in the Unlicensed component. It may also improve the network performance modeling in both scenarios.

Chapter 6

Conclusions

This dissertation has presented a new data-driven approach to network performance analysis and optimization by gathering and utilizing cellular operator data from public LAA deployments. Three primary contributions have been put forward.

First, the thesis utilized machine learning algorithms to analyze and optimize unlicensed cellular networks. Feature relationship analysis was used to present a comparative study of unlicensed cellular standards, viz., LAA and LTE-U. The network data for analysis was collected through comprehensive experiments on an LAA/LTE-U testbed. The gathered data was then analyzed through a family of regression algorithms. The thesis highlighted the utility of network feature relationships in analyzing unlicensed network performance through various machine learning model parameters such as R-sq, residual error, outliers, *etc.* It offered several insightful inferences on aspects such as the impact of bandwidth, residual error, and outliers on coexistence network performance. The analysis conclusively shows that LAA data models are more stable and precise than LTE-U models, effectively settling the LAA vs. LTE-U debate. More importantly, the thesis demonstrated how machine learning could be leveraged to enhance classical network optimization techniques. NeFRO, a feature relationship-based optimization framework, was proposed and validated through signal strength and capacity optimization. NeFRO reduced the convergence times by as much as 24%, and its accuracy with respect to baseline classical optimization models was as high as 97.16% on average. Further, the thesis addressed the unexplored problem of "Accuracy Speed trade-off" in the data-driven optimization of unlicensed networks. It proposed a context-aware network feature relationship-based optimization framework (CANEFRO), which was validated through decision matrix analysis. CANEFRO demonstrated that network context and machine learning enhance the capabilities of classical network optimization.

Second, data was gathered from public LAA deployments of three major cellular service providers, viz., AT&T, T-Mobile, and Verizon. An innovative computer-vision-based solution was engineered to extract LAA data gathered through the Network Signal Guru tool. Thereafter, the LAA dataset was analyzed to study the impact of PCI or cell selection in public LAA networks. It was learned that the differences in Licensed and Unlicensed components could be attributed to factors such as

operator deployment architecture, the impact of cooperating and rogue Wi-Fi transmissions in the unlicensed band, and resource block allocation. The thesis also studied the variation in the performance of numerosity reduction techniques in the Licensed and Unlicensed components of an LTE-LAA system. Through rigorous analysis using multiple machine learning algorithms, the thesis inferred that parameters of an ML model trained on network data, such as R-sq, Accuracy, and residual error, are reliable metrics for cell quality estimation. Cell quality has a direct correlation with network performance. Thus, the thesis hypothesized that cell association guided by cell quality estimates derived from operator data could greatly enhance the end user experience in unlicensed cellular networks. The proposed NeFRO framework was used to validate the hypothesis. The results showed that data-driven cell selection can reduce Unlicensed cell association time by as much as 34.89%.

Validation of the proposed data-driven optimization approach is of great relevance. As coexistence network densification continues and the number of small cells increases, the convergence time required for network optimization will increase significantly as well. Cell association time will become a major impediment to QoS delivery to the end user. Thus, an operator-data-driven cell selection approach will be highly beneficial in alleviating this problem.

Finally, from the observations made at the LAA sites and the analysis of the dataset gathered from the three LAA service providers, a unique phenomenon was observed that is specific to the unlicensed networks. Two cell selection scenarios were identified, i.e., the Same PCI scenario and the Different PCI scenario. The Same PCI for LTE and LAA components implies that the deployment has a common backhaul connectivity, which facilitates an efficient splitting of Licensed and Unlicensed data. In the Same PCI scenario, the packet aggregation will likely be more seamless and efficient. Consequently, the performance at the transport layer will improve, offering improved QoS to the end user. The analysis showed that the impact of PCI as a categorical parameter when LTE and LAA components are camped on different cells varies significantly from the Same PCI scenario. Further, when coexisting with Wi-Fi, the performance of the two PCI scenarios differs considerably, as well. The thesis also showed that resource block allocation not only differs in the Licensed and Unlicensed components but is also dependent on the PCI scenario a UE is in. Given the significance of this phenomenon, the thesis aimed to solve the PCI scenario identification problem through an imbalanced classifier using a minimal feature set. The proposed PCI scenario classification solution is highly suitable for UE-driven procedures in the unlicensed band where the scenario prediction performance is high (AUC=0.84). For example, reliable PCI scenario prediction will pave the way for UE-initiated cell attachment by offering a choice to the UE during the cell selection or handover process. The proposed solutions and analysis are extremely important in light of the upcoming 5G-NR Unlicensed deployments where the number of PCI scenarios will multiply.

There are a few additional noteworthy findings from the data analysis and field experiments carried out in this thesis. First, cellular operators are not yet offering services in the 5GHz U-NII-2 band. The LAA operators have only deployed LAA networks in the 5GHz U-NII-1 and U-NII-3 bands.

The U-NII-2 band is used for military, radar, and ship (X or S band radar) transmissions. A plausible reason is that a sensing protocol needs to be implemented to avoid interference with ongoing radar/ship transmissions. This may be expensive for operators, given the low penetration of LAA-equipped mobile devices. Although operators are not utilizing the U-NII-2 band currently, it may change as devices capable of offering LAA and 5G-NRU services achieve greater penetration. Further, the analysis indicates that Wi-Fi and LAA coexist fairly in the 5 GHz band, which is encouraging. Finally, over 90% of the available LAA RBs were allocated to the client device, which could be because of fewer active users during the pandemic and limited penetration of the LAA devices.

To conclude, this thesis aimed to leverage machine learning and network data to propose new methodologies for performance analysis and optimization in unlicensed networks. It has demonstrated how cellular operator data can be utilized to make the mechanisms in unlicensed networks, such as cell selection, more efficient. These contributions will add value to the upcoming 5G NR-U networks and cellular operation in other unlicensed bands. For fair spectrum sharing and cellular operation in all future unlicensed bands, cellular operators will require these data-driven solutions to analyze and optimize network performance.

Acknowledgement

Success in any endeavor depends on effort and environment. I started working on this thesis at the onset of the COVID-19 pandemic, a rather precarious and uncertain time. Despite the countless challenges, personal and professional, this thesis was successfully completed within the stipulated time.

Huge credit goes to my supervisor, Dr. Hirozumi Yamaguchi, and co-supervisor, Dr. Teruo Higashino, who have been my anchors over the past three years. They have offered me excellent advice and guidance. They not only supervised my research but also worked with me proactively when faced with hard deadlines, especially Dr. Yamaguchi. Research work is only half the battle for an international student in Japan, and my supervisors have been the most kind and gracious mentors. They have extended all possible help and support I needed during this time. Dr. Yamaguchi has been extremely encouraging and provided a nurturing environment that enabled me to learn new skills in a wide variety of fields. I am eternally grateful to both of my supervisors. They have been exceptional.

I would like to express my gratitude to Dr. Hideyuki Shimonishi, Dr. Toru Hasegawa, Dr. Takashi Watanabe, and Dr. Masayuki Murata for taking out the time to have a discussion on my thesis. Their questions, feedback, and suggestions for improvement were valuable in revising the manuscript. Thank you very much.

A sincere thank you to my collaborators, Dr. Vanlin Sathya, Dr. Kunal Dahiya, Dr. Monisha Ghosh, Dr. Eitaro Yamatsuta, Dr. Winston Seah, and Dr. Bheemarjuna Reddy, for their efforts, contributions, and suggestions. Especially Dr. Vanlin and Dr. Kunal. They are excellent teammates - brilliant, hardworking, and compassionate.

The professors in my lab have shared great feedback and raised interesting questions during the presentations and seminars. For that, I sincerely thank Dr. Akihito Hiromori, Dr. Akira Uchiyama, Dr. Tatsuya Amano, Dr. Erdélyi Viktor, Dr. Hiroki Yoshikawa, Dr. Hamada Rizk, and Dr. Teruhiro Mizumoto. I also thank my lab mates and the lab secretaries for making Mobile Computing Lab a lively and happy place to work and have fun.

A heartfelt thank you to Dr. Betty Lala for being a wonderful, patient, and supportive partner. She has always cheered me on and stood by me on all days - good, bad, and ugly. She has been a perfect sounding board and offered critical help during countless deadlines. Thank you for your unceasing love and encouragement.

A huge thank you to my family back home. To my parents, Mr. Kalika Kala and Mrs. Pushpa Manas Kala, who haven't seen their only child in almost four years and dealt with all of life's problems on their own. To my brother Kalyan for the constant support and for holding down the fort. Thank you all for your love, patience, and encouragement.

I also extend my earnest gratitude to Dr. Aya Hagishima for her support over the past year.

A special vote of thanks to Yohei and Deepanker, who have been my lifeline on several occasions.

And a warm thank you to the JICA team and my friends and colleagues for their help and support.

Last but not least, I would like to thank myself for keeping at it, pushing through the pain, making mistakes and learning from them, being relentless, and showing up.

Dedication

This thesis is dedicated to the two loved ones I lost but could not mourn.
And to DMX.
May you find the peace in the afterlife that eluded you in this one.

Bibliography

[1] D. Jiang and G. Liu, "An overview of 5g requirements," *5G Mobile Communications*, pp. 3–26, 2017.

[2] C. Fishman, "The story of how NASA created the first worldwide high-speed data network—in 1968, url=https://www.fastcompany.com/90366549/the-story-of-how-nasa-created-the-first-worldwide-high-speed-data-network-in-1968," 2019.

[3] Ericcson, "Ericsson mobility report, url=https://www.ericsson.com/en/reports-and-papers/mobility-report," 2022.

[4] G. M. S. Association, "LTE Unlicensed Reports, url=https://gsacom.com/technology/lte-unlicensed/," 2020.

[5] V. Sathya, M. I. Rochman, and M. Ghosh, "Measurement-based coexistence studies of laa & wi-fi deployments in chicago," *IEEE Wireless Communications*, vol. 28, no. 1, pp. 136–143, 2020.

[6] G. S. for Mobile Communications Association, "Spectrum Sharing GSMA Public Policy Position, url=https://www.gsma.com/spectrum/wp-content/uploads/2021/06/Spectrum-Sharing-Positions.pdf," 2021.

[7] S. M. Kala, K. Dahiya, V. Sathya, T. Higashino, and H. Yamaguchi, "Lte-laa cell selection through operator data learning and numerosity reduction," *Pervasive and Mobile Computing*, vol. 83, p. 101586, 2022. [Online]. Available: https://www.sciencedirect.com/science/article/pii/S1574119222000335

[8] S. M. Kala, V. Sathya, E. Yamatsuta, H. Yamaguchi, and T. Higashino, "Operator data driven cell-selection in lte-laa coexistence networks," in *International Conference on Distributed Computing and Networking 2021*, 2021, pp. 206–214.

[9] A. Abedi and T. Brecht, "Examining relationships between 802.11 n physical layer transmission feature combinations," in *Proceedings of the 19th ACM International Conference on Modeling, Analysis and Simulation of Wireless and Mobile Systems*, 2016, pp. 229–238.

[10] L. Kriara, M. K. Marina, and A. Farshad, "Characterization of 802.11 n wireless lan performance via testbed measurements and statistical analysis," in *2013 IEEE International Conference on Sensing, Communications and Networking (SECON)*. IEEE, 2013, pp. 158–166.

[11] S. Biswas, J. Bicket, E. Wong, R. Musaloiu-e, A. Bhartia, and D. Aguayo, "Large-scale measurements of wireless network behavior," in *Proceedings of the 2015 ACM Conference on Special Interest Group on Data Communication*, 2015, pp. 153–165.

[12] L. Kriara and M. K. Marina, "Samplelite: A hybrid approach to 802.11 n link adaptation," *ACM SIGCOMM Computer Communication Review*, vol. 45, no. 2, pp. 4–13, 2015.

[13] S. M. Kala, V. Sathya, S. W. KG, and B. R. Tamma, "Cirno: Leveraging capacity interference relationship for dense networks optimization," in *2020 IEEE Wireless Communications and Networking Conference (WCNC)*. IEEE, 2020, pp. 1–6.

[14] M. H. Ly, Y. Hussein, E. Mhanna, and M. Assaad, "Initial access optimization for millimeter wave wireless networks," in *2021 IEEE Wireless Communications and Networking Conference (WCNC)*, 2021, pp. 1–6.

[15] J. Zhang and D. M. Blough, "Optimizing coverage with intelligent surfaces for indoor mmwave networks," in *IEEE INFOCOM 2022 - IEEE Conference on Computer Communications*, 2022, pp. 830–839.

[16] J. Zeng, H. Wang, and W. Luo, "Self-optimizing traffic steering for 5g mmwave heterogeneous networks," *Sensors*, vol. 22, no. 19, p. 7112, 2022.

[17] T. Kudo and T. Ohtsuki, "Cell range expansion using distributed q-learning in heterogeneous networks," *Eurasip journal on wireless communications and networking*, vol. 2013, no. 1, p. 61, 2013.

[18] A. Pratap, R. Singhal, R. Misra, and S. K. Das, "Distributed randomized k-clustering based pcid assignment for ultra-dense femtocellular networks," *IEEE Transactions on Parallel and Distributed Systems*, vol. 29, no. 6, pp. 1247–1260, 2018.

[19] N. Trabelsi, C. S. Chen, R. El Azouzi, L. Roullet, and E. Altman, "User association and resource allocation optimization in lte cellular networks," *IEEE Transactions on Network and Service Management*, vol. 14, no. 2, pp. 429–440, 2017.

[20] D. Fooladivanda and C. Rosenberg, "Joint user association and resource allocation in heterogeneous cellular networks: Comparison of two modeling approaches," in *2019 31st International Teletraffic Congress (ITC 31)*. IEEE, 2019, pp. 66–74.

[21] J. Tan, S. Xiao, S. Han, Y.-C. Liang, and V. C. Leung, "Qos-aware user association and resource allocation in laa-lte/wifi coexistence systems," *IEEE Transactions on Wireless Communications*, vol. 18, no. 4, pp. 2415–2430, 2019.

[22] V. Huang, A. Bertze, and S. Corroy, "Adaptive cell selection in heterogeneous networks," Apr. 16 2019, uS Patent 10,264,496.

[23] Y. Shi, J. Zhang, W. Chen, and K. B. Letaief, "Generalized sparse and low-rank optimization for ultra-dense networks," *IEEE Communications Magazine*, vol. 56, no. 6, pp. 42–48, 2018.

[24] G. Cheung, J. Lee, S.-J. Lee, and P. Sharma, "On the complexity of system throughput derivation for static 802.11 networks," *IEEE Communications Letters*, vol. 14, no. 10, pp. 906–908, 2010.

[25] H. Zhang, X. Chu, W. Guo, and S. Wang, "Coexistence of wi-fi and heterogeneous small cell networks sharing unlicensed spectrum," *IEEE Communications Magazine*, vol. 53, no. 3, pp. 158–164, 2015.

[26] V. Sathya, S. M. Kala, and K. Naidu, "Heterogenous networks: From small cells to 5g nr-u," *Wireless Personal Communications*, pp. 1–32, 2022.

[27] Z. Zhong, P. Kulkarni, F. Cao, Z. Fan, and S. Armour, "Issues and challenges in dense WiFi networks," in *Proc. of the Int'l Wireless Communications and Mobile Computing Conference (IWCMC)*, Dubrovnik, Croatia, 2015, pp. 947–951.

[28] Y. Kao, H. Chiu, S. Wu, H. Chao, and C. Gan, "Throughput analysis of lte and wifi heterogeneous dense small cell networks," pp. 1–6, 2019.

[29] H. Song, Q. Cui, Y. Gu, G. L. Stüber, Y. Li, Z. Fei, and C. Guo, "Cooperative lbt design and effective capacity analysis for 5g nr ultra dense networks in unlicensed spectrum," *IEEE Access*, vol. 7, pp. 50 265–50 279, 2019.

[30] H. Zhang, X. Chu, W. Guo, and S. Wang, "Coexistence of wi-fi and heterogeneous small cell networks sharing unlicensed spectrum," *IEEE Communications Magazine*, vol. 53, no. 3, pp. 158–164, 2015.

[31] L. Ho and H. Gacanin, "Design principles for ultra-dense Wi-Fi deployments," in *Proc. of the IEEE Wireless Communications and Networking Conference (WCNC)*, Barcelona, Spain, 15-18 April 2018, pp. 1–6.

[32] M. S. Afaqui, E. Garcia-Villegas, and E. Lopez-Aguilera, "Ieee 802.11 ax: Challenges and requirements for future high efficiency wifi," *IEEE Wireless Communications*, vol. 24, no. 3, pp. 130–137, 2017.

[33] S. M. Kala, M. P. K. Reddy, R. Musham, and B. R. Tamma, "Interference mitigation in wireless mesh networks through radio co-location aware conflict graphs," *Wireless Networks*, vol. 22, no. 2, pp. 679–702, 2016.

[34] D. Chafekar, V. Anil Kumar, M. V. Marathe, S. Parthasarathy, and A. Srinivasan, "Capacity of wireless networks under sinr interference constraints," *Wireless Networks*, vol. 17, no. 7, pp. 1605–1624, 2011.

[35] K. Jain, J. Padhye, V. N. Padmanabhan, and L. Qiu, "Impact of interference on multi-hop wireless network performance," *Wireless networks*, vol. 11, no. 4, pp. 471–487, 2005.

[36] P. Gupta and P. R. Kumar, "The capacity of wireless networks," *IEEE Transactions on Information Theory*, vol. 46, no. 2, pp. 388–404, 2000.

[37] Y. Shi, J. Zhang, K. B. Letaief, B. Bai, and W. Chen, "Large-scale convex optimization for ultra-dense cloud-ran," *IEEE Wireless Communications*, vol. 22, no. 3, pp. 84–91, 2015.

[38] M. X. Cheng, Y. Li, and D.-Z. Du, *Combinatorial optimization in communication networks*. Springer Science & Business Media, 2006, vol. 18.

[39] J. Park, S.-L. Kim, and J. Zander, "Asymptotic behavior of ultra-dense cellular networks and its economic impact," in *2014 IEEE Global Communications Conference*. IEEE, 2014, pp. 4941–4946.

[40] E. Björnson, L. Sanguinetti, and M. Kountouris, "Deploying dense networks for maximal energy efficiency: Small cells meet massive mimo," *IEEE Journal on Selected Areas in Communications*, vol. 34, no. 4, pp. 832–847, 2016.

[41] B. Li, D. Zhu, and P. Liang, "Small cell in-band wireless backhaul in massive mimo systems: A cooperation of next-generation techniques," *Ieee transactions on wireless communications*, vol. 14, no. 12, pp. 7057–7069, 2015.

[42] X. Ge, H. Cheng, M. Guizani, and T. Han, "5g wireless backhaul networks: challenges and research advances," *IEEE Network*, vol. 28, no. 6, pp. 6–11, 2014.

[43] A. Y. Al-Zahrani, F. R. Yu, and M. Huang, "A joint cross-layer and colayer interference management scheme in hyperdense heterogeneous networks using mean-field game theory," *IEEE Transactions on Vehicular Technology*, vol. 65, no. 3, pp. 1522–1535, 2015.

[44] M. Manjrekar, V. R. Pillai, V. R. Raja, and S. Shakkottai, "A mean field game approach to scheduling in cellular systems," *IEEE Transactions on Control of Network Systems*, 2019.

[45] M. A. Hirzallah, "Protocols and algorithms for harmonious coexistence over unlicensed bands in next-generation wireless networks," Ph.D. dissertation, The University of Arizona, 2020.

[46] Y. C. Hu, M. Patel, D. Sabella, N. Sprecher, and V. Young, "Mobile edge computing—a key technology towards 5g," *ETSI white paper*, vol. 11, no. 11, pp. 1–16, 2015.

[47] K. Apicharttrisorn, B. Balasubramanian, J. Chen, R. Sivaraj, Y.-Z. Tsai, R. Jana, S. Krishnamurthy, T. Tran, and Y. Zhou, "Characterization of multi-user augmented reality over cellular networks," in *2020 17th Annual IEEE International Conference on Sensing, Communication, and Networking (SECON)*. IEEE, 2020, pp. 1–9.

[48] M. Kamel, W. Hamouda, and A. Youssef, "Ultra-dense networks: A survey," *IEEE Communications Surveys & Tutorials*, vol. 18, no. 4, pp. 2522–2545, 2016.

[49] A. Rouskas, G. Kyriazis, and D. I. Komnakos, "Green optimization schemes for mobile network design and operation," *Wireless Personal Communications*, vol. 96, no. 2, pp. 3227–3247, 2017.

[50] E. Amaldi, A. Capone, M. Cesana, I. Filippini, and F. Malucelli, "Optimization models and methods for planning wireless mesh networks," *Computer Networks*, vol. 52, no. 11, pp. 2159–2171, 2008.

[51] J. Tian, H. Zhang, D. Wu, and D. Yuan, "QoS-constrained medium access probability optimization in wireless interference-limited networks," *IEEE Trans. on Communications*, vol. 66, no. 3, pp. 1064–1077, 2018.

[52] F. C. Commission, "Notice of proposed rulemaking on unlicensed use of the 6 GHz band," https://docs.fcc.gov/public/attachments/FCC-18-147A1.pdf, 2018.

[53] G. P. Project, "3GPP release 13 specification," http://www.3gpp.org/release-13/, 2015, accessed: 2019-12-12.

[54] A. M. Baswade, M. Reddy, B. R. Tamma, V. Sathya *et al.*, "Performance analysis of spatially distributed lte-u/nr-u and wi-fi networks: an analytical model for coexistence study," *Journal of Network and Computer Applications*, vol. 191, p. 103157, 2021.

[55] A. M. Baswade and B. R. Tamma, "Channel sensing based dynamic adjustment of contention window in laa-lte networks," in *2016 8th International Conference on Communication Systems and Networks (COMSNETS)*, 2016, pp. 1–2.

[56] P. V. Klaine, M. A. Imran, O. Onireti, and R. D. Souza, "A survey of machine learning techniques applied to self-organizing cellular networks," *IEEE Communications Surveys & Tutorials*, vol. 19, no. 4, pp. 2392–2431, 2017.

[57] G. L. Masini and A. Centonza, "Neighbor selection for handover in a radio access network," Mar. 22 2016, uS Patent 9,294,963.

[58] F. H. Khan and M. Portmann, "Joint qos-control and handover optimization in backhaul aware sdn-based lte networks," *Wireless Networks*, pp. 1–23, 2019.

[59] S. Xu, A. Nikravesh, and Z. M. Mao, "Leveraging context-triggered measurements to characterize lte handover performance," in *International Conference on Passive and Active Network Measurement*. Springer, 2019, pp. 3–17.

[60] V. Sathya, S. M. Kala, S. Bhupeshraj, and B. R. Tamma, "Raptap: a socio-inspired approach to resource allocation and interference management in dense small cells," *Wireless Networks*, pp. 1–24, 2020.

[61] 3GPP, "3gpp tsg-ran wg2 meeting89bis, bratislava, slovakia," April "20 - 24" 2015.

[62] A. Pratap, R. Misra, and U. Gupta, "Randomized graph coloring algorithm for physical cell id assignment in lte-a femtocellular networks," *Wireless Personal Communications*, vol. 91, no. 3, pp. 1213–1235, 2016.

[63] J. Jeon, R. D. Ford, V. V. Ratnam, J. Cho, and J. Zhang, "Coordinated dynamic spectrum sharing for 5g and beyond cellular networks," *IEEE Access*, vol. 7, pp. 111 592–111 604, 2019.

[64] V. Sathya, S. M. Kala, M. I. Rochman, M. Ghosh, and S. Roy, "Standardization advances for cellular and wi-fi coexistence in the unlicensed 5 and 6 ghz bands," *GetMobile: Mobile Computing and Communications*, vol. 24, no. 1, pp. 5–15, 2020.

[65] S. M. Kala, V. Sathya, K. Dahiya, T. Higashino, and H. Yamaguchi, "Optimizing unlicensed coexistence network performance through data learning," in *Mobile and Ubiquitous Systems: Computing, Networking and Services*. Cham: Springer International Publishing, 2022, pp. 128–149.

[66] J. Yi, W. Sun, S. Park, and S. Choi, "Performance analysis of lte-laa network," *IEEE Communications Letters*, vol. 22, no. 6, pp. 1236–1239, 2017.

[67] A. M. Cavalcante, E. Almeida, R. D. Vieira, S. Choudhury, E. Tuomaala, K. Doppler, F. Chaves, R. C. Paiva, and F. Abinader, "Performance evaluation of lte and wi-fi coexistence in unlicensed bands," in *2013 IEEE 77th Vehicular Technology Conference (VTC Spring)*. IEEE, 2013, pp. 1–6.

[68] B. Bojović, L. Giupponi, Z. Ali, and M. Miozzo, "Evaluating unlicensed lte technologies: Laa vs lte-u," *IEEE Access*, vol. 7, pp. 89 714–89 751, 2019.

[69] V. Sathya, M. I. Rochman, and M. Ghosh, "Measurement-based coexistence studies of laa amp; wi-fi deployments in chicago," *IEEE Wireless Communications*, vol. 28, no. 1, pp. 136–143, 2021.

[70] Ericcson, "Ericcson mobility report, 2021," *Update*, 2021. [Online]. Available: www.ericsson.com/en/mobility-report/reports/june-2021

[71] V. Sathya, S. M. Kala, M. I. Rochman, M. Ghosh, and S. Roy, "Standardization advances for cellular and wi-fi coexistence in the unlicensed 5 and 6 ghz bands," *GetMobile: Mobile Computing and Communications*, vol. 24, no. 1, pp. 5–15, 2020.

[72] Z. Ali, B. Bojovic, L. Giupponi, and J. M. Bafalluy, "On fairness evaluation: Lte-u vs. laa," in *Proceedings of the 14th ACM International Symposium on Mobility Management and Wireless Access*, ser. MobiWac '16. New York, NY, USA: Association for Computing Machinery, 2016, p. 163–168. [Online]. Available: https://doi.org/10.1145/2989250.2989255

[73] H. Laaki, Y. Miche, and K. Tammi, "Prototyping a digital twin for real time remote control over mobile networks: Application of remote surgery," *Ieee Access*, vol. 7, pp. 20 325–20 336, 2019.

[74] S. Abadal, A. Mestres, J. Torrellas, E. Alarcon, and A. Cabellos-Aparicio, "Medium access control in wireless network-on-chip: A context analysis," *IEEE Communications Magazine*, vol. 56, no. 6, pp. 172–178, 2018.

[75] K.-L. A. Yau, P. Komisarczuk, and P. D. Teal, "Reinforcement learning for context awareness and intelligence in wireless networks: Review, new features and open issues," *Journal of Network and Computer Applications*, vol. 35, no. 1, pp. 253–267, 2012, collaborative Computing and Applications. [Online]. Available: https://www.sciencedirect.com/science/article/pii/S1084804511001755

[76] S. M. Kala, V. Sathya, K. Dahiya, T. Higashino, and H. Yamaguchi, "Identification and analysis of a unique cell selection phenomenon in public unlicensed cellular networks through machine learning," *IEEE Access*, vol. 10, pp. 87 282–87 301, 2022.

[77] K. P. Murphy, *Machine learning: a probabilistic perspective*. MIT press, 2012.

[78] I. Minitab, "Minitab release 17: statistical software for windows," *Minitab Inc, USA*, 2014.

[79] Q. Mao, F. Hu, and Q. Hao, "Deep learning for intelligent wireless networks: A comprehensive survey," *IEEE Communications Surveys & Tutorials*, vol. 20, no. 4, pp. 2595–2621, 2018.

[80] B. Bellalta, "Ieee 802.11 ax: High-efficiency wlans," *IEEE Wireless Communications*, vol. 23, no. 1, pp. 38–46, 2016.

[81] Q. Chen, G. Yu, and Z. Ding, "Enhanced LAA for Unlicensed LTE Deployment Based on TXOP Contention," *IEEE Transactions on Communications*, vol. 67, no. 1, pp. 417–429, 2019.

[82] V. Valls, A. Garcia-Saavedra, X. Costa, and D. J. Leith, "Maximizing lte capacity in unlicensed bands (lte-u/laa) while fairly coexisting with 802.11 wlans," *IEEE Communications Letters*, vol. 20, no. 6, pp. 1219–1222, 2016.

[83] V. Sathya, A. Ramamurthy, and B. R. Tamma, "On placement and dynamic power control of femtocells in LTE HetNets," in *Proc. of IEEE Globecom*, Austin, TX, USA, 8-12 December 2014, pp. 4394–4399.

[84] A. M. Baswade, K. M. Shashi, B. R. Tamma, and F. A. Antony, "On Placement of LAA/LTE-U Base Stations in Heterogeneous Wireless Networks," in *Proc. of the 19th Int'l Conference on Distributed Computing and Networking (ICDCN)*, Varanasi, India, 4-7 January 2018.

[85] GAMS, "General Algebraic Modeling System," retrieved March 2019 from http://www.gams.com.

[86] V. Belton and T. Stewart, *Multiple criteria decision analysis: an integrated approach*. Springer Science & Business Media, 2002.

[87] V. Sathya, S. M. Kala, M. I. Rochman, M. Ghosh, and S. Roy, "Standardization advances for cellular and wi-fi coexistence in the unlicensed 5 and 6 ghz bands," *GetMobile: Mobile Computing and Communications*, vol. 24, no. 1, pp. 5–15, 2020.

[88] W.-F. Alliance, "AT&T more than halfway to enabling LAA in 24 markets this year, url=https://www.fiercewireless.com/wireless/at-t-more-than-half-way-to-enabling-laa-24-markets-year," 2018.

[89] V. Sathya, M. I. Rochman, and M. Ghosh, "Measurement-based coexistence studies of laa & wi-fi deployments in chicago," *IEEE Wireless Communications*, 2020.

[90] T. Han, X. Ge, L. Wang, K. S. Kwak, Y. Han, and X. Liu, "5g converged cell-less communications in smart cities," *IEEE Communications Magazine*, vol. 55, no. 3, pp. 44–50, 2017.

[91] T. RAN, "Scenarios and requirements for small cell enhancements for e-utra and e-utran (release 12)," *3GPP, TR*, vol. 36, p. V12.

[92] B. Chen, J. Chen, Y. Gao, and J. Zhang, "Coexistence of lte-laa and wi-fi on 5 ghz with corresponding deployment scenarios: A survey," *IEEE Communications Surveys & Tutorials*, vol. 19, no. 1, pp. 7–32, 2016.

[93] X. Wang, S. Mao, and M. X. Gong, "A survey of lte wi-fi coexistence in unlicensed bands," *GetMobile: Mobile Computing and Communications*, vol. 20, no. 3, pp. 17–23, 2017.

[94] C. Wu, X. Chen, T. Yoshinaga, Y. Ji, and Y. Zhang, "Integrating licensed and unlicensed spectrum in the internet of vehicles with mobile edge computing," *IEEE Network*, vol. 33, no. 4, pp. 48–53, 2019.

[95] X. Lu, E. Sopin, V. Petrov, O. Galinina, D. Moltchanov, K. Ageev, S. Andreev, Y. Koucheryavy, K. Samouylov, and M. Dohler, "Integrated use of licensed-and unlicensed-band mmwave radio technology in 5g and beyond," *IEEE Access*, vol. 7, pp. 24 376–24 391, 2019.

[96] V. Sathya, M. I. Rochman, and M. Ghosh, "Hidden-nodes in coexisting laa & wi-fi: a measurement study of real deployments," *arXiv preprint arXiv:2103.15591*, 2021.

[97] Ericssion, "T-mobile, ericsson exceed 1 gbps with laa demo," https://www.ericsson.com/en/press-releases/2017/12/t-mobile-ericsson-exceed-1-gbps-with-laa-demo, 2017.

[98] S. M. Kala, "Extracted LAA Network Dataset from ATT, T-Mobile, and Verizon, url=https://drive.google.com/drive/folders/1h3H9i-P9wIwUqtbdznKr7Rre3XGF0c8H?usp=share$_l ink$,″ 2022.

[99] "XCAL-Mobile, Handheld Air Interface Field Testing Solution, url=https://accuver.com/sub/products/view.php?idx=10ckattempt=2."

[100] "QualiPoc Android, The premium handheld troubleshooter, url=https://www.rohde-schwarz.com/us/products/test-and-measurement/network-data-collection/qualipoc-android$_6$3493 − 55430.*html*.″

[101] "Network Signal Guru, url=https://play.google.com/ store/apps/details?id=com.qtrun.QuickTest&hl=en_US," 2020.

[102] "Network Cell Info Lite Wifi, url=https://www.appbrain.com/app/network-cell-info-lite-wifi/com.wilysis.cellinfolite."

[103] "FCC Speed Test App, url=https://play.google.com/store/apps/details?id=com.samknows.fcc."

[104] Y. Li, C. Peng, Z. Yuan, J. Li, H. Deng, and T. Wang, "Mobileinsight: Extracting and analyzing cellular network information on smartphones," in *Proceedings of the 22nd Annual International Conference on Mobile Computing and Networking*, 2016, pp. 202–215.

[105] Y. Sun, M. Peng, Y. Zhou, Y. Huang, and S. Mao, "Application of machine learning in wireless networks: Key techniques and open issues," *IEEE Communications Surveys & Tutorials*, vol. 21, no. 4, pp. 3072–3108, 2019.

[106] S. Ali, W. Saad, N. Rajatheva, K. Chang, D. Steinbach *et al.*, *6G White Paper on Machine Learning in Wireless Communication Networks*, 2020.

[107] G. E. Hinton, "Connectionist learning procedures," in *Machine learning*. Elsevier, 1990, pp. 555–610.

[108] J. Friedman, T. Hastie, R. Tibshirani *et al.*, *The elements of statistical learning*. Springer series in statistics New York, 2001.

[109] L. Breiman, "Random forests," *Machine learning*, 2001.

[110] J. H. Friedman, "Stochastic gradient boosting," *Computational statistics & data analysis*, 2002.

[111] C.-J. Hsieh, "Big data and high performance statistical computing," www.stat.ucdavis.edu/~chohsieh/teaching/STA141C_Spring2017/lecture7.pdf, 2018.

[112] S. M. Kala, V. Sathya, S. W. KG, and B. R. Tamma, "Cirno: Leveraging capacity interference relationship for dense networks optimization," in *2020 IEEE Wireless Communications and Networking Conference (WCNC)*. IEEE, 2020, pp. 1–6.

[113] S. M. Kala, V. Sathya, S. S. Magdam, and B. R. Tamma, "Odin : Enhancing resilience of disaster networks through regression inspired optimized routing," in *2019 IEEE International Conference on Advanced Networks and Telecommunications Systems (ANTS)*, 2019, pp. 1–6.

[114] E. Pekalska, R. P. Duin, and P. Paclík, "Prototype selection for dissimilarity-based classifiers," *Pattern Recognition*, pp. 189–208, 2006. [Online]. Available: https://www.sciencedirect.com/science/article/pii/S0031320305002633

[115] D. R. Wilson and T. R. Martinez, "Instance pruning techniques," in *MACHINE LEARNING: PROCEEDINGS OF THE FOURTEENTH INTERNATIONAL CONFERENCE (ICML'97*, 1997, pp. 404–411.

[116] H.-S. Park and C.-H. Jun, "A simple and fast algorithm for k-medoids clustering," *Expert Systems with Applications*, 2009. [Online]. Available: https://www.sciencedirect.com/science/article/pii/S095741740800081X

[117] J. L. Carbonera and M. Abel, "A density-based approach for instance selection," in *2015 IEEE 27th International Conference on Tools with Artificial Intelligence (ICTAI)*, 2015, pp. 768–774.

[118] European Commision Radio Spectrum Committee, "Commission paper on a draft mandate to CEPT on RLAN in the 6 GHz band (5925-6725 MHz)," https://circabc.europa.eu/d/d/workspace/SpacesStore/d63ea67f-8171-4619-a53d-8feb57387c27/RSCOM17-40_RLAN%206%20GHz.pdf, 2017.

[119] S. M. Kala, V. Sathya, M. P. K. Reddy, B. Lala, and B. R. Tamma, "A socio-inspired calm approach to channel assignment performance prediction and wmn capacity estimation,"

Journal of Network and Computer Applications, vol. 125, pp. 42 – 66, 2019. [Online]. Available: http://www.sciencedirect.com/science/article/pii/S1084804518303126

[120] V. Loginov, E. Khorov, A. Lyakhov, and I. Akyildiz, "Cr-lbt: Listen-before-talk with collision resolution for 5g nr-u networks," *IEEE Transactions on Mobile Computing*, 2021.

[121] 3GPP, "3rd generation partnership project; technical specification group services and system aspects; release 16 description; summary of rel-16 work items (release 16)," 2019.

[122] J. Moysen and M. García-Lozano, "Learning-based tracking area list management in 4g and 5g networks," *IEEE Transactions on Mobile Computing*, vol. 19, no. 8, pp. 1862–1878, 2019.

[123] S. Sundberg and J. Garcia, "Locating enodebs through sectorization inference—sector fitting evaluated on a railway use case," *Computer Networks*, vol. 190, p. 107945, 2021.

[124] "derf's collection, url=https://media.xiph.org/video/derf/."

[125] K. Chounos, S. Keranidis, A. Apostolaras, and T. Korakis, "Fast spectral assessment for handover decisions in 5g networks," in *2019 16th IEEE Annual Consumer Communications & Networking Conference (CCNC)*. IEEE, 2019, pp. 1–6.

[126] I. Ashraf, F. Boccardi, and L. Ho, "Power savings in small cell deployments via sleep mode techniques," in *2010 IEEE 21st International Symposium on Personal, Indoor and Mobile Radio Communications Workshops*. IEEE, 2010, pp. 307–311.

[127] R. Honarvar, A. Zolghadrasli, and M. Monemi, "Context-oriented performance evaluation of network selection algorithms in 5g heterogeneous networks," *Journal of Network and Computer Applications*, p. 103358, 2022.

[128] J. M. Johnson and T. M. Khoshgoftaar, "Survey on deep learning with class imbalance," *Journal of Big Data*, vol. 6, no. 1, pp. 1–54, 2019.

[129] A. K. Bairagi, N. H. Tran, W. Saad, Z. Han, and C. S. Hong, "A game-theoretic approach for fair coexistence between lte-u and wi-fi systems," *IEEE Transactions on Vehicular Technology*, vol. 68, no. 1, pp. 442–455, 2019.